GUTs in Type IIB Orientifold Compactifications

Ralph Blumenhagen[1], Volker Braun[2], Thomas W. Grimm[3], and Timo Weigand[4]

[1] *Max-Planck-Institut für Physik, Föhringer Ring 6,*
80805 München, Germany

[2] *Dublin Institute for Advanced Studies, 10 Burlington Road, Dublin 4, Ireland*

[3] *Bethe Center for Theoretical Physics and*
Physikalisches Institut der Universität Bonn, Nussallee 12,
53115 Bonn, Germany

[4] *SLAC National Accelerator Laboratory, Stanford University,*
2575 Sand Hill Road, Menlo Park, CA 94025, USA

blumenha@mppmu.mpg.de, vbraun@stp.dias.ie,
grimm@th.physik.uni-bonn.de, timo@slac.stanford.edu

Abstract

We systematically analyse globally consistent $SU(5)$ GUT models on intersecting D7-branes in genuine Calabi-Yau orientifolds with O3- and O7-planes. Beyond the well-known tadpole and K-theory cancellation conditions there exist a number of additional subtle but quite restrictive constraints. For the realisation of $SU(5)$ GUTs with gauge symmetry breaking via $U(1)_Y$ flux we present two classes of suitable Calabi-Yau manifolds defined via del Pezzo transitions of the elliptically fibred hypersurface $\mathbb{P}_{1,1,1,6,9}[18]$ and of the Quintic $\mathbb{P}_{1,1,1,1,1}[5]$, respectively. To define an orientifold projection we classify all involutions on del Pezzo surfaces. We work out the model building prospects of these geometries and present five globally consistent string GUT models in detail, including a 3-generation $SU(5)$ model with no exotics whatsoever. We also realise other phenomenological features such as the $\mathbf{10\,10\,5_H}$ Yukawa coupling and comment on the possibility of moduli stabilisation, where we find an entire new set of so-called swiss-cheese type Calabi-Yau manifolds. It is expected that both the general constrained structure and the concrete models lift to F-theory vacua on compact Calabi-Yau fourfolds.

Contents

1 Introduction

The LHC experiment is widely expected not only to confirm the existence of the Higgs particle as the last missing ingredient of the Standard Model of Particle Physics, but also to reveal new structures going far beyond. As experiments are proceeding into this hitherto unexplored energy regime, string theory, with its claim to represent the unified theory of all interactions, will have to render an account of its predictions for physics beyond the Standard Model. Clearly, these depend largely on the value of the string scale M_s, the most dramatic outcome corresponding to M_s close to the TeV scale. While this is indeed a fascinating possibility, in concrete string models it often leads to severe cosmological issues such as the cosmological moduli problem. In this light it might be fair to say that a more natural (but also more conservative) scenario involves a value of M_s at the GUT, Planck or intermediate scale.

During the last years, various classes of four-dimensional string compactifications with $\mathcal{N} = 1$ spacetime supersymmetry have been studied in quite some detail (see the reviews [1, 2, 3, 4, 5] for references). From the viewpoint of realising the Minimal Supersymmetric Standard Model (MSSM) and some extension thereof the best understood such constructions are certainly the perturbative heterotic string and Type IIA orientifolds with intersecting D6-branes. On the contrary, as far as moduli stabilisation is concerned Type IIB orientifolds with O7- and O3-planes look very promising. The combination of three-form fluxes and D3-brane instantons can stabilise all closed string moduli [6] even within the solid framework of (conformal) Calabi-Yau manifolds where reliable computations can be performed. Moreover, supersymmetry breaking via Kähler moduli mediation and the resulting structure of soft terms bear some attractive features and have been studied both for the LARGE volume scenario [7,8] with an intermediate string scale and for a GUT scenario with the string scale at the GUT scale [9,10].

These considerations are reason enough to seriously pursue model building within type IIB orientifolds. The observation that the MSSM gauge couplings appear to meet at the GUT scale furthermore suggests the existence of some GUT theory at high energies. GUT gauge groups such as $SU(5)$ and $SO(10)$ appear naturally in string theories based on gauge group E_8 like the heterotic string. On the other hand, it has become clear that for perturbative orientifolds with D-branes, exceptional gauge groups and features like the spinor representations of $SO(10)$ do not emerge. For $SU(5)$ D-brane models, by contrast, the gauge symmetry and the desired chiral matter spectrum can be realised, a fact welcome in view of the described progress in

Type IIB moduli stabilisation. Still, at first sight there appears a serious problem in the Yukawa coupling sector. The $\mathbf{10\,10\,5_H}$ Yukawa coupling violates global perturbative $U(1)$ symmetries which are the remnants of former $U(1)$ symmetries rendered massive by the Stückelberg mechanism [11]. As a consequence of these considerations it is sometimes argued that the natural context for Type II GUT model building is the strong coupling limit, where the crucial couplings in question are not "perturbatively" forbidden. The strongly coupled duals of type IIA and Type IIB orientifolds are given by singular M-theory compactifications on G_2 manifolds and, respectively, by F-theory compactifications on elliptically fibred Calabi-Yau fourfolds [12]. The local model building rules for such F-theory compactifications have been worked out recently in [13, 14, 15, 16, 17, 18, 19]; For recent studies of 7-branes from the F-theory perspective see [20, 21, 22, 23, 24].

On the other hand, investigations of non-perturbative corrections for Type II orientifold models [25, 26, 27] have revealed that the $\mathbf{10\,10\,5_H}$ Yukawa coupling can be generated by Euclidean D-brane instantons wrapping suitable cycles Γ in the internal manifold with the right zero mode structure [28]. Of course these couplings are suppressed[1] by the exponential of the instanton action $\Re(T_{\mathrm{inst}}) = g_s^{-1}\mathrm{Vol}(\Gamma)$. It is crucial to appreciate that this suppression is *not* tied to the inverse gauge coupling of the Standard Model, as would be the case for effects related to gauge (as opposed to "stringy") instantons, but can in principle take any value, depending on the geometric details of our compactification manifold. This feature, which holds both for Type IIA and Type IIB orientifolds, opens up the prospect of $SU(5)$ GUT model building already in the limit $T_{\mathrm{inst}} \to 0$ of perturbative Type II orientifolds. Once we also take the nice features of moduli stabilisation in Type IIB into account, one might seriously hope that the strong coupling limit of Type IIB orientifolds, either in their genuinely F-theoretic disguise or in their perturbative description as D-brane models with O7- and O3- planes and $T_{inst} \to 0$, may indeed provide a promising starting point to construct realistic GUT models.

In the recent work [14, 16], the authors draw the first conclusion (see also [13, 17]). Taking into account that F-theory models on elliptically fibred fourfolds can admit degenerations of the elliptic fibre such that exceptional gauge groups appear naturally, these references pursue the program of studying GUT type F-theory compactifications. As a physical input, the authors of [14, 16] propose the working hypothesis

---

[1]Note that for a Georgi-Glashow $SU(5)$ GUT the $\mathbf{10\,10\,5_H}$ Yukawa gives masses to up-type quarks, whereas for flipped $SU(5)$ it provides the down-type quark masses. In the latter case, the exponential suppression might explain the little hierarchy between up and down quarks [28].

that the Planck scale ought to be decouple-able from the GUT scale, even if only in principle. From the Type IIB perspective, these F-theoretic models do not only contain usual D-branes, but also so-called (p, q) seven-branes which carry charge under both the R-R and the NS-NS eight-forms. The new non-perturbative states, such as the gauge bosons of exceptional groups or the spinor representations of $SO(10)$, are given by (p, q) string junctions starting and ending on these branes. Unlike fundamental strings, these string junctions can have more than two ends thus providing extra states.

From the guiding principle of decoupled gravity it is further argued in [16] that the (p, q) 7-branes should wrap shrinkable four-cycles in the internal geometry. These are given by del Pezzo surfaces[2]. Lacking a global description of Calabi-Yau fourfolds with the desirable degeneration, the authors provide a local set-up of singularities or (p, q) 7-branes and line bundles so that the GUT particle spectrum is realised. At a technical level there arises a challenge with GUT symmetry breaking because a theory on a del Pezzo surface has neither adjoints of $SU(5)$ nor discrete Wilson lines at its disposal to break $SU(5)$ to $SU(3) \times SU(2) \times U(1)_Y$. One option would be to adopt the philosophy of heterotic compactifications and embed a further non-trivial $U(1)$ line bundle, as discussed for the heterotic string originally in [31] and more recently in [32,33,34,35]. For line bundles non-trivial on the Calabi-Yau manifold, the associated $U(1)$ generically becomes massive due to the Stückelberg mechanism, but in presence of several line bundles special linear $U(1)$ combinations remain massless. In the heterotic context of [34], in order to maintain gauge coupling unification without relying on large threshold corrections it is necessary to consider the large g_s limit of heterotic M-theory [36].

As a new and very central ingredient the authors of [16] propose to break the GUT gauge group instead by a line bundle embedded into $U(1)_Y$ such that it circumvents the sort of no-go theorem mentioned above (see also [17]). The idea is to support the bundle on a non-trivial two-cycle inside the del Pezzo surface which is trivial on the ambient four-fold base. It was argued in [16] that with this mechanism some of the notorious problems of GUTs such as the doublet-triplet splitting problem, dangerous dimension five proton decay operators and even neutrino masses can be addressed and actually solved by appropriate choices of matter localisations and line bundles on the del Pezzo divisors. Studies of supersymmetry breaking mechanisms for this class of local models have appeared in [37, 38, 39].

The Planck-scale decoupling principle might be a justification for a local approach

---

[2]Local quiver type models on del Pezzo singularities have been studied, for example, in [29, 30].

to string model building (and indeed a quite constraining one), but in absence of a realisation of the described mechanisms in globally consistent string compactifications it remains an open question if these local GUT models do really consistently couple to gravity. In fact, it is the global consistency conditions of string theory which decide whether a given construction is actually part of the string landscape or merely of the "swampland" of gauge theories. At a technical level, it is therefore no wonder that they constitute some of the biggest challenges in string model building, and many interesting local constructions fail to possess a compact embedding satisfying each of these stringy consistency conditions. For example, whether or not a given $U(1)_Y$ flux actually leads to a massless hypercharge depends on the global embedding of the divisor supporting the 7-brane into the ambient geometry and cannot be decided within a local context.

In F-theory the global consistency conditions, in particular the D7-brane tadpole cancellation condition, are geometrised: They are contained in the statement that indeed a compact elliptically fibred fourfold exists such that the degenerations of the fibre realise the GUT model. This is a very top-down condition and given the complexity and sheer number of fourfolds it is extremely hard to implement in practise.

It is the aim of this paper to address these global consistency conditions by taking a different route. As described above Georgi-Glashow $SU(5)$ GUT models can naturally be realised on two-stacks of D7-branes in a perturbative Type IIB orientifold. Here we have quite good control over the global consistency conditions as they are very similar to the well-studied Type I or Type IIA orientifolds. Therefore, our approach is to first construct a GUT model on a Type IIB orientifold, satisfy all consistency conditions, check whether the top quark Yukawa is really generated by an appropriate D3-instanton and then take the local $T_{\text{inst.}} \rightarrow 0$ limit[3].

To follow this path, we start by partly newly deriving, partly summarising the model building rules for Type IIB orientifolds. We then study how much of the appealing structure proposed in the F-theoretic context, such as the $U(1)_Y$ GUT gauge breaking, can already be realised in perturbative Type IIB orientifolds on Calabi-Yau threefolds with intersecting D7-branes wrapping holomorphic surfaces with non-trivial vector- or line-bundles.

In order for the $U(N)$ gauge factors on the D7-banes not to exhibit chiral mul-

---

[3]Here we make the working assumption that a Type IIB vacuum satisfying all K-theory and supersymmetry constraints has an uplift to F-theory on a Calabi-Yau fourfold. We are aware that this may not be so straightforward to show [40].

tiplets transforming in the adjoint representation, the four-cycle wrapped by the 7-brane should be rigid. A natural class of such complex four-manifolds is again given by del Pezzo surfaces, which therefore remain important ingredients from a phenomenological point of view[4]. This leads us to the study of a class of suitable Calabi-Yau threefolds admitting complex divisors of del Pezzo type whose non-trivial two-cycles are partially trivial when considered as two-cycles of Y. A large class of such Calabi-Yau threefolds is given by del Pezzo transitions, as have been recently discussed in a slightly different context in [41]. The idea is to start for instance with the well-studied "swiss cheese" type Calabi-Yau hypersurface $\mathbb{P}_{1,1,1,6,9}[18]$, which is elliptically fibred over $\mathbb{P}_2$, and blow up points on the base. As a second starting point for such del Pezzo transitions we consider the quintic $\mathbb{P}_4[5]$. As we will see such Calabi-Yau manifolds are natural candidates for GUT model building.

More concretely, in Section 2 we collect the string model building rules for Type IIB orientifolds with O7- and O3-planes. Since these involve intersecting D7-branes supporting non-trivial gauge bundles, the relevant structure is a combination of Type I and Type IIA orientifold features and as such is slightly more complicated and subtle. In particular, since the del Pezzo surfaces wrapped by the D7-branes are not $Spin$, one has to take into account the Freed-Witten anomaly [42] shifting the proper quantisation for the gauge fluxes[5]. Moreover, for involutions with $h_-^2 > 0$ one encounters dynamical B-field moduli, which have to be appropriately dealt with.

In Section 3 we discuss how we can realise a D-brane sector supporting a Georgi-Glashow $SU(5)$ GUT model. In many respects this is very analogous to $SU(5)$ GUTs in intersecting D6-brane scenarios (for concrete examples see, for example, [43, 11, 44, 45, 46, 47, 48]). We show that the GUT symmetry breaking via $U(1)_Y$ flux can be realised in the perturbative Type IIB orientifold framework and provide the conditions under which this flux can solve the doublet-triplet splitting problem and the suppression of dimension five proton decay operators. By studying which quantities are affected by this flux we find that not only the gauge group is broken but also the non-chiral spectrum and the D3-brane tadpole generically changes. Very analogous features are expected to arise also in F-theory compactifications on compact Calabi-Yau fourfolds equipped with non-vanishing four-form flux.

The slightly more mathematical Section 4 defines a class of compact Calabi-Yau

---

[4]Note, however, that the class of rigid surfaces is larger than that of shrinkable, that is, del Pezzo, surfaces. For example, the surface dP$_9$, which is rigid, but not contractible, is still an interesting candidate for a GUT D7-brane in this respect.

[5]An analogous quantisation condition is expected to also arise for the four-form flux in F-theory compactifications on compact as well as on non-compact Calabi-Yau fourfolds.

manifolds naturally containing del Pezzo surfaces. These compact manifolds have recently been considered in [41] and contain the kind of holomorphic surfaces allowing for the realisation of many of the GUT features we are interested in. They can be described as elliptic fibrations over del Pezzo surfaces dP_n, $n = 1, \ldots, 8$ and their various connected phases related via flop transitions. In the elliptic fibration itself, besides the dP_n basis, we find various dP_9 surfaces, which via the flop transitions become dP_8 surfaces or $\mathbb{P}_2$ surfaces with more than nine points blown up. In the course of this section, to define the orientifold actions we have to investigate the existence of appropriate involutions. In order not to interrupt the physics elaborations too much this rather technical though central discussion has mainly been shifted to appendix A. The mathematically interested reader is encouraged to consult this appendix for more details on the classification of involutions and the determination of the fixed point loci. As an important part of our analysis we will prove the "swiss cheese" structure of those del Pezzo transitions where the dP_9 surfaces have all been flopped to dP_8 surfaces. We will show that as a consequence of this structure the D-term supersymmetry conditions force the cycles supporting D-branes to take a vanishing volume, that is, they are dynamically driven to the quiver locus.

In Sections 5 and 6 we present some first concrete $SU(5)$ GUT models. These are the outcome of an essentially manual search which has succeeded in implementing all known global consistency conditions. As a warm-up, Section 5 discusses at length an $SU(5)$ model on the Weierstraß model over dP_2 with two chiral families of $SU(5)$ GUT matter, one vector-like pair of Standard Model Higgs and no chiral exotics. The GUT matter transforming in the **10** is localised in the bulk of the GUT branes, while the $\overline{\mathbf{5}}$ and the Higgs pair arise at matter curves. Upon breaking $SU(5)$ by means of $U(1)_Y$ flux there arise extra vector-like pairs of Standard Model matter. As one of its phenomenologically appealing features, this model contains a $\mathbf{10\,10\,5_H}$ Yukawa coupling of order one induced by a Euclidean D3-brane instanton in the limit $T_{inst.} \to 0$, but the global consistency conditions do not allow for the construction of a three-generation model on this particular geometry. To remedy this we present, in Section 6, a string vacuum of a similar type on the del Pezzo transition of this Weierstraß model, but featuring three chiral families of Standard Model matter, no chiral exotics and only two pairs of extra vector-like states. As a consequence of the swiss cheese structure of the manifold, the D-term supersymmetry conditions drive the vacuum to the boundary of the Kähler cone. This can be avoided in a three-generation GUT model on the Weierstraß model over dP_3 as discussed in the remainder of this section. The key phenomenological achievements and drawbacks of these three examples are summarised in Tables 9, 13, and 15.

In Section 7 we analyse yet another class of geometries based on the quintic hypersurface which also contain del Pezzo surfaces suitable for GUT model building by extending the examples of [41]. In this type of geometries it is possible to localise all GUT matter at matter curves, thus avoiding the appearance of extra vector-like pairs in the bulk. The D-term supersymmetry conditions can be realised for non-zero cycle volume. Once again due to subtle global consistency constraints we only present a two-generation GUT model exhibiting these features realised on dP_8 surfaces, but remarkably we do find an interesting model with just three generations of Standard Model matter and no exotics whatsoever on a related geometry featuring dP_9 surfaces. The detailed properties of these two examples are summarised in Tables 17 and 19, respectively.

In Section 8 we comment on the possibilities of moduli stabilisation in our class of models. Taking our findings for GUT model building into account, the most natural realisation of the LARGE volume scenario of moduli stabilisation seems to place the GUT branes and the instantons contributing to the superpotential on different, non-intersecting dP_n surfaces. This is expected to lead to a new pattern of soft terms at the GUT scale and consequently to different collider signatures compared to the studies which have appeared in the literature so far. Furthermore, we clearly need to stabilise the string scale not at an intermediate, but at the GUT scale, for example along the lines of [10]. The explicit elaboration of such aspects is, however, beyond the scope of the present article.

2 Orientifolds with Intersecting D7-Branes

In this section we will introduce some preliminaries on Type IIB Calabi-Yau orientifold compactifications with space-time filling D7 branes. In order for such a scenario to be globally consistent and to preserve $\mathcal{N} = 1$ supersymmetry in the four flat dimensions we consider an orientifold projection which allows for O3 and O7 planes and takes the form $\mathcal{O} = (-1)^{F_L} \Omega_p \sigma$. Here σ is a holomorphic and isometric involution of the internal Calabi-Yau manifold Y. The action of σ on the Kähler form J of Y is $\sigma^* J = J$, while the holomorphic $(3,0)$ form transforms as $\sigma^* \Omega = -\Omega$. Similarly, for the other string fields to remain in the spectrum they have to transform with the appropriate parity under σ.

To determine the four-dimensional effective theory one first needs to examine the surviving bulk and brane fields. At least locally, each such field can be identified with an element of an appropriate bundle valued cohomology group on the internal mani-

fold and the cycles wrapped by the D-branes. The involution σ splits the cohomology groups into eigenspaces, and allows one to identify the spectrum preserved by the orientifold. Focusing on the bulk fields corresponding to closed string excitations, one notes that $H^{p,q}(Y, \mathbb{C})$ splits as $H^{p,q}_+ \oplus H^{p,q}_-$ with dimensions $h^{p,q}_\pm$ respectively. One thus obtains the complex dilaton $\tau = C_0 + ie^{-\phi}$, $h^{1,1}_+$ complexified Kähler moduli T_I and $h^{1,1}_-$ B-field moduli G^i given by [49, 50]

$$T_I = \int_{\Gamma^+_I} \Pi \,, \qquad G^i = \int_{\gamma^i_-} \Pi \,, \qquad \Pi = e^{-B}\Big(e^{-\phi}\mathrm{Re}\big[e^{iJ}\big] + iC_{\mathrm{RR}}\Big) \tag{1}$$

where $C_{\mathrm{RR}} = C_0 + C_2 + C_4$. The cycles Γ^+_I and γ^i_- form a basis of the homology groups $H^+_{2,2}$ and $H^-_{1,1}$, respectively. We will call the continuous moduli G^i simply B_- moduli, since they encode the variations of the NS-NS and R-R two-forms. While no dynamical moduli are associated with the reduction of the B-field along the positive 2-cycles $\Gamma^I_+ \in H^+_{1,1}$ there can still be discrete non-zero B-flux $\frac{1}{2\pi}\int_{\Gamma^I_+} B = \frac{1}{2}$. This survives the orientifold action due to the axionic shift symmetry $\int_{\Gamma^I_+} B \to \int_{\Gamma^I_+} B + 2\pi$ and will sometimes be referred to as B_+ flux. In the following we will determine which quantities in the four-dimensional action depend on which of these closed string moduli.

2.1 Intersecting D7-Branes With Gauge Bundles

We first discuss the inclusion of space-time filling D7-branes in more detail. Consider wrapping a stack of N_a D7-branes around a four-cycle D_a in Y. The calibration condition for the D7-branes requires D_a to be a holomorphic divisor [51]. The orientifold symmetry σ maps D_a to its orientifold image D'_a so that in the upstairs geometry each brane is accompanied by its image brane. There are three different cases to be distinguished:

1. $[D_a] \neq [D'_a]$,

2. $[D_a] = [D'_a]$ but $D_a \neq D'_a$ point-wise, and

3. $D_a = D'_a$ point-wise, that is, D7-branes coincide with an O-plane.

In the first two situations, the D7-brane may or may not intersect an O7-plane. For vanishing gauge flux, branes of the first type carry unitary gauge groups, while those of the other two types yield symplectic or orthogonal gauge groups. In absence of

11

CFT methods to uniquely distinguish SO vs. SP Chan-Paton factors the rule of thumb is that a stack of N_a branes plus their N_a image branes on top of an $O7^{-/+}$-plane[6] gives rise to a gauge group $SO(2N_a)/SP(2N_a)$. The same configuration along a cycle of type 2 with locally four Dirichlet-Neumann boundary conditions to the $O7^{-/+}$-plane yields gauge group $SP(2N_a)/SO(2N_a)$.

Gauge fluxes on D7-branes

Each stack of D7-branes can carry non-vanishing background flux for the Yang-Mills field strength F_a. Recall that the field strength F_a appears in the Chern-Simons and DBI action only in the gauge invariant combination $\mathcal{F}_a = F_a + \iota^* B \mathbf{1}$, where $\iota : D_a \to Y$ denotes the embedding of the divisor D_a into the ambient space. Therefore all physical quantities depend a priori only on $\mathcal{F}_a$. However, as we will describe in detail below, with the exception of the D-term supersymmetry condition only the discrete B_+-flux effectively enters the consistency conditions.

A consistent configuration of internal gauge flux is mathematically described in terms of a stable holomorphic vector bundle[7] by identifying the curvature of its connection with the Yang-Mills field strength. For all concrete applications in this article it will be sufficient to restrict ourselves to the simplest case of line bundles L_a, corresponding to Abelian gauge flux. For a single D-brane wrapping a simply connected divisor these are determined uniquely by their first Chern class $c_1(L_a)$ as an element of $H^2(D_a)$ or equivalently by a two-cycle l_a with class in $H_2(D_a)$ as $L_a = \mathcal{O}(l_a)$. For stacks of several coincident branes wrapping the divisor D_a we also have to specify the embedding of the $U(1)$ structure group of the line bundle into the original gauge group on the branes.

Let us start with a stack of N_a branes of type 1 and decompose the background value of the physical Yang-Mills field strength $\mathcal{F}$ as

$$\mathcal{F}_a = T_0 \left(F_a^{(0)} + \iota^* B \right) + \sum_i T_i \, F_a^{(i)}. \tag{2}$$

Here $T_0 = 1_{N_a \times N_a}$ refers to the diagonal $U(1)_a \subset U(N_a)$ while T_i are the traceless Abelian[8] elements of $SU(N_a)$. This defines the line bundles $L_a^{(i)}$ as

$$c_1(L_a^{(0)}) = \frac{1}{2\pi}(F_a^{(0)} + \iota^* B) \in H^2(D_a), \quad c_1(L_a^{(i)}) = \frac{1}{2\pi}F_a^{(i)} \in H^2(D_a). \tag{3}$$

---

[6]A $O7^{-/+}$-plane carries $-8/+8$ times the charge of a D7-brane in the upstairs geometry.

[7]More generally, gauge flux is described by coherent sheaves, but for our purposes it suffices to consider vector bundles on the divisors.

[8]This can be generalised to non-Abelian vector bundles. For example, on a stack of N_a coincident

Note that in view of the appearance of $\mathcal{F}_a$ in all physical equations the B-field is to be included in $c_1(L_a^0)$.

While the effect of $L_a^{(0)}$ is merely to split $U(N_a) \to SU(N_a) \times U(1)_a$, the other $L_a^{(i)}$ will break $SU(N_a)$ further. The relevant example we will be studying in detail is the breaking of $U(5)_a \to SU(5) \times U(1)_a \to SU(3) \times SU(2) \times U(1)_Y \times U(1)_a$ by means of diagonal flux and another line bundle corresponding to the hypercharge generator T_Y. Note that the Abelian gauge factors may become massive via the Stückelberg mechanism [54].

For a stack of $2N_a$ invariant branes of type 2 and 3 a non-trivial bundle $L_a^{(0)}$ breaks $SO(2N_a)/SP(2N_a) \to SU(N_a) \times U(1)_a$ and the embedding of $L_a^{(i)}$ works in an analogous manner. We will be more specific in the context of the concrete setup described in Subsection 3.1.

In general it is possible for some components of[9] $c_1(L_a)$ along $H^2(D_a)$ to be trivial as elements of $H^2(Y)$. Recall that the inclusion $\iota : D_a \to Y$ defines the pushforward $\iota_* : H_2(D_a) \to H_2(Y)$ and pullback $\iota^* : H^2(Y) \to H^2(D_a)$. Then one can split L_a as

$$L_a = \iota^* \mathbb{L}_a \otimes R_a, \tag{4}$$

with $\mathbb{L}_a = \mathcal{O}(\ell_a)$ defined as a line bundle on the Calabi-Yau Y. The part of L_a trivial in Y, denoted as $R_a = \mathcal{O}(r_a)$, corresponds to a two-cycle r_a which is non-trivial on D_a but a boundary in Y, that is, $[r_a] \in \ker(\iota_*)$. The possibility of considering such gauge flux in the relative cohomology of D_a in Y was first pointed out in [55, 56] and its relevance for model building was stressed in [30, 41].

We need to understand which quantities are affected by a relative flux R. In this context, we will make heavy use of the following integrals

$$\int_{D_a} c_1(\iota^* \mathbb{L}_b) \wedge c_1(\iota^* \mathbb{L}_c) = \int_Y [D_a] \wedge c_1(\mathcal{O}(\ell_b)) \wedge c_1(\mathcal{O}(\ell_c)) = \kappa_{abc},$$

$$\int_{D_a} c_1(\iota^* \mathbb{L}_b) \wedge c_1(R_c) = \int_{D_a \cap \ell_b} c_1(R_c) = 0, \tag{5}$$

$$\int_{D_a} c_1(R_b) \wedge c_1(R_c) = \eta_{abc} ,$$

---

branes one can define a holomorphic rank n_a bundle (with n_a dividing N_a) and embed its structure group $U(n_a)$ into the original $U(N_a)$ theory. This breaks the four-dimensional gauge group down to the commutant $U(N_a/n_a)$ of $U(n_a)$ in $U(N_a)$. See [52, 53] for a general discussion in terms of D9-branes on Calabi-Yau manifolds.

[9]In the sequel we will sometimes omit the superscripts in $L_a^{(i)}$ to avoid cluttering of notation.

where κ_{abc} and η_{abc} are not necessarily zero. We conclude that the integral over a divisor of a pull-back two form wedge a two-form which is trivial in Y vanishes. As will be detailed below, this implies that a bundle in the cohomology which is trivial in Y but non-trivial on D_a does not affect the chiral spectrum, the D-term supersymmetry conditions and the D5-brane tadpole of the brane configuration. However, it does affect the gauge symmetry, the D3-brane tadpole and the non-chiral spectrum of the model.

Quantisation condition

Essential both for consistency of the theory and for concrete applications is to appreciate the correct quantisation conditions on the gauge flux. Following [42] they are determined by requiring that the worldsheet path integral for an open string wrapping the two-surface Σ with boundary $\partial\Sigma$ along D_a be single-valued. Consider first a single brane wrapping the divisor D_a and carrying Abelian gauge flux F_a. The quantity to be well-defined is given by

$$\text{Pfaff}(D) \; \exp\left(i \int_{\partial\Sigma} A_a\right) \; \exp\left(i \int_\Sigma B\right) \tag{6}$$

in terms of the Pfaffian of the Dirac operator, the connection A of the Abelian gauge bundle and the B-field. If D_a is not *Spin*, that is, if $c_1(K_{D_a}) \neq 0 \mod 2$, the Pfaffian picks up a holonomy upon transporting $\partial\Sigma$ around a loop on D_a [42]. This holonomy must be cancelled by the second factor in eq. (6). For internal line bundles this is guaranteed if the gauge flux obeys the condition

$$\int_\omega F_a + \frac{1}{2} \int_\omega K_{D_a} \in \mathbb{Z} \qquad \forall \omega \in H_2(D_a, \mathbb{Z}), \tag{7}$$

or equivalently, using our convention eq. (3),

$$c_1(L_a) - \iota^* B + \frac{1}{2} c_1(K_{D_a}) \in H^2(D_a, \mathbb{Z}). \tag{8}$$

Note in particular that for trivial B flux along D_a, $\iota^* B = 0$, the Abelian gauge bundle on the single brane D_a has to be half-integer[10] quantised if the divisor D_a is not *Spin*.

---

[10]The quantisation condition eq. (8) with non-trivial B-field is related to the concept of vector bundles without vector structure [57] in Type I theory as studied recently, for example, in [58,?].

This condition is readily generalised to line bundles on stacks of D-branes. The probe argument of [42] now implies that the path integral has to be well-defined for every disk worldsheet Σ with boundary on each of the branes in the stack of N_a D-branes wrapping D_a. This requires

$$T_0 \left(c_1(L_a^{(0)}) - \iota^* B \right) + \sum_i T_i \, c_1(L_a^{(i)}) + \frac{1}{2} T_0 \, c_1(K_{D_a}) \in H^2(D_a, \mathbb{Z})_{N_a \times N_a}. \qquad (9)$$

where the notation on the right hand side means that all elements of the $N_a \times N_a$ matrix on the left hand side are in $H_2(D_a, \mathbb{Z})$. One concludes that depending on the precise from of T_i the bundles $L_a^{(i)}$ can in general be fractionally quantised, a fact that will be very important for our applications.

A second constraint arises for the continuous B_- moduli in H_-^2: the restriction to D_a of the characteristic class ζ of the B_--field, introduced in [42], has to equal the third Stiefel-Whitney class of D_a. Recall from [42] that modulo torsion, ζ is given by the field strength $H = dB_-$ and that for complex divisors the third Stiefel-Whitney class is always zero. Moreover, for all surfaces considered in this paper, we have $H^3(D_a, \mathbb{Z}) = 0$ so that $H = dB_-$ always restricts to zero on the divisor. Therefore no further condition on the B-field moduli G^i introduced in (1) arises from these considerations.

Orientifold action

Let us now describe the orientifold action on the gauge flux. To this end note that the orientifold action $\sigma : D \to D'$ induces a map on cohomology, $\sigma^* : H^2(D_a, \mathbb{Z}) \to H^2(D'_a, \mathbb{Z})$. The full orientifold action on a vector bundle on D_a is given by the composition $\sigma^* \Omega_p$. Here Ω_p acts as dualisation, $L_a \to L_a^\vee$. In particular, the Chern character of the image bundle is

$$\mathrm{ch}_k(L'_a) = (-1)^k \sigma^* \mathrm{ch}_k(L_a) = \sigma^* \mathrm{ch}_k(L_a^\vee). \qquad (10)$$

We now discuss the three cases introduced at the beginning of Subsection 2.1 in turn. In the first situation, where not even the homology class of the brane is preserved, one can define two divisors $D_a^\pm$ and two vector bundles $L_a^\pm$ by setting

$$D_a^\pm = D_a \cup (\pm D'_a) \, , \qquad L_a^\pm|_{D_a} = L_a \, , \qquad L_a^\pm|_{D'_a} = \pm L'_a, \qquad (11)$$

where $-D'_a$ is the cycle D'_a with reversed orientation. Upon setting $H^2(D_a^+) = H^2(D_a) \oplus H^2(D'_a)$ and decomposing the latter into positive and negative eigenspaces under σ^*, $H^2(D_a^+) = H_+^2(D_a^+) \oplus H_-^2(D_a^+)$ [55], it follows that $c_1(L_a^+) \in H_-^2(D_a^+)$.

In the second case the homology class is preserved but the brane is not point-wise fixed. Hence, the homology class of D_a^- in eq. (11) is trivial and we can use $[D_a] = \frac{1}{2}[D_a^+]$. The degree-2 cohomology group of D_a thus splits again as $H^2(D_a, \mathbb{Z}) = H_+^2(D_a) \oplus H_-^2(D_a)$. On the covering space of the orientifold one requires an even number of branes in the homology class of D_a which are pairwise identified under the involution σ. Clearly, this corresponds to an integer number of branes on D_a^+. The Chern class $c_1(L_a)$ on D_a is in the full $H^2(D_a)$ and (D_a, L_a) is mapped to (D_a, L_a') as in eq. (10).

In the third case, for D_a on top of the orientifold, $H^2(D_a) = H_+^2(D_a)$ and (D_a, L_a) is mapped to $(D_a, L_a^\vee)$. This case directly parallels the situation for D9-branes in Type I compactifications. An odd number of branes stuck on top of the orientifold plane is not possible, as discussed recently in [23]. Formally we therefore work upstairs with the system $2N_a D_a$ carrying the invariant bundle $L_a \oplus L_a^\vee$.

2.2 Tadpole Cancellation for Intersecting D7-Branes

In consistent compactifications it is crucial to cancel the tadpoles of the space-time filling intersecting D7-branes. Satisfying the tadpole cancellation condition ensures that the spectrum is free of non-Abelian gauge anomalies. In general, D7-branes carry also induced D3- and D5- charges arising due to a non-trivial gauge-field configuration on the seven branes and through curvature corrections. All induced tadpoles for a compactification have to be cancelled.

Throughout this article we will be working upstairs on the ambient Calabi-Yau manifold before taking the quotient by σ. Recall that the K-theoretic charges Γ of a D7-brane and the O7-plane along divisors D_a and D_{O7} are encoded in the Chern-Simons coupling to the closed RR-forms $2\pi \int_{\mathcal{R}^{1,3} \times D_a} \sum_{2p} C_{2p} \Gamma$. Concretely these are given by

$$S_{D7} = 2\pi \int_{\mathcal{R}^{1,3} \times D_a} \sum_{2p} C_{2p} \, \mathrm{tr} \left[e^{\frac{1}{2\pi} \mathcal{F}_a} \right] \sqrt{\frac{\hat{A}(TD)}{\hat{A}(ND)}},$$

$$S_{O7} = -16\pi \int_{\mathcal{R}^{1,3} \times D_{O7}} \sum_{2p} C_{2p} \sqrt{\frac{L(\frac{1}{4} T D_{O7})}{L(\frac{1}{4} N D_{O7})}} \qquad (12)$$

in terms of the Â-roof and the Hirzebruch genus associated with the tangent and normal bundles to the respective divisors. The D7-, D5-, and D3-brane charges follow upon straightforward decomposition of eq. (12).

Let us start by discussing cancellation of the D7-charge. In a consistent orientifold compactification the D7-brane charge has to equal the charge carried by the O7-planes,

$$\sum_a N_a \left([D_a] + [D'_a]\right) = 8 \left[D_{\text{O7}}\right], \tag{13}$$

where the sum is over all D7$_a$-branes. Since supersymmetric D7-branes together with their orientifold images wrap cycles $D_a + D'_a$ in the homology classes of $H_4^+(Y)$, the orientifold invariant charges are captured by the Poincaré dual cohomology $H_+^2(Y)$ on the ambient Calabi-Yau manifold Y.

A net D5-brane charge can be induced by a gauge-field configuration $\mathcal{F}_a$ on D_a (and the respective orientifold images) if there exist non-trivial elements in $H_-^2(Y)$. The D5-brane charge along the element $\omega_b \in H^2(Y, \mathbb{Z})$ of a stack of N_a branes carrying Abelian gauge flux as in eq. (3) reads

$$\Gamma_\omega^{D5} = \frac{1}{2\pi} \int_Y \omega \wedge [D_a] \wedge \text{tr} \mathcal{F}_a , \tag{14}$$

where

$$\frac{1}{2\pi} \text{tr} \mathcal{F}_a = \sum_I \text{tr} \left[T_I\right] \, c_1(L_a^{(I)}), \qquad I = 0, i . \tag{15}$$

The condition for cancellation of D5-brane charge therefore takes the form

$$\sum_a \int_Y \omega \wedge \left([D_a] \wedge \text{tr} \mathcal{F}_a + [D'_a] \wedge \text{tr} \mathcal{F}_{a'} \right) = 0 , \tag{16}$$

and has to be satisfied for all elements $\omega \in H_-^2(Y)$. Clearly this condition is vacuous if all branes are of the type $[D_a] = [D'_a]$ and $c_1(L_{a'}^{(I)}) = c_1\big((L_a^{(I)})^\vee\big)$, but it may be quite restrictive in more general situations.

The general condition for cancellation of the D3-brane tadpole takes the form

$$(N_{\text{D3}} + N_{\text{D3}'}) + N_{\text{flux}} - \sum_a (Q_{\text{D7}}^a + Q_{\text{D7}}'^a) = \frac{N_{\text{O3}}}{2} + Q_{\text{O7}} . \tag{17}$$

Here N_{D3} counts the number of $D3$-branes, each of which is accompanied by its orientifold image[11]. N_{flux} denotes the possible contributions from $G_3 = F_3 + \tau H_3$

---

[11]In particular, if n_{D3} D3-branes lie inside an $O7$-plane they come together with their images and yield gauge group $Sp(2n_{D3})$.

form flux, which is in particular important for complex structure moduli stabilisation. The induced D3-charge on the O7-planes is given by

$$
\begin{aligned}
Q_{\mathrm{O7}} = \frac{\chi(D_{\mathrm{O7}})}{6} &= \frac{1}{6} \int_Y c_2(D_{\mathrm{O7}}) \wedge [D_{\mathrm{O7}}] \\
&= \frac{1}{6} \int_Y [D_{\mathrm{O7}}]^3 + c_2(T_Y) \wedge [D_{\mathrm{O7}}] \, .
\end{aligned}
\tag{18}
$$

If a stack of N_a D7-branes wraps a smooth divisor of type 1 or 3, as defined on page 11, their D3-charge reads

$$
Q_{\mathrm{D7}}^a = N_a \frac{\chi(D_a)}{24} + \frac{1}{8\pi^2} \int_{D_a} \operatorname{tr} \mathcal{F}_a^2
\tag{19}
$$

with

$$
\frac{1}{8\pi^2} \operatorname{tr} \mathcal{F}_a^2 = \frac{1}{2} \sum_{I,J} \operatorname{tr}[T_I \, T_J] \, c_1\!\left(L_a^{(I)}\right) c_1\!\left(L_a^{(J)}\right) .
\tag{20}
$$

More subtle is the case 2, since eq. (17) will be modified as discussed in [21, 23]. One replaces the Euler characteristic by

$$
Q_{\mathrm{D7}}^a = N_a \frac{\chi_o(D_a)}{24} + \frac{1}{8\pi^2} \int_{D_a} \operatorname{tr} \mathcal{F}_a^2 \, , \qquad \chi_o(D_a) = \chi(\Sigma_a) - n_{\mathrm{pp}},
\tag{21}
$$

where Σ_a is an auxiliary surface obtained by blowing up the singular points in D_a, while n_{pp} counts the number of pinch points in D_a.

The relation to the F-theory D3-brane tadpole condition becomes obvious if one slightly reorders the terms in eq. (17) and divides by two,

$$
N_{\mathrm{D3}} + \frac{N_{\mathrm{flux}}}{2} + N_{\mathrm{gauge}} = \frac{N_{\mathrm{O3}}}{4} + \frac{\chi(D_{\mathrm{O7}})}{12} + \sum_a N_a \frac{\chi_o(D_a)}{24}
\tag{22}
$$

with

$$
N_{\mathrm{gauge}} = -\sum_a \frac{1}{8\pi^2} \int_{D_a} \operatorname{tr} \mathcal{F}_a^2 = -\frac{1}{2} \sum_a N_a \int_{D_a} \sum_{I,J} \operatorname{tr}[T_I \, T_J] \, c_1\!\left(L_a^{(I)}\right) c_1\!\left(L_a^{(J)}\right) . \tag{23}
$$

The right-hand side of equation (22) is precisely $\chi(Y_4)/24$ in the F-theory lift of this Type IIB orientifold, where Y_4 denotes the Calabi-Yau fourfold. This implies that generically each topologically different arrangement of D7-branes cancelling the RR

18

eight-form tadpole constraints lifts to a different Calabi-Yau fourfold with different Euler characteristic. For the trivial solution with eight D7-branes placed right on top of the smooth orientifold plane with $n_{\rm pp} = 0$ the right hand side of (22) simplifies to $\frac{N_{\rm O3}}{4} + \frac{\chi(D_{\rm O7})}{4}$. It is a consistency check that this number is indeed an integer.

Let us emphasise that for the cancellation of anomalies only the D7 and D5-tadpole constraints are important. The D3-brane tadpole is in some sense only related to the non-chiral sector of the D-brane theory. This is related to the fact that a D3-brane can never carry any chiral modes, as it can in principle be moved to a position away from the D7-branes. The expectation is that a globally consistent Type IIB orientifold model with a supersymmetric D7- and D5-brane sector lifts up to F-theory on a compact Calabi-Yau fourfold. The cancellation of the D3-brane tadpole is an additional attribute both in Type IIB orientfolds and in F-theory models. Taking also into account that for moduli stabilisation and the realisation of inflation, the presence of (a small number of) anti-D3-branes is very welcome, in this paper we take all the D7- and D5-brane supersymmetry constraints very seriously but are a bit more relaxed about the existence of anti- D3-branes in the system. In fact, we will find that in our semi-realistic GUT examples the D3-brane tadpole can easily be saturated by already modest addition of gauge fluxes on the D7-branes.

Role of B_-moduli

Before proceeding we would like to comment on the role of the continuous B_--moduli appearing in $\mathcal{F}$ and thus in the D-brane charges. It is natural to wonder how to reconcile their contribution with the discrete nature of a quantity such as the D5- or D3-brane charge.

In fact the B_- moduli decouple from the tadpole equations by means of the $D7$-brane tadpole cancellation condition (13) and the simple observation that the B_- field restricts trivially to the O7-plane,

$$\int_{D_{O7}} \omega \wedge B_- = 0 , \qquad \forall \omega \in H^2_-(Y) . \tag{24}$$

Concretely, the B_--contribution to the D5-brane tadpole condition (16)

$$\sum_a N_a \int_Y \omega \wedge \left([D_a] \wedge B_- + [D'_a] \wedge B_- \right) = 8 \int_Y \omega \wedge [D_{O7}] \wedge B_- = 0 \tag{25}$$

indeed vanishes due to (13) and (24).

19

To isolate the B_--moduli in the D3-brane tadpole let us introduce the quantity

$$c_1(\widetilde{L}_a) = c_1(L_a) - B_- \tag{26}$$

and rewrite the induced D3-brane tadpole as

$$-\sum_a N_a \left[\int_{D_a} \left(c_1(\widetilde{L}_a) + B_- \right)^2 + \int_{D'_a} \left(c_1(\widetilde{L}'_a) + B_- \right)^2 \right] . \tag{27}$$

For simplicity we are sticking to gauge flux $\frac{1}{2\pi}\mathcal{F} = T_0 c_1(L_a)$. For the mixed term we find that

$$-\sum_a N_a \int_Y \left([D_a] \wedge c_1(\widetilde{L}_a) + [D'_a] \wedge c_1(\widetilde{L}'_a) \right) \wedge B_- = 0 , \tag{28}$$

where we have used the D5-brane tadpole cancellation condition (16). Finally, we evaluate

$$-\sum_a N_a \int_Y \left([D_a] \wedge B_-^2 + [D'_a] \wedge B_-^2 \right) = -8 \int_{D_{O7}} B_-^2 = 0 \tag{29}$$

so that as anticipated the continuous B_--moduli do not appear in the tadpole cancellation conditions.

K-Theory charge cancellation

Apart from cancellation of these homological charges, also all K-theoretic torsion charges have to sum up to zero. In general it is a very non-trivial task to compute all in particular torsional K-theory constraints. However, according to the probe brane argument of [59] cancellation of torsion charges is equivalent to absence of a global $SU(2)$ Witten anomaly on the worldvolume of every probe brane supporting symplectic Chan-Paton factors. In concrete compactifications this amounts to requiring an even number of fundamental representations in the sector between the physical D7-branes and each symplectic probe brane. Note that in a concrete model determining all symplectic four-cycles is also far from trivial.

2.3 The Massless Spectrum

For applications to phenomenology it is essential to understand the massless matter arising from open strings stretching between two stacks of D7-branes.

Non-chiral matter transforming in the adjoint representation emerges from strings with both endpoints on the same D-brane along D_a. It consists of the vector multiplet

together with $h^{1,0}(D_a)$ and $h^{2,0}(D_a)$ chiral multiplets describing the Wilson line and deformation moduli of the D7-branes. Matter in the bifundamental representation[12] $(\overline{N}_a, N_b)$ and (N_a, N_b) arises from open strings stretching between two different D7-branes in the (a, b) and (a', b) sector, respectively. Intersections between a brane and its image, that is, of type (a', a), yield matter in the (anti)symmetric representation. For example, if all branes are on top of a $O7^{(-)}$-plane, then all states in the (a', a) sector are anti-symmetrised. On an invariant brane with four Dirichlet-Neumann boundary conditions with an $O7^{(-)}$-plane, the (a', a) states are symmetrised. The chiral spectrum is summarised in Table 1, see also [60]. For the concrete computation

sector	$U(N_a)$	$U(N_b)$	chirality
(ab)	$\overline{\square}_{(-1)}$	$\square_{(1)}$	I_{ab}
$(a'b)$	$\square_{(1)}$	$\square_{(1)}$	$I_{a'b}$
$(a'a)$	$\boxminus_{(2)}$	1	$\frac{1}{2}(I_{a'a} + 2I_{\mathrm{O7a}})$
$(a'a)$	$\square\square_{(2)}$	1	$\frac{1}{2}(I_{a'a} - 2I_{\mathrm{O7a}})$

Table 1: *Chiral spectrum for intersecting D7-branes. The subscripts denote $U(1)$ charges.*

of the chiral index I_{ab} and to determine the vector-like spectrum we have to distinguish two situations according to the localisation of matter on sub-loci of different dimensions. For simplicity we again only discuss the case where all D7-branes carry holomorphic line bundles.

2.3.1 Matter Divisors

For two D7-branes wrapping the same divisor $D_a = D_b = D$ and carrying line bundles L_a and L_b, matter in the bifundamental representation $(\overline{N}_a, N_b)$ is counted by the extension groups [61]

$$\mathrm{Ext}^n(\iota_* L_a, \iota_* L_b), \qquad n = 0, \ldots 3, \tag{30}$$

---

[12]For the general overview we only consider diagonal embeddings and postpone a discussion of more general line bundles to the applications in Section 5.

where $i : D \to Y$ defines the embedding of D in the Calabi-Yau Y. The value $n = 1$ refers to anti-chiral multiplets transforming as $(\overline{N}_a, N_b)$, while $n = 2$ corresponds to chiral multiplets in the same representation. For consistency, the states counted by the groups corresponding to $n = 0$ and $n = 3$ have to absent. These states do not correspond to matter fields but rather gauge fields and have been named ghosts in [13]. We show in Subsection 2.4 that for supersymmetric configurations with the Kähler form inside the Kähler cone these ghosts are automatically absent. By running through the spectral sequence, one can show that the sheaf extension groups eq. (30) are given by appropriate cohomology groups for line bundles on the divisor D, concretely

$$
\begin{aligned}
\mathrm{Ext}^0(\iota_* L_a, \iota_* L_b) &= H^0(D, L_a \otimes L_b^\vee), \\
\mathrm{Ext}^1(\iota_* L_a, \iota_* L_b) &= H^1(D, L_a \otimes L_b^\vee) + H^0(D, L_a \otimes L_b^\vee \otimes N_D), \\
\mathrm{Ext}^2(\iota_* L_a, \iota_* L_b) &= H^2(D, L_a \otimes L_b^\vee) + H^1(D, L_a \otimes L_b^\vee \otimes N_D), \\
\mathrm{Ext}^3(\iota_* L_a, \iota_* L_b) &= \qquad\qquad H^2(D, L_a \otimes L_b^\vee \otimes N_D).
\end{aligned}
\tag{31}
$$

By Serre duality and $N_D = K_D$ we can relate $H^i(D, L_a \otimes L_b^\vee \otimes N_D) = H^{2-i}(D, L_a^\vee \otimes L_b)$. It straightforwardly follows that for the chiral index I_{ab} counting bifundamental matter transforming as $(\overline{N}_a, N_b)$ one obtains

$$
\begin{aligned}
I_{ab}^{bulk} &= \sum_{n=0}^{3} (-1)^n \dim \mathrm{Ext}^n(\iota_* L_a, \iota_* L_b) \\
&= \chi(D, L_a \otimes L_b^\vee) - \chi(D, L_a \otimes L_b^\vee \otimes N_D) \\
&= -\int_Y [D] \wedge [D] \wedge (c_1(L_a) - c_1(L_b)).
\end{aligned}
\tag{32}
$$

In these conventions $I_{ab} > 0$ if there is an excess of chiral states in the representation $(\overline{N}_a, N_b)$. Note that this expression only depends on the components of $c_1(L_i)$ which are non-trivial on the ambient Calabi-Yau manifold, cf. eq. (5).

We have the additional freedom to twist the line bundle L_a on D by a line bundle R_a with $\iota_* R_a = \mathcal{O}$. This does not change the chiral spectrum, though it can change the vector-like one and will in general contribute to the D3-tadpole.

2.3.2 Matter Curves

If the two D7-branes wrap different divisors D_a and D_b intersecting over a curve C of genus g and carrying line bundles L_a and L_b, the cohomology groups counting

matter in $(\overline{N}_a, N_b)$ are

$$H^i\left(C, L_a^\vee \otimes L_b \otimes K_C^{\frac{1}{2}}\right). \tag{33}$$

Here $i = 0$ and $i = 1$ refer to chiral and anti-chiral states in the representation $(\overline{N}_a, N_b)$, respectively[13]. The chiral index I_{ab} counting the excess of chiral over anti-chiral states transforming as $(\overline{N}_a, N_b)$ follows from the Riemann-Roch-Hirzebruch theorem as

$$I_{ab}^{loc.} = \chi(C, L_a^\vee \otimes L_b \otimes K_C^{\frac{1}{2}}) = -\int_Y [D_a] \wedge [D_b] \wedge (\, c_1(L_a) - c_1(L_b)\,)\,. \tag{34}$$

In terms of extension groups we therefore get

$$\mathrm{Ext}^i(\iota_* L_a, \iota_* L_b) = \begin{cases} 0 & i = 0 \\ H^1(C, L_a^\vee \otimes L_b \otimes K_C^{\frac{1}{2}}) & i = 1 \\ H^0(C, L_a^\vee \otimes L_b \otimes K_C^{\frac{1}{2}}) & i = 2 \\ 0 & i = 3. \end{cases} \tag{35}$$

Finally, the index I_{O7a} in Table 1 is

$$I_{O7a} = \int_Y [D_{O7}] \wedge [D_a] \wedge c_1(L_a), \tag{36}$$

reflecting the absence of a gauge bundle on top of the orientifold plane.

We leave it to the readers to convince themselves that, as in the context of the tadpole cancellation conditions, the B_--moduli also drop out automatically from all cohomology groups describing the massless spectrum.

2.4   F- and D-Term Supersymmetry Constraints

Let us discuss the constraints which need to be imposed in order for the brane configuration to be supersymmetric. In the four-dimensional effective action these constraints manifest themselves through the vanishing of F- and D-terms in the vacuum. In the following we will discuss both sets of constraints in turn.

We first turn to the supersymmetry constraints imposed by the vanishing of the D-terms. Recall that the D-term induced by a gauging of a field-independent

---

[13]Note the different assignment of chiral and anti-chiral multiplets with the extension groups of even and odd degree for bulk and localised matter. This can be derived, for example, by T-duality from the analogous phenomenon in D9-D5 systems [52,53].

symmetry with Killing vector X_a^L is of the form $D_a = \bar{X}_a^L \partial_{\bar{M}^L} K$, where K is the Kähler potential. Let us recall the induced gauging for the complex scalars T_I and G^i defined in (1). A gauging of T_I can be induced for a non-trivial line bundle on a D7-brane (D_a, L_a), while G^i can be gauged if there exists a D'_a which is not homologous to D_a, that is, if we are in the case 1 defined at the beginning of Subsection 2.1, page 11. The Killing vectors for these gaugings are of the form

$$X_{a\,I} = \int_{D_a} [\Gamma_+^I] \wedge c_1(\widetilde{L}_a) \, , \qquad X_a^i = \int_{D_a} [\gamma_-^i] \wedge B_- \, , \tag{37}$$

where Γ_+^I, γ_-^i are the two-cycles introduced in eq. (1) and thereafter to define T_I, G^i. Note that there is no continuous moduli dependence in $X_{a\,I}$ since we have explicitly split off the B_- field as in eq. (26). One next notes that [49, 62]

$$\partial_{T_I} K \sim r^I \, , \qquad \partial_{G^i} K \sim s_i, \tag{38}$$

where r^I, s_i arise in the expansions $J = r^I [\Gamma_I^+]$ and $J \wedge B_- = s_i[\gamma_-^i]$. It is important to note that the expression for $\partial_{T_I} K$ in eq. (38) is also valid away from the large volume limit. For example, one of the r^I can become small while $\partial_{G^i} K$ will receive additional corrections, for example, due to world-sheet instantons. We thus encounter a moduli dependent Fayet-Iliopoulos term for the configuration of the form [51, 55]

$$\xi_a \sim \int_{D_a} \iota^* J \wedge (c_1(\widetilde{L}_a) + B_-) = \int_{D_a} \iota^* J \wedge c_1(L_a) \, . \tag{39}$$

Note that ξ_a depends on the pullback of the Kähler form J of Y to the D7-brane and as a consequence of eq. (5) only on the components of $c_1(L_a)$ which are non-trivial on Y. Furthermore the B_--moduli, encoded in $c_1(L_a)$, do not drop out of the D-terms. For vanishing VEVs of the chiral fields charged under the $U(1)$ supported on the D7-branes, the D-term supersymmetry condition requires these FI-terms to vanish. This imposes conditions on the combined Kähler and B_- moduli space. As long as the Kähler moduli are chosen such that J is indeed invariant under the orientifold action, the Fayet-Iliopoulos term for (D_a, L_a) and (D'_a, L'_a) coincide. We will encounter that in a concrete example in Subsection 6.2.

For line bundles $L_a \neq \mathcal{O}$ satisfying the D-term constraint eq. (39), we will now derive two important consequences:

No ghosts

First, we realise that the FI-term is nothing else than the slope $\mu(L_a)$ of the line bundle L_a. Now to come back to the question of ghosts in the massless spectrum in

eq. (31), it is important to recall the general fact that

- For two vector bundles V_a, V_b of equal slope and rank, $\mu(V_a) = \mu(V_b)$ and $\mathrm{rk}(V_a) = \mathrm{rk}(V_b)$, the existence of a map $0 \to V_a \to V_b$ implies that $V_a = V_b$.

We thus conclude for the extension groups between two supersymmetric line bundles $L_a \neq L_b$ that $\mathrm{Ext}^0(\iota_* L_a, \iota_* L_b) = \mathrm{Ext}^3(\iota_* L_a, \iota_* L_b) = 0$. Indeed, if $H^0(D, L_a \otimes L_b^\vee)$ were non-vanishing, we could define a map $0 \to \mathcal{O} \to L_a \otimes L_b^\vee$ where both $\mathcal{O}$ and, by hypothesis, $L_a \otimes L_b^\vee$ have vanishing slope. Therefore, $L_a = L_b$ in contradiction to our assumption. The same reasoning for the dual bundle $L_a^\vee \otimes L_b$ shows that $\mathrm{Ext}^3(\iota_* L_a, \iota_* L_b) = 0$.

D3-tadpole contribution

Second we note that for line bundles with vanishing slope for a Kähler form inside the Kähler cone, the contribution of the gauge flux to the D3-brane tadpole always has the same sign

$$-\frac{N_a}{2} \int_{D_a} c_1^2(L_a) \geq 0. \tag{40}$$

Indeed, on a surface D_a the set of $c_1(L_a)$ with vanishing slope is given by $H_2(D_a) - \{M \cup -M\}$, where M denotes the Mori cone of D_a. However, the Mori cone contains all classes C with $C^2 > 0$ and $C \cdot K > 0$. Therefore, $c_1^2(L_a) \leq 0$. This result implies that for supersymmetric brane configurations the possible choices of line bundles are rather limited if we do not want to introduce anti–D3-branes in the system.

Finally, let us mention that the other supersymmetry conditions, namely the holomorphy of the divisor and the bundle, arise from a superpotential

$$W_{D7} = \int_{\mathcal{C}(L_a, L_a')} \Omega, \tag{41}$$

where $\mathcal{C}(L_a, L_a')$ is a chain ending on the two-cycle Poincaré dual to $c_1(L_a^+)$ on the divisor $D_a + D_a'$.

3   SU(5) GUTs and Their Breaking

After this discussion of the general model building rules for Type IIB orientifolds with O7- and O3- planes we can now become more specific about the realisation of

$SU(5)$ Georgi-Glashow GUTs. Parts of the logic are very similar to the implementation of GUT models in Type IIA intersecting D-branes [43, 11, 45] as described, for example, in [11, 28]. Let us first transfer these rules to our Type IIB setting. Then we move forward to describe how the mechanism of GUT symmetry breaking via $U(1)_Y$ flux, exploited by [16] in the local F-theory context, can also be realised in this perturbative orientifold limit.

3.1 Georgi-Glashow SU(5) GUT

The starting point is the construction of a $U(5) \times U(1)$ gauge theory from a stack of five D7-branes wrapping a four-cycle D_a and one additional brane wrapping D_b. These brane stacks carry holomorphic bundles L_a and L_b, respectively.

The orientifold action maps $(D_a, L_a) \rightarrow (D_{a'}, L'_a)$ (and similarly for (D_b, L_b)). As previously discussed, this includes the case that D_a is invariant under σ. First we diagonally embed two line bundles L_a and L_b by identifying their structure group with the diagonal $U(1)_a$ and $U(1)_b$, respectively. Each of the two Abelian factors $U(1)_a$ and $U(1)_b$ separately acquires a mass by the Stückelberg mechanism as long as D_a and D_b are non-trivial homology cycles [54].

A more group theoretic way of describing the gauge group and its matter content is to start with an $SO(12)$ gauge group. The embedding of two line bundles with structure groups $U(1)_{a,b}$ can break this to $U(5) \times U(1)$, where the generators of the two $U(1)$s are embedded into $SO(12)$ as

$$
\begin{aligned}
U(1)_a &\in \text{diag}\,(\,1_{5\times5}, 0\,|\,0, -1_{5\times5}\,)\,, \\
U(1)_b &\in \text{diag}\,(\,0_{5\times5}, 1\,|\,-1, 0_{5\times5}\,)\,.
\end{aligned}
\tag{42}
$$

The adjoint of $SO(12)$ decomposes into $SU(5) \times U(1)_a \times U(1)_b$ representations as

$$
\begin{aligned}
[66] &= [24]_{(0,0)} + [1]_{(0,0)} + [10]_{(2,0)} + [\overline{10}]_{(-2,0)} + [5]_{(1,-1)} + [\overline{5}]_{(-1,1)} \\
&\quad + [5]_{(1,1)} + [\overline{5}]_{(-1,-1)}.
\end{aligned}
\tag{43}
$$

To ensure absence of a massless combination of $U(1)$ factors we require that $[D_a]$ and $[D_b]$ be linearly independent in $H_4(Y, \mathbb{Z})$. Note that in the presence of further tadpole cancelling D7-branes it has to be ensured that the full mass matrix is of maximal rank.

The MSSM spectrum

The massless states transforming in the adjoint representation are given by the deformations of the four-cycles, which are counted by $H^1(D, \mathcal{O})$ (Wilson lines) and $H^2(D, \mathcal{O})$ (transversal deformations). In principle we could allow for precisely one such adjoint of $SU(5)$, which might break the $SU(5)$ symmetry to the Standard model by the Higgs mechanism. An example of such a surface with $h^{(2,0)} = 1$ is $K3$. However, a complete GUT model relying on this mechanism would have to address the generation of a suitable potential for the GUT Higgs field from string dynamics such that $SU(5)$ is broken dynamically to the Standard Model. Since we will rather be breaking the GUT symmetry by embedding $U(1)_Y$ flux, we insist that the $SU(5)$ stack wraps a rigid four-cycle. This is satisfied for del Pezzo surfaces, which have $h^{1,0}(D) = h^{2,0}(D) = 0$. In view of the rules of Table 1 the charged GUT spectrum requires the chiral intersection pattern listed in Table 2.

state	number	sector	$U(5)$	$U(1)$
10	3	$(a'a)$	$\boxminus_{(2)}$	1
$\overline{\mathbf{5}}$	3	(ab')	$\overline{\square}_{(-1)}$	$\overline{\square}_{(-1)}$
$\mathbf{1}_N$	3	$(b'b)$	1	$\square\square_{(2)}$
$\mathbf{5}_H + \overline{\mathbf{5}}_H$	$1 + 1$	(ab)	$\overline{\square}_{(-1)}$	$\square_{(1)}$

Table 2: *Chiral spectrum for intersecting D7-brane model. The indices denote the $U(1)$ charges. The last line gives the Higgs particles.*

The first two lines contain the antisymmetric representation **10** of $SU(5)$ and the fundamental $\overline{\mathbf{5}}$. The states from the $b'b$ sector are necessary to satisfy the "formal" $U(N_b)$ anomaly ($3 \times (4 + 1) - 3 \times 5 = 0$) and carry the charges of right-handed neutrinos. States from the $(a'b)$ carry the right quantum numbers to be identified with the pair of Higgs fields $\mathbf{5_H} + \overline{\mathbf{5}}_\mathbf{H}$. However, one can also realise the Higgs fields from intersections (ac) between the $SU(5)$ brane stack and a third one. In contrast to $SO(10)$ GUTs, here all massless fields are perturbatively realised by open string stretched between stacks of D7-branes.

The various fields are localised on the intersection of the various divisors. As mentioned already in Subsection 2.1, these are either curves or divisors. In the latter

case one has to compute cohomology classes over a del Pezzo surface, which in general gives also vector-like matter. On the contrary, if two divisors intersect over a curve vector-like states are much easier to suppress. We will exemplify this feature in the concrete examples to be discussed later.

Yukawa couplings

The Yukawa couplings which give masses to the MSSM fields after GUT and electroweak symmetry breaking are

$$\mathbf{10}^{(2,0)}\,\mathbf{10}^{(2,0)}\,\mathbf{5_H}^{(1,-1)}, \qquad \mathbf{10}^{(2,0)}\,\overline{\mathbf{5}}^{(-1,-1)}\,\overline{\mathbf{5}}_{\mathbf{H}}^{(-1,1)} \qquad \mathbf{1}_N^{(0,2)}\,\overline{\mathbf{5}}^{(-1,-1)}\,\mathbf{5_H}^{(1,-1)}\ , \quad (44)$$

where the upper indices denote the Abelian $U(1)_a \times U(1)_b$ charges. If as indicated we realise the matter and Higgs fields as in Table 2, the last two Yukawa couplings, i.e. the ones generating masses for the d-quarks and leptons, are allowed already at the perturbative level. For them to be present the wave functions of the massless modes have to overlap. If all states are localised on curves, this means that the three divisors have to meet at a point. On a Calabi-Yau threefold, this is generically the case. Note that to first order the wavefunctions of the fields localise strictly along the matter curves and these perturbative Yukawa couplings are of rank one. Only higher order corrections to the wavefunction profile are responsible for a non-trivial family structure. If on the other hand the $\mathbf{10}$ and the $\mathbf{1_N}$ arise from the bulk of the GUT brane and the $U(1)_b$ brane while the $\overline{\mathbf{5}}$ and the Higgs are localised on curves, the perturbative Yukawa couplings involve the triple-product of the restriction of corresponding powers of L_a and L_b to the matter curve.

By contrast, it is obvious from their $U(1)$ charges in eq. (44) that the u-quark Yukawa couplings $\mathbf{10\,10\,5_H}$ are perturbatively forbidden. For quite some time this was considered the main obstacle to the construction of open string SU(5) GUT models. This no-go was bypassed in [28] where it was pointed out that an isolated, rigid Euclidean D3-brane instanton wrapping a four-cycle D_{inst} of $O(1)$ type (that is, in particular invariant under orientifold action) can generate these missing Yukawa couplings. This requires extra fermionic charged matter zero modes localised at the intersection of the instanton with the two stacks of D7-branes. Concretely, a necessary condition is that the chiral intersection numbers are

$$I_{a,\text{inst}} = 1, \qquad I_{b,\text{inst}} = -1 \ . \tag{45}$$

The resulting six chiral zero modes λ_a^i, λ_b, $i = 1, \ldots 5$, can then be absorbed by the

disc diagrams

$$\mathbf{10}^{(2,0)} \, \lambda_a^i \lambda_a^j, \qquad \mathbf{10}^{(2,0)} \, \lambda_a^k \lambda_a^l, \qquad \mathbf{5}_H^{(1,-1)} \, \lambda_a^m \lambda_b \, . \tag{46}$$

As detailed [28] this results in non-perturbative couplings proportional to

$$Y^\alpha \, Y^\beta \, \epsilon_{ijklm} \, \mathbf{10}_\alpha^{ij} \, \mathbf{10}_\beta^{kl} \, \mathbf{5}_H^m \tag{47}$$

with $i, j, \ldots$ denoting $SU(5)$ group indices and α, β labelling families. Note that the coupling eq. (47) is of unit rank in family space so that a single instanton gives rise to masses only for one particular generation of u-quarks. This is a consequence of the fact that the multiplicities of the λ^i-modes are only due to their $SU(5)$ Chan-Paton factors. As stated above, this is a similar situation to the one for the perturbative couplings, which to first order are also of rank one. For non-perturbative couplings of the form (47) the resolution has to involve several distinct instantons whose combined effect may be to give rise to higher rank couplings.

Of course the amplitude is suppressed by the instanton action

$$\exp\left(-\frac{1}{2g_s} \int_{D_{\text{inst}}} J \wedge J \right). \tag{48}$$

As such the scale of the coupling is independent of the GUT coupling, which is controlled by the cycle volume of the GUT brane. The instanton cycle entering the above suppression, however, is a priori unrelated to the GUT cycle. Still in the perturbative regime $g_s \ll 1$ there is the danger that the coupling tends to be too small. In our approach we will eventually take the small T_{inst} limit of the orientifold model and, besides imposing the tadpole constraints, will require that at least for the third family this Yukawa coupling is generated by a Euclidean D3-brane instanton. Of course we have to ensure that when $T_{\text{inst}} \to 0$ not the whole manifold degenerates. In principle the large hierarchy in the u-quark masses between the third and the first two families can be engineered by different instantons with suitable suppression.

Very similarly, if the Higgs fields originate from the intersection of the $SU(5)$ branes with a third stack then the bottom Yukawa couplings carry $U(1)^3$ charges

$$\mathbf{10}^{(2,0,0)} \, \overline{\mathbf{5}}^{(-1,-1,0)} \, \overline{\mathbf{5}}_{\mathbf{H}}^{(-1,0,1)} \tag{49}$$

and are therefore not gauge invariant any more. In this case, also these couplings can only be generated non-perturbatively by an appropriate D3-brane instanton, which intersects the $U(1)$ stacks b and c just once.

Dim=4 proton decay

In GUT theories there is the danger of generating dimension-four operators violating baryon or lepton number

$$U\,D\,D,\quad Q\,D\,L,\quad L\,L\,E\,. \tag{50}$$

Clearly if present they generate unacceptably fast proton decay. In Georgi-Glashow $SU(5)$ all these operators descend from the

$$\mathbf{10}^{(2,0)}\,\overline{\mathbf{5}}^{(-1,-1)}\,\overline{\mathbf{5}}^{(-1,-1)}\,, \tag{51}$$

coupling, which is perturbatively forbidden due to $U(1)_b$ violation. However, as just described, even perturbatively absent couplings can be generated non-perturbatively by D3-brane instantons. In certain domains of the Kaähler moduli space such instanton-induced dimension-four operators would be dangerous. For an instanton to generate such a coupling three situations are in principle conceivable in view of the $U(1)_a$ and $U(1)_b$ charges: it either carries the six charged matter zero modes $\lambda_a^i, \overline{\lambda}_a^j, \overline{\lambda}_b^k$ with $i, j, k = 1, 2$ or alternatively the four zero modes $\lambda_a, \overline{\lambda}_a, \overline{\lambda}_b^k$ with $k = 1, 2$. The third possibility is that it carries just the two zero modes $\overline{\lambda}_b^k$ with $k = 1, 2$. On the other hand, charged matter zero modes from intersections of the instanton with the $SU(5)$ stack always appear in multiples of five. We thus conclude that in absence of any known mechanism to absorb the extra zero modes without pulling down more charged matter fields, in the two first cases no such dangerous dimension-four operators are generated. However, the third option is not a priori excluded. Of course, if such an instanton exists the coupling is exponentially suppressed, but we just learnt in the context of the $\mathbf{10\,10\,5_H}$ Yukawa coupling that this need not be the case in the $T_{\text{inst}} \to 0$ limit. Therefore, to be on the safe side we require that such an instanton does not exist.

Neutrino masses

We have already seen that the Yukawa coupling $\mathbf{1_N}^{(0,2)}\,\overline{\mathbf{5}}^{(-1,-1)}\,\mathbf{5_H}^{(1,-1)}$ generates Dirac type masses for the neutrinos. In order to realise for instance the see-saw mechanism one also needs Majorana type masses of the order $10^{12} - 10^{15}\text{GeV}$. These can be either generated by higher dimensional couplings involving some additional $SU(5)$ singlet fields or by D3-brane instantons [25, 26, 63, 64]. Higher dimensional couplings are of course suppressed by the string scale, so that one needs to explain the high scale of these terms.

30

For directly generating a mass term

$$S_{\text{mass}} = M_N \, \mathbf{1}_N^{(0,2)} \, \mathbf{1}_N^{(0,2)} \tag{52}$$

via an instanton, it has to carry the four charged matter zero modes λ_b^i, $i = 1, \ldots, 4$. In this case the Majorana mass scale is $M_s \exp(-S_{inst})$ which, that is, depending on the size of the four-cycle, can still give a suppression by a few orders of magnitude.

3.2   Breaking SU(5) to SU(3) × SU(2) × U(1)

Let us describe how one can break the $SU(5)$ GUT via a line bundle L_Y whose structure group is embedded into $U(1)_Y$. This method was used in the context of local F-theory GUT models in [16]. Here we will discuss its implementation within the perturbative orientifold and find important quantisation constraints on the bundle L_Y. Clearly these have to be taken into account in a string theoretically consistent framework.

Suppose we have designed the model such that the $SU(5)$ gauge symmetry is supported on a D7-brane wrapping a rigid divisor, which is a del Pezzo surface $\mathrm{dP}_r \subset Y$ containing $r + 1$ homological 2-cycles. Therefore, even though we cannot turn on (discrete) Wilson lines (as $\pi^1(D)$ is vanishing), we have the chance to break the $SU(5)$ gauge symmetry to the Standard Model by turning on non-vanishing flux in $U(1)_Y$. This Abelian flux F_Y is embedded into the fundamental representation of $SU(5)$ as $F_Y \, T_Y \subset SU(5)$ with

$$T_Y = \begin{pmatrix} -2 & & & & \\ & -2 & & & \\ & & -2 & & \\ & & & 3 & \\ & & & & 3 \end{pmatrix}. \tag{53}$$

Such gauge flux through a non-trivial 2-cycle in Y would lead, via the Green-Schwarz mechanism, to a mass term by mixing with an axion. However for flux supported on a two-cycle of the dP_r trivial in Y, there is no axion to pair with and the $U(1)_Y$ remains massless after gauge symmetry breaking [30, 16]. As discussed in Subsection 2.1, this means that for $U(1)_Y$ to remain massless we have to choose $U(1)_Y$ such that its first Chern class $c_1(L_Y) \in H^2(D_a, \mathbb{Q})$ is trivial on the ambient Calabi-Yau space Y, that is, the element $d_Y \in H_2(D_a, \mathbb{Q})$ specifying $L_Y = \mathcal{O}_{D_a}(d_Y)$ must lie in the kernel of the pushforward $\iota_* H_2(D_a) \to H_2(Y)$. From the relations eq. (5) it is immediately

clear that this flux does not change the chiral spectrum, the D7- and D5-tadpole constraints and the Fayet-Iliopoulos terms.

Cancellation of the Freed-Witten anomaly again constrains the quantisation of the bundles L_a and L_Y. In view of the diagonal embedding of L_a into $U(5)$ condition eq. (9) becomes

$$T_0\left(c_1(L_a) - \iota^*B\right) + T_Y\, c_1(L_Y) + \frac{1}{2}\, T_0\, c_1(K_{D_a}) \in H^2(D_a, \mathbb{Z})_{5\times 5} \qquad (54)$$

with $T_0 = 1_{5\times 5}$. This equation has two important consequences: First, $c_1(L_a) - \iota^*B$ and $c_1(L_Y)$ can take fractional values. For example, for a Spin divisor the choice $c_1(L_a) - \iota^*B = \frac{2}{5}$, $c_1(L_Y) = \frac{1}{5}$ would be consistent. Second, the two independent conditions encoded in the matrix valued equation (54) cannot be satisfied simultaneously for non-spin divisors without turning on non-trivial flux F_a as well[14].

The breaking of $SU(5)$ by means of L_Y flux induces the standard splitting of the GUT multiplets into MSSM representations,

$$
\begin{aligned}
\mathbf{24} &\to (\mathbf{8},\mathbf{1})_{0_Y} + (\mathbf{1},\mathbf{3})_{0_Y} + (\mathbf{1},\mathbf{1})_{0_Y} + (\mathbf{3},\mathbf{2})_{5_Y} + (\overline{\mathbf{3}},\mathbf{2})_{-5_Y}, \\
\overline{\mathbf{5}} &\to (\overline{\mathbf{3}},\mathbf{1})_{2_Y} + (\mathbf{1},\mathbf{2})_{-3_Y}, \\
\mathbf{10} &\to (\mathbf{3},\mathbf{2})_{1_Y} + (\overline{\mathbf{3}},\mathbf{1})_{-4_Y} + (\mathbf{1},\mathbf{1})_{6_Y}, \\
\mathbf{5}_H &\to (\mathbf{3},\mathbf{1})_{-2_Y} + (\mathbf{1},\mathbf{2})_{3_Y}, \quad \overline{\mathbf{5}}_H \to (\overline{\mathbf{3}},\mathbf{1})_{2_Y} + (\mathbf{1},\mathbf{2})_{-3_Y}.
\end{aligned}
\qquad (55)
$$

As is familiar from the analogous embedding of U(1) bundles in heterotic compactifications [32] the number of massless states after GUT symmetry breaking is computed by dressing the bundles appearing in the cohomology groups by a factor of L_Y^q. Here q denotes the hypercharge of the MSSM fields.

From the decomposition of the adjoint of $SU(5)$ one deduces that $H^*(D_a, L_Y^{\pm 5})$ gives rise to extra massless states. Clearly, these vector-like exotics are phenomenologically unappealing, so we require that these cohomology groups vanish. This is a very strong requirement and for fifth powers of *integer quantised* line-bundles on dP_r impossible to satisfy.

However, as discussed above, $c_1(L_Y)$ can really take values in $\mathbb{Z}/5$. To illustrate this further one can modify the embedding as follows. Instead of embedding the line bundle L_a entirely into the diagonal $U(1)_a$ of $U(5)$ as in eq. (42), one defines

---

[14]Note that this conclusion holds also in the context of F-theory compactifications. In a globally consistent setup, non-trivial L_Y cannot be switched on at will, but only in combination with non-trivial and suitably quantised 4-form flux that takes the role of L_a.

two line bundles $\mathcal{L}_a$ and $\mathcal{L}_Y$ and identifies their field strengths with the following combinations of generators T_a and T_Y of the diagonal $U(1)_a$ and hypercharge $U(1)_Y$,

$$\mathcal{L}_a \leftrightarrow T_a, \tag{56}$$

$$\mathcal{L}_Y \leftrightarrow \frac{2}{5}T_a + \frac{1}{5}T_Y.$$

The analogue of condition eq. (54),

$$c_1(\mathcal{L}_a) - \iota^*B + \frac{1}{2}K_{D_a} \in \mathbb{Z}, \tag{57}$$

$$c_1(\mathcal{L}_a) + c_1(\mathcal{L}_Y) - \iota^*B + \frac{1}{2}K_{D_a} \in \mathbb{Z},$$

leads to $c_1(\mathcal{L}_Y) \in \mathbb{Z}$ and in general half-integer quantised $\mathcal{L}_a$ bundles. This agrees with the fact that all cohomology groups involve integer powers of $\mathcal{L}_a$ and $\mathcal{L}_Y$. It is important to realise that the gauge flux $U(1)_Y$, though being trivial in the cohomology on Y nevertheless does contribute to the D3-tadpole condition. The contribution of the fluxes L_a and L_Y reads

$$N_{\text{gauge}} = -\frac{5}{2}\int_{D_a} c_1^2(L_a) - 15\int_{D_a} c_1^2(L_Y), \tag{58}$$

where we have taken into account $\text{tr}(T_Y^2) = 30$. Redefining as above $L_a = \mathcal{L}_a \otimes \mathcal{L}_Y^{\frac{2}{5}}$ and $L_Y = \mathcal{L}_Y^{\frac{1}{5}}$ yields

$$N_{\text{gauge}} = -\frac{5}{2}\int_{D_a} c_1^2(\mathcal{L}_a) - \int_{D_a} c_1^2(\mathcal{L}_Y) - 2\int_{D_a} c_1(\mathcal{L}_a)\, c_1(\mathcal{L}_Y). \tag{59}$$

$\mathcal{L}_Y$ being trivial on the Calabi-Yau, the mixed term $\int c_1(\mathcal{L}_a)\, c_1(\mathcal{L}_Y)$ may be non-vanishing only if also $\mathcal{L}_a$ has components trivial on Y.

Let us discuss the effect of $\mathcal{L}_Y$ in more detail:

Massless $U(1)_Y$

Since we have now embedded the line bundle $\mathcal{L}_Y$ into a combination of T_0 and T_Y, one might be worried that due to the Green-Schwarz mechanism it is not directly $U(1)_Y$ which remains massless. To find the massive Abelian gauge symmetry, we have to evaluate the relevant axion coupling

$$\int_{\mathbb{R}_{1,3}\times Y} C_4 \wedge \text{Tr}(F_{\text{GUT}}^2), \tag{60}$$

33

where F_{GUT} is the total $U(5)$ field strength supported on the GUT brane stack. Splitting this into the four-dimensional parts F^{4D} and the internal background values given by the first Chern classes, we can write

$$F_{\mathrm{GUT}} = T_0 \left(F_0^{4D} + c_1(\mathcal{L}_a) - \iota^* B + \frac{1}{2} c_1(K_{D_a}) + \frac{2}{5} c_1(\mathcal{L}_Y) \right) + T_Y \left(F_Y^{4D} + \frac{1}{5} c_1(\mathcal{L}_Y) \right) . \quad (61)$$

Inserting this into (60) and extracting the relevant term with two legs of $\mathrm{Tr}(F_{\mathrm{GUT}}^2)$ in the four-dimensional Minkowski space and two legs on the GUT $D7$-brane, one immediately realises that it is still the diagonal F_0^{4D} which mixes with the axions.

Exotics

As already described the decomposition of the adjoint of $SU(5)$ yields massless states counted by the cohomology groups $H^*(D_a, \mathcal{L}_Y)$. For phenomenological reasons we require that these cohomology groups vanish. This gives already a very strong constraint on the possible line bundles.

MSSM matter fields

Using the bundles $\mathcal{L}_a$ and $\mathcal{L}_Y$, we now express the relevant cohomology groups counting the number quarks and lepton fields. As mentioned these modes localise either on surfaces or on curves. To treat both cases simultaneously we express the number of modes in terms of sheaf extension groups. It is understood that for the actual computation one uses the formulae collected in Subsection 2.3.

The anti-fundamental matter representation of $SU(5)$ splits as

$$\begin{aligned}
(\bar{\mathbf{3}}, \mathbf{1})_{2_Y} &\quad : \quad \mathrm{Ext}^*(\mathcal{L}_a, \mathcal{L}_b^{-1}), \\
(\mathbf{1}, \mathbf{2})_{-3_Y} &\quad : \quad \mathrm{Ext}^*(\mathcal{L}_a \otimes \mathcal{L}_Y, \mathcal{L}_b^{-1})
\end{aligned} \quad (62)$$

with $\mathcal{L}_b = L_b$. Similarly, for the anti-symmetric representation, we have to compute the three cohomology classes

$$\begin{aligned}
(\mathbf{3}, \mathbf{2})_{1_Y} &\quad : \quad \mathrm{Ext}^*(\mathcal{L}_a^{-1} \otimes \mathcal{L}_Y^{-1}, \mathcal{L}_a), \\
(\bar{\mathbf{3}}, \mathbf{1})_{-4_Y} &\quad : \quad \mathrm{Ext}^*(\mathcal{L}_a^{-1}, \mathcal{L}_a), \\
(\mathbf{1}, \mathbf{1})_{6_Y} &\quad : \quad \mathrm{Ext}^*(\mathcal{L}_a^{-1} \otimes \mathcal{L}_Y^{-2}, \mathcal{L}_a).
\end{aligned} \quad (63)$$

Since $\mathcal{L}_Y$ is trivial in Y it is guaranteed that the chiral index of these representations does not change. However, in general the vector-like matter will change and will

34

be different for MSSM states descending from the same GUT multiplet. This is avoidable if all matter is localised on curves (and not on surfaces) such that the restriction of $\mathcal{L}_Y$ to this matter curve vanishes.

Higgs field and 3-2 splitting

The fundamental representation for the Higgs field of $SU(5)$ splits as

$$
\begin{aligned}
(\mathbf{3}, \mathbf{1})_{-2_Y} \quad &: \quad \mathrm{Ext}^*(\mathcal{L}_a^{-1}, \mathcal{L}_b^{-1}), \\
(\mathbf{1}, \mathbf{2})_{3_Y} \quad &: \quad \mathrm{Ext}^*(\mathcal{L}_a^{-1} \otimes \mathcal{L}_Y^{-1}, \mathcal{L}_b^{-1}).
\end{aligned}
\tag{64}
$$

Note that all these states are vector-like. We need that the $SU(2)$ doublets remain massless and that the $SU(3)$ triplets get a mass of the GUT scale. This translates into requiring that $\mathrm{Ext}^*(\mathcal{L}_a^{-1}, \mathcal{L}_b^{-1}) = (0, 0, 0, 0)$ and $\mathrm{Ext}^*(\mathcal{L}_a^{-1} \otimes \mathcal{L}_Y^{-1}, \mathcal{L}_b^{-1}) = (0, 1, 1, 0)$. For the Higgs fields localised on the intersection curve C_{ab} of the $U(5)$ divisor D_a and the $U(1)$ divisor D_b, two possibilities can occur.

The first option is that the intersection locus is a *single* elliptic curve, that is, $C_{ab} = T^2$. In this case the restriction of the line bundles to C_{ab} have to be of degree zero so that indeed no chiral matter is localised on C_{ab}. Recall that a degree zero line bundle on the elliptic curve C_{ab} can be written as $\mathcal{O}(p - q)$, where p, q denote points different from the origin 0 of the elliptic curve. The trivial bundle $\mathcal{O}$ corresponds to $p - q = 0$ and has cohomology $H^*(C_{ab}, \mathcal{O}) = (1, 1)$. If $p - q \neq 0$ the line bundle has a non-trivial Wilson line and the cohomology groups vanish. It is therefore clear that for an appropriate choice of the line bundles appearing in eq. (64) it can be arranged that only the doublet remains massless while the triplets acquire string scale masses. According to what we just said this happens provided the restriction of the line bundles appearing in eq. (64) to the genus one matter curve C_{ab} take the form

$$
\begin{aligned}
\mathcal{L}_a^{-1} \otimes \mathcal{L}_b|_{C_{ab}} &= \mathcal{O}(p - q), \quad p - q \neq 0, \\
\mathcal{L}_a^{-1} \otimes \mathcal{L}_Y^{-1} \otimes \mathcal{L}_b|_{C_{ab}} &= \mathcal{O}.
\end{aligned}
\tag{65}
$$

To see how to arrange for this, suppose one has found a model where the line bundles $\mathcal{L}_a$ and $\mathcal{L}_b$ can both be written as the pullback of line bundles from the Calabi-Yau,

$$
\mathcal{L}_a = \iota_a^* \mathbb{L}_a, \qquad \mathcal{L}_b = \iota_b^* \mathbb{L}_b.
\tag{66}
$$

Since $\mathcal{L}_a^{-1} \otimes \mathcal{L}_b|_{C_{ab}}$ is of degree zero in this case $\mathcal{L}_a^{-1} \otimes \mathcal{L}_b|_{C_{ab}} = \mathcal{O}$ with trivial Wilson lines. The relations eq. (65) can now simply be met by twisting $\mathcal{L}_a$ by a line bundle

R_a on D_a which is trivial on the ambient manifold and satisfies

$$R_a = \mathcal{L}_Y^{-1}. \tag{67}$$

As with everything desirable in life this surgery is not for free, as the new contribution of the GUT brane to the D3-brane tadpole is increased from eq. (59) to[15]

$$N_{\text{gauge}}^a = -\frac{5}{2} \int_{D_a} c_1^2(\mathcal{L}_a) - \frac{3}{2} \int_{D_a} c_1^2(\mathcal{L}_Y). \tag{68}$$

We will however also encounter cases[16] in which eq. (66) is not the situation to begin with. In particular it may be inconsistent to define the final GUT bundle as $\iota_a^* \mathbb{L}_a \otimes \mathcal{L}_Y^{-1}$ because this bundle might exhibit ghosts in its spectrum. For the line bundle appearing in (64), in this case we have, supposing for definiteness that $\mathcal{L}_b = \iota_b^* \mathbb{L}_b$,

$$\mathcal{L}_a^{-1} \otimes \mathcal{L}_Y^{-1} \otimes \mathcal{L}_b|_{C_{ab}} = \mathcal{O}(p_1 - q_1). \tag{69}$$

We then need to twist $\mathcal{L}_b$ by a line bundle R_b trivial on the ambient space, and every such bundle satisfies $R_b|_{C_{ab}} = \mathcal{O}(p_2 - q_2)|_{C_{ab}}$. To ensure $p_1 + p_2 - (q_1 + q_2) = 0$, as desired, might require adjusting some of the complex structure moduli of the manifold.

On the other hand, it was argued in [16] that in case H_u and H_d are localised on a single curve, dimension five proton decay operators $Q\,Q\,Q\,L$ can be generated by exchanging Kaluza-Klein modes of the Higgs-triplet. To avoid such operators, it was suggested that the intersection locus $D_a \cap D_b$ consists of two components $C_1 \cup C_2$, such that the $\mathbf{5}_H$ originates from $H^*(C_1, \mathcal{L}_a^{-1} \otimes \mathcal{L}_b \otimes \sqrt{K_{C_1}}) = (1,0)$ and $\overline{\mathbf{5}}_H$ from $H^*(C_2, \mathcal{L}_a^{-1} \otimes \mathcal{L}_b \otimes \sqrt{K_{C_1}}) = (0,1)$. This is the second option we have for the localisation of the Higgs field.

The top Yukawa couplings

We have seen that in the $SU(5)$ GUT model the top quark Yukawa coupling $\mathbf{10}\,\mathbf{10}\,\mathbf{5_H}$ can be generated by a single rigid $O(1)$ instanton with the right charged matter zero mode structure. We need to check whether this is compatible with the breaking of the $SU(5)$ GUT group by the $U(1)_Y$ flux.

---

[15]Here we are using that $\mathcal{L}_a = \iota_a^* \mathbb{L}_a$ prior to twisting by R_a so that the cross-term in eq. (59) vanishes.

[16]This discussion is only relevant for the models proposed in Section 5 and Subsection 6.1.

Recall that the five zero modes λ_a^i transform in the $\overline{\mathbf{5}}$ representation of the $SU(5)$ and the single zero mode λ_b in the singlet representation of $SU(5)$ with $U(1)_b$ charge $q_b = +1$. The $U(1)_Y$ flux splits the $\overline{\mathbf{5}}$ representation according to (55), that is, the $(\overline{\mathbf{3}}, \mathbf{1})_{2_Y}$ zero modes are counted by $\text{Ext}^*(\mathcal{L}_a, \mathcal{O})$ and the $(\overline{\mathbf{1}}, \mathbf{2})_{-3_Y}$ modes by $\text{Ext}^*(\mathcal{L}_a \otimes \mathcal{L}_Y, \mathcal{O})$. As long as the $SU(5)$ stack of branes and the instanton brane intersect over a 2-cycle non-trivial in the Calabi-Yau manifold, the restriction of $\mathcal{L}_Y$ to the intersection locus vanishes and we get precisely three instanton zero modes λ_a^i transforming in the $(\overline{\mathbf{3}}, \mathbf{1})_{2_Y}$ representation and two zero modes $\tilde{\lambda}_a^j$ transforming in the $(\overline{\mathbf{1}}, \mathbf{2})_{-3_Y}$ representation. Since $\mathcal{L}_Y$ is supported on the $SU(5)$ stack, the single zero mode λ_b also still exists. Then the Standard Model top-Yukawa couplings $(\mathbf{3}, \mathbf{2})\,(\overline{\mathbf{3}}, \mathbf{1})\,(\mathbf{1}, \mathbf{2})_H$ are generated by the instanton via the following absorption of the six charged instanton zero modes

$$
\begin{array}{c|c}
(\mathbf{3}, \mathbf{2})_{1_Y} & (\overline{\mathbf{3}}, \mathbf{1})_{2_Y}^{\lambda_a} \; (\mathbf{1}, \mathbf{2})_{-3_Y}^{\tilde{\lambda}_a} \\
(\overline{\mathbf{3}}, \mathbf{1})_{-4_Y} & (\overline{\mathbf{3}}, \mathbf{1})_{2_Y}^{\lambda_a} \; (\overline{\mathbf{3}}, \mathbf{1})_{2_Y}^{\lambda_a} \\
(\mathbf{1}, \mathbf{2})_{3_Y} & (\mathbf{1}, \mathbf{2})_{-3_Y}^{\tilde{\lambda}_a} \; (\mathbf{1}, \mathbf{1})_{0_Y}^{\lambda_b} \; .
\end{array}
\tag{70}
$$

The μ-term

The supersymmetric μ term clearly vanishes at tree-level. For having it directly generated non-perturbatively, the rigid $O(1)$ instanton must carry the four charged matter zero modes $\lambda_a, \overline{\lambda}_a$ and $\lambda_b, \overline{\lambda}_b$. However, due to the $SU(2)$ Chan-Paton factor the λ always come in multiples of two, so that these simple non-perturbative μ-terms are absent. However, they can be generated by higher dimensional operators involving $SU(5)$ gauge singlets, which have to receive some non-vanishing vacuum expectation value.

3.3   Summary of GUT Model Building Constraints

In this section we have collected a number of perturbative and non-perturbative stringy mechanisms to first realise Georgi-Glashow $SU(5)$ GUTs and second to solve some of their inherent problems. The perfect string model, besides being globally consistent would of course satisfy all these constraints. Eventually, one also has to address the issue of moduli stabilisation by fluxes and instantons, some aspects of which we discuss in Section 8. A more thorough and complete analysis is beyond the main scope of this paper but truly on the agenda.

Let us summarise in Table 3 the main properties a realistic string GUT model should have

property	mechanism	status
globally consistent	tadpoles + K-theory	✓
D-term susy	vanishing FI-terms inside Kähler cone	✓
gauge group $SU(5)$	$U(5) \times U(1)$ stacks	✓
3 chiral generations	choice of line bundles $\mathcal{L}_{a,b}$	✓
no vector-like matter	localisation on curves	✓
1 vector-like of Higgs	choice of line bundles	✓
no adjoints	rigid 4-cycles ← del Pezzo	✓
GUT breaking	$U(1)_Y$ flux $\mathcal{L}_Y$ on trivial 2-cycles	✓
3-2 splitting	Wilson lines on $g = 1$ curve	✓
3-2 split + no dim=5 p^+-decay	local. of H_u, H_d on disjoint comp.	✓
$\mathbf{10}\,\overline{\mathbf{5}}\,\overline{\mathbf{5}}_H$ Yukawa	perturb. or D3-instanton	✓
$\mathbf{10}\,\mathbf{10}\,\mathbf{5}_H$ Yukawa	presence of appropriate D3-instanton	✓
Majorana neutrino masses	presence of appropriate D3-instanton	✓

Table 3: *Summary of $SU(5)$ properties and their realisations by different Type IIB orientifold mechanisms. The mark ✓ in the last column indicates that all features can in principle be realised.*

4   Del Pezzo Transitions on $\mathbb{P}_{1,1,1,6,9}[18]$

In this section we discuss a first class of Calabi-Yau orientifold backgrounds which will later support our GUT models. The underlying geometries are compact Calabi-Yau manifolds M_n which can be either constructed as elliptic fibrations over del Pezzo surfaces dP_n, or by performing del Pezzo transitions. To set the stage for our analysis of the Calabi-Yau orientifolds we will first recall some basic geometric facts about

the surfaces dP_n in Subsection 4.1 and classify all involutions on these surfaces. In Subsection 4.2 we argue that the elliptically fibred Calabi-Yau threefolds over dP_n can also be obtained by del Pezzo transitions starting from the degree 18 hypersurface in $\mathbb{P}_{1,1,1,6,9}$ after flop transitions. Simple examples are obtained if the base is one of the toric del Pezzo surfaces dP_2 or dP_3. In Sections 4.3 and 4.4 we construct the corresponding Calabi-Yau threefolds and study their different topological phases using toric geometry. In a second step we introduce viable orientifold involutions σ on these compact Calabi-Yau manifolds and derive the induced tadpoles from O7 and O3 planes.

In the second part of this section we will have a closer look at the topological phases of M_n with n dP_8 surfaces. We show in Subsection 4.5 that these are examples of so-called swiss-cheese Calabi-Yau manifolds which can support large volume vacua with one large and $n+1$ small four-cycles [7,8,65]. In Subsection 4.6 we discuss the D-term conditions arising from wrapping a D7-brane on the small del Pezzo surfaces with orientifold invariant homology class.

4.1   Del Pezzo Surfaces and Their Involutions

The compact orientifold geometries for our GUT models will be obtained from elliptic fibrations over del Pezzo surfaces dP_n. In order to study these threefolds it will be necessary to review some basic facts about del Pezzo surfaces first. We will also discuss involutions on these dP_n. We will determine their fix-point locus and action on the exceptional curves of the del Pezzo surface. Since these involutions on the base will descend to involutions on the entire Calabi-Yau manifold, this will enable us to identify viable brane configurations later on.

On the geometry of del Pezzo surfaces

By definition, del Pezzo surfaces are the Fano surfaces, that is, the algebraic surfaces with ample canonical bundle. These are either the surfaces $\mathcal{B}_n = dP_n$, which are obtained by blowing up $\mathbb{P}^2$ on $0 \leq n \leq 8$ points[17], or $\mathbb{P}^1 \times \mathbb{P}^1$. Their Hodge numbers

---

[17]The points must be general in the sense that no two points are infinitesimally close, no three are on one line, no six on a conic, no eight on a cubic with a node at one of them. In other words, one is not allowed to blow up points sitting on a (-1)-curve. If one were to blow up a point on a (-1)-curve, then the proper transform would be a (-2)-curve. So yet another characterisation of the allowed points is that there be no curves of self-intersection -2 or less. Moreover, note that different sets of points can correspond to the same (complex structure on the) del Pezzo surface.

are $h^{0,0} = h^{2,2} = 1$, $h^{1,1}(\mathcal{B}_n) = n + 1$ and $h^{1,1}(\mathbb{P}^1 \times \mathbb{P}^1) = 2$, while all other $h^{p,q}$ vanish. A basis of homologically nontrivial two-cycles in $\mathcal{B}_n$ consists of the class of a line l in $\mathbb{P}^2$, and the n exceptional curves e_i, one for each blown-up point. Their intersection numbers are $l^2 = 1$, $e_i \cdot e_j = -\delta_{ij}$, $e_i \cdot l = 0$. Written in this basis, the first Chern class is

$$c_1(T\mathcal{B}_n) = -K = 3l - \sum_{i=1}^{n} e_i \ . \tag{71}$$

The square of the canonical class

$$K^2 = \int_{\mathcal{B}_n} c_1^2 = 9 - n \tag{72}$$

is also called the degree[18] of the del Pezzo surface. The second (top) Chern class is the Euler density, hence

$$\chi(\mathcal{B}_n) = \int_{\mathcal{B}_n} c_2 = 3 + n \ . \tag{73}$$

Let C be a curve in the del Pezzo surface. Then its degree $\deg(C)$ and its arithmetic genus g read

$$\deg(C) = -K \cdot C \ , \qquad g = \tfrac{1}{2}(C \cdot C + K \cdot C) + 1 \ . \tag{74}$$

Of particular interest are the rigid genus-0 instantons, that is rational curves of self-intersection (-1). For convenience of the reader we reproduce the classification of such (-1)-curves, see [66], in Table 4.

The del Pezzo surfaces $\mathbb{P}^2 = \mathcal{B}_0$, $\mathbb{P}^1 \times \mathbb{P}^1$, $\mathcal{B}_1$, $\mathcal{B}_2$, and $\mathcal{B}_3$ (that is, those of degree $K^2 \geq 6$) are toric varieties. The remaining surfaces $\mathcal{B}_4$, ..., $\mathcal{B}_8$ are not toric varieties, but can of course be embedded into toric varieties. In particular, the del Pezzo surfaces $\mathcal{B}_5$, ..., $\mathcal{B}_8$ are hypersurfaces or complete intersections in weighted projective spaces. For this, let us denote by $\mathbb{P}(d_1, \ldots, d_r | w_0, \ldots, w_m)$ the complete intersection of r equations of homogeneous degree $d_1, \ldots, d_r$ in weighted projective space with weights $w_0, \ldots, w_m$. These del Pezzo surfaces are listed in Table 5. One infers that the dimension of the complex deformation spaces for del Pezzo surfaces $\mathcal{B}_n$ with $n \geq 5$ is $\dim H^1(T\mathcal{B}_n) = 2n - 8$.

---

[18]To understand this notation, note that a degree $d = K^2$ del Pezzo surface with $d \geq 3$ can be realised as a degree-d hypersurface in $\mathbb{P}^d$.

class $\in H_2(\mathcal{B}_n, \mathbb{Z})$	$\mathcal{B}_1$	$\mathcal{B}_2$	$\mathcal{B}_3$	$\mathcal{B}_4$	$\mathcal{B}_5$	$\mathcal{B}_6$	$\mathcal{B}_7$	$\mathcal{B}_8$
$(0;1)$	1	2	3	4	5	6	7	8
$(1;-1^2)$		1	3	6	10	15	21	28
$(2;-1^5)$					1	6	21	56
$(3;-2,-1^6)$							7	56
$(4;-2^3,-1^5)$								56
$(5;-2^6,-1^2)$								28
$(6;-3,-2^7)$								8
Total no.	1	3	6	10	16	27	56	240

Table 4: *Number of (-1)-curves on the $\mathcal{B}_n$ del Pezzo surfaces. The coefficients $(a;b_1,\ldots b_n)$ are with respect to the standard basis $(l;e_1,\ldots,e_n)$. For example, $(1,-1^2)$ denotes all $\binom{n}{2}$ homology classes of the form $l - e_i - e_j$, $1 \le i < j \le n$. Note that there are no (-1)-curves on $\mathcal{B}_0 = \mathbb{P}^2$ and $\mathbb{P}^1 \times \mathbb{P}^1$, which are omitted.*

del Pezzo	K^2	hypersurface	coordinates
$\mathcal{B}_5$	4	$\mathbb{P}(2,2|1,1,1,1,1)$	(x_1,x_2,x_3,x_4,x_5)
$\mathcal{B}_6$	3	$\mathbb{P}(3|1,1,1,1)$	(x_1,x_2,x_3,x_4)
$\mathcal{B}_7$	2	$\mathbb{P}(4|2,1,1,1)$	(y,x_1,x_2,x_3)
$\mathcal{B}_8$	1	$\mathbb{P}(6|3,2,1,1)$	(y,z,x_1,x_2)

Table 5: *The del Pezzo surfaces of degree $K^2 \le 4$.*

Classification of involutions on del Pezzo surfaces

In order to systematically study GUT models on elliptically fibred Calabi-Yau manifolds with del Pezzo base, one needs to classify all different, non-trivial, holomorphic involutions on del Pezzo surfaces. In the following we intend to discuss the final classification in Table 6 and give a first impression of the necessary steps needed for this derivation. Most of the technical details and geometric constructions are shifted into Appendix A. The classification in Table 6 completes the list obtained in ref. [41].

For a systematic classification of involutions we will look at the pattern of rigid $\mathbb{P}^1$ instantons, that is, the (-1)-curves. Clearly, every involution induces a $\mathbb{Z}_2$ automorphism of the (-1)-curves. Conversely, up to degree 6, the automorphism of the (-1)-curves determines the involution. In the remaining degrees ≥ 7 there either are no (-1)-curves, or they lie over a line or point of the blown-up $\mathbb{P}^2$. Hence, in the latter case they do not "fill out" the space to uniquely determine the involution. Technically, the (-1)-curves generate all of $H_2(S, \mathbb{Z})$ if and only if the degree is 6 or less. In a next step, one has to find all conjugacy classes of involutions acting on the (-1) curves and check that these descend to actual geometric involutions on the corresponding del Pezzo surface. The details of this analysis can be found in Appendix A. Here we will discuss the final classification summarised in Table 6.

In Table 6 the complete list of del Pezzo surfaces $\mathcal{B}_n$ with involutions σ_i is shown. For each pair $(\mathcal{B}_n, \sigma_i)$ it also includes detailed information about the fix-point set. We use the following notation:

- $\Sigma(\sigma)$ is the homology class of the genus-g curve with $g \geq 1$ in the fixed point set of σ. As discussed in Appendix A, there is at most one such curve.

- $R(\sigma)$ are the homology classes of the rational genus 0 curves in the fixed point set.

- $B(\sigma)$ is the number of isolated fixed points that do not lie on (-1)-curves.

- $P(\sigma)$ is the number of isolated fixed points that do lie on (-1)-curves, and hence may not be blown up further.

- (b_2^+, b_2^-) are the dimensions of the $\pm$ eigenspaces of σ_i in $H_2(\mathcal{B}_n)$.

In the last column we also displayed the explicit action of the involution on the basis $(l, e_1, \ldots, e_n)$ of $H_2(\mathcal{B}_n)$ and basis (l_1, l_2) of $H_2(\mathbb{P}^1 \times \mathbb{P}^1)$. The k-dimensional identity matrix is simply denoted by $\mathbf{1}_k$, while H exchanges two elements $e_i \leftrightarrow e_j$ or $l_1 \leftrightarrow l_2$.

In addition there are also five involutions $(I^{(2)}_{\mathcal{B}_3}, I^{(3)}_{\mathcal{B}_3}, I^{(5)}_{\mathcal{B}_5}, I^{(9)}_{\mathcal{B}_7}, I^{(9)}_{\mathcal{B}_8})$ which should be viewed as the additional building blocks for all non-trivial involutions on del Pezzo surfaces. We will introduce the explicit form of these involutions in turn.

To define the special involutions we will specify their action on the basis elements $(l, e_1, \ldots, e_n)$. On the third del Pezzo surface we define the two involutions

$$I^{(2)}_{\mathcal{B}_3} = \begin{pmatrix} 2 & 1 & 1 & 1 \\ -1 & -1 & 0 & -1 \\ -1 & 0 & -1 & -1 \\ -1 & -1 & -1 & 0 \end{pmatrix} , \qquad I^{(3)}_{\mathcal{B}_3} = \begin{pmatrix} 2 & 1 & 1 & 1 \\ -1 & 0 & -1 & -1 \\ -1 & -1 & 0 & -1 \\ -1 & -1 & -1 & 0 \end{pmatrix} . \tag{75}$$

The remaining three involutions we need to introduce are well-known classical involutions. They are minimal since they satisfy $\sigma(E) \neq E$ and $\sigma(E) \cap E \neq \emptyset$ for each (-1)-curve E. This implies that such an involution cannot be obtained by blowing up a higher degree del Pezzo and extending an involution defined on the del Pezzo surface before blow-up. On $\mathcal{B}_5$ there is a minimal involution known as the de Jonquières involution which acts as

$$I^{(5)}_{\mathcal{B}_5} = \begin{pmatrix} 3 & 2 & 1 & 1 & 1 & 1 \\ -2 & -1 & -1 & -1 & -1 & -1 \\ -1 & -1 & -1 & 0 & 0 & 0 \\ -1 & -1 & 0 & -1 & 0 & 0 \\ -1 & -1 & 0 & 0 & -1 & 0 \\ -1 & -1 & 0 & 0 & 0 & -1 \end{pmatrix} . \tag{76}$$

There is one minimal involution for the del Pezzo surfaces of degree 1 and 2, respectively. The del Pezzo surface $\mathcal{B}_7$ admits the Geiser involution

$$I^{(9)}_{\mathcal{B}_7} : \quad l \mapsto -l - 3K , \quad e_i \mapsto -K - e_i . \tag{77}$$

while on $\mathcal{B}_8$ one has the Bertini involution acting as

$$I^{(9)}_{\mathcal{B}_8} : \quad l \mapsto -l - 6K , \quad e_i \mapsto -2K - e_i . \tag{78}$$

Note that one can explicitly check that each involution on each del Pezzo surface preserves its canonical class K defined in eq. (71).

With these definitions at hand, the involutions in Table 6 can be used for explicit computations. This will be particularly useful for the elliptically fibred threefolds over a del Pezzo base, since all involutions can be lifted to the corresponding Calabi-Yau threefold. We are then in the position to construct explicit Calabi-Yau orientifolds and compute the tadpoles induced by the O3- and O7-planes.

4.2 The Geometry of Del Pezzo Transitions of $\mathbb{P}_{1,1,1,6,9}[18]$

We are now in the position to construct compact Calabi-Yau threefolds M_n associated to a del Pezzo base. The first construction is via an elliptic fibration over a del Pezzo base $\mathcal{B}_n$, while the second construction is by employing del Pezzo transitions.

Involution	g	$\Sigma = [\Sigma_g]$	R	B	P	(b_2^+, b_2^-)	action on H_2
$(\mathbb{P}^2, \sigma)$			l	1		$(1,0)$	$\mathbf{1}_1$
$(\mathbb{P}^1 \times \mathbb{P}^1, \sigma_1)$			$(l_1) \cup (l_2)$			$(2,0)$	$\mathbf{1}_2$
$(\mathbb{P}^1 \times \mathbb{P}^1, \sigma_2)$				4		$(2,0)$	$\mathbf{1}_2$
$(\mathbb{P}^1 \times \mathbb{P}^1, \sigma_3)$			$l_1 + l_2$			$(1,1)$	H
$(\mathcal{B}_1, \sigma_1)$			$(l) \cup (e_1)$			$(2,0)$	$\mathbf{1}_2$
$(\mathcal{B}_1, \sigma_2)$			$l - e_1$	1	1	$(2,0)$	$\mathbf{1}_2$
$(\mathcal{B}_2, \sigma_1)$			$(l - e_1) \cup (e_2)$		1	$(3,0)$	$\mathbf{1}_3$
$(\mathcal{B}_2, \sigma_2)$			$l - e_1 - e_2$	1	2	$(3,0)$	$\mathbf{1}_3$
$(\mathcal{B}_2, \sigma_3)$			l		1	$(2,1)$	$\mathbf{1}_1 \oplus H$
$(\mathcal{B}_3, \sigma_1)$			$(l - e_1 - e_2) \cup (e_3)$		2	$(4,0)$	$\mathbf{1}_4$
$(\mathcal{B}_3, \sigma_2)$			$l - e_1$		2	$(3,1)$	$\mathbf{1}_2 \oplus H$
$(\mathcal{B}_3, \sigma_3)$			$2l - e_1 - e_2$			$(2,2)$	$I^{(2)}_{\mathcal{B}_3}$
$(\mathcal{B}_3, \sigma_4)$				4		$(3,1)$	$I^{(3)}_{\mathcal{B}_3}$
$(\mathcal{B}_4, \sigma_1)$			$l - e_1 - e_2$		3	$(4,1)$	$\mathbf{1}_3 \oplus H$
$(\mathcal{B}_4, \sigma_2)$			l		1	$(3,2)$	$\mathbf{1}_1 \oplus 2H$
$(\mathcal{B}_5, \sigma_1)$			$l - e_1$		2	$(4,2)$	$\mathbf{1}_2 \oplus 2H$
$(\mathcal{B}_5, \sigma_2)$			$2l - e_1 - e_2$			$(3,3)$	$I^{(2)}_{\mathcal{B}_3} \oplus H$
$(\mathcal{B}_5, \sigma_3)$				4		$(4,2)$	$I^{(3)}_{\mathcal{B}_3} \oplus H$
$(\mathcal{B}_5, \sigma_{\mathrm{dJ}})$	1	$3l - \sum_{i=1}^5 e_i$				$(2,4)$	$I^{(5)}_{\mathcal{B}_5}$
$(\mathcal{B}_6, \sigma_1)$			$l - e_1 - e_2$		3	$(5,2)$	$\mathbf{1}_3 \oplus 2H$
$(\mathcal{B}_6, \sigma_2)$	1	$3l - \sum_{i=1}^6 e_i$			1	$(3,4)$	$I^{(5)}_{\mathcal{B}_5} \oplus \mathbf{1}_1$
$(\mathcal{B}_7, \sigma_1)$				4		$(5,3)$	$I^{(3)}_{\mathcal{B}_3} \oplus 2H$
$(\mathcal{B}_7, \sigma_2)$	1	$3l - \sum_{i=1}^7 e_i$			2	$(4,4)$	$I^{(5)}_{\mathcal{B}_5} \oplus \mathbf{1}_2$
$(\mathcal{B}_7, \sigma_3)$	1	$3l - \sum_{i=1}^5 e_i$				$(3,5)$	$I^{(5)}_{\mathcal{B}_5} \oplus H$
$(\mathcal{B}_7, \sigma_{\mathrm{G}})$	3	$6l - 2\sum_{i=1}^7 e_i$				$(1,7)$	$I^{(9)}_{\mathcal{B}_7}$
$(\mathcal{B}_8, \sigma_1)$	1	$3l - \sum_{i=1}^8 e_i$			3	$(5,4)$	$I^{(5)}_{\mathcal{B}_5} \oplus \mathbf{1}_3$
$(\mathcal{B}_8, \sigma_2)$	1	$3l - \sum_{i=1}^6 e_i$			1	$(4,5)$	$I^{(5)}_{\mathcal{B}_5} \oplus \mathbf{1}_1 \oplus H$
$(\mathcal{B}_8, \sigma_{\mathrm{B}})$	4	$9l - 3\sum_{i=1}^7 e_i$		1		$(1,8)$	$I^{(9)}_{\mathcal{B}_8}$

Table 6: *All involutions on del Pezzo surfaces. See page 42 for the definition of Σ, R, B, and P.*

Elliptically fibred Calabi-Yau threefolds with del Pezzo base

Let us construct Calabi-Yau threefolds M_n as elliptic fibrations over the del Pezzo base dP_n. We consider elliptic fibrations which are generically smooth with the worst degeneration of the fibre of Kodaira type I_1 [67,68]. In the following we will restrict further to elliptic fibrations with generic elliptic fibres of type E_8 such that the generic elliptic fibres can be represented by a degree 6 hypersurface in $\mathbb{P}_{1,2,3}$ denoted by $\mathbb{P}_{1,2,3}[6]$. As shown, for example, in [69], one then finds that the Euler number of the elliptic fibration M_n is given by

$$\chi(M_n) = -C_{(8)} \int_{\mathcal{B}_n} c_1^2 = 60(n-9), \tag{79}$$

where $C_{(8)} = 30$ is the dual Coxeter number of E_8 and we have used (72) for the del Pezzo base $\mathcal{B}_n$. One can also count the number of Kähler classes for these geometries. One finds that there are $n+1$ classes corresponding to the non-trivial two-cycles of the del Pezzo base as well as the fibre class of the elliptic fibration. This implies that M_n has Hodge numbers

$$h^{1,1}(M_n) = n + 2 , \qquad h^{2,1}(M_n) = 272 - 29n, \tag{80}$$

where we have used that $\chi = 2(h^{1,1} - h^{2,1})$.

The specification of M_n as an elliptic fibration over the base dP_n will turn out to be particularly useful in the study of orientifold involutions and brane configurations on M_n. Let us introduce the map

$$\pi : \ M_n \ \rightarrow \ \mathcal{B}_n , \tag{81}$$

which is the projection from the threefold M_n to the base. Note that every (-1) curve class E in $\mathcal{B}_n$ can be pulled back to a divisor in M_n using $\pi^* : E \mapsto \pi^*(E) \in H_4(M_n, \mathbb{Z})$. In fact, each such divisor is a dP_9 surface. This surface is defined as blow up of $\mathbb{P}^2$ at nine points which arise at the intersections of two cubic curves. Thus, dP_9 is an elliptic fibration over $\mathbb{P}^1$ which has 12 singular fibres[19]. The dP_9 is not strictly a del Pezzo surface, but the equations (72) and (73) remain to be valid. Recall that the (-1) curve in the base have been listed in Table 4. It it thus straightforward to determine the intersections of these curves. In case two curves E_1, E_2 intersect at a point the corresponding two dP_9 divisors $\pi^*(E_1)$ and $\pi^*(E_2)$ in M_n will intersect

---

[19]Roughly speaking, the dP_9 is half a K3 surface which is an elliptic fibration over $\mathbb{P}^1$ with 24 singular fibres.

over a Riemann surface of genus 1. Clearly each $\pi^*(E)$ intersects the base $\mathcal{B}_n$ in a $\mathbb{P}^1$. Already this simple analysis allows us to infer the necessary information on the triple intersections of the threefold $\mathcal{M}_n$ in the elliptically fibred phase.

We want to apply a similar logic also for the extension of an involution on the del Pezzo base to an involution σ on the threefold $\mathcal{M}_n$. In fact, by appropriately defining σ the action on the (-1) curves of $\mathcal{B}_n$ lifts to an action of their π^* pull-backs. The fixed divisors wrapped by the O7-planes can then be determined using Table 6. Determining the number of O3-planes in the full set-up also depends on the precise form of the involution on M_n. In particular, it is not generally the case that each isolated fix-point in the base lifts to a single fix-point in M_n. Let us consider the case where the torus fibre over the fix-point is smooth, which will turn out to be the case in our explicit examples. In this simple situation, we have to distinguish three cases. Firstly, the fibre over the isolated fix-point can be fixed itself. This extension of the involution should be omitted, since this would imply the presence of O5-planes and violate the condition $\sigma^*\Omega = -\Omega$. Secondly, the involution can act as shift on the torus fibre and hence have no fix-points in M_n. Thirdly, σ can act as the inversion of the torus fibre. Such an involution has 4 fix-points, one on the zero section and three on the tri-section

$$D_T = 3\mathcal{B}_n - 3\pi^*(K) \, , \tag{82}$$

where K is the canonical class of the del Pezzo base. To define viable involutions on M_n one needs to extend this analysis to the singular Kodaira fibres.

Del Pezzo transitions of $\mathbb{P}_{1,1,1,6,9}[18]$

An alternative way to construct the threefolds M_n is to perform del Pezzo transitions starting with the degree 18 hypersurface in weighted projective space $\mathbb{P}_{1,1,1,6,9}$. This Calabi-Yau manifold $M_0 = \mathbb{P}_{1,1,1,6,9}[18]$ is an elliptic $\mathbb{P}_{1,2,3}[6]$ fibration over the base $\mathcal{B} = \mathbb{P}_2$ and has $h^{1,1} = 2$. In order to perform the del Pezzo transition $M_0 \rightarrow M_1$ one generates a dP$_8$ singularity by fixing 29 complex structure deformations [70, 41]. This singularity is then resolved by blowing up a del Pezzo surface dP$_8$. Clearly, in this process the Hodge numbers precisely change as required in eq. (80). This process can be repeated to obtain the manifolds M_n. However, it is important to note that the manifold constructed via the elliptic fibration only coincide with the one obtained by del Pezzo transitions after performing appropriate flop transitions. In order to obtain del Pezzo surfaces dP$_8$ out of the dP$_9$ surfaces of the elliptic fibred phase, one has to perform a flop transition for the $\mathbb{P}^1$ intersecting the base.

4.3   Orientifold of An Elliptic Fibration Over dP_2

The first Calabi-Yau threefold which we investigate in detail is the manifold M_2 which corresponds to the elliptic fibration over dP_2. The geometry of M_2 and its topological phases has been studied from a different point of view in [71]. Note that, using eqns. (80) and (79), one finds the Hodge numbers $h^{1,1}(M_2) = 4$, $h^{2,1}(M_2) = 214$ and the Euler number $\chi(M_2) = -420$. It will be important that the manifold M_2 has actually 5 distinct topological phases which are connected by flop transitions. They correspond to the five triangulations of the toric dP_2 base. dP_2 can be represented torically by the points $(1,0)$, $(0,1)$, $(-1,0)$, $(0,-1)$, $(-1,-1)$ in two dimensions. The five triangulations of this polyhedron are depicted in Figure 1.
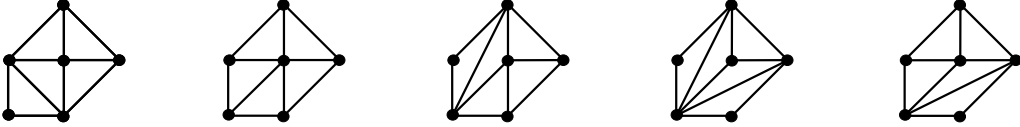
Figure 1: *The five different triangulations of the toric* dP_2 *base.*

To study the Calabi-Yau space M_2 in detail, we will also invoke the methods of toric geometry. Note that $\mathbb{P}_{1,1,1,6,9}$ is described by the six points $v_1^* = (1,0,0,0)$, $v_2^* = (0,1,0,0)$, $v_3^* = (0,0,1,0)$, $v_4^* = (0,0,0,1)$, $v_5^* = (-9,-6,-1,-1)$, $v_6^* = (-3,-2,0,0)$. Each of these points corresponds to a divisor D_i and the hypersurface $\mathbb{P}_{1,1,1,6,9}[18]$ is defined to admit the anti-canonical class $-\sum_{i=1}^{6} D_i$. To obtain the manifold M_2 one introduces two blowing-up divisors D_7, D_8 corresponding to the points $v_7^* = (-6,-4,-1,0)$ and $v_8^* = (-6,-4,0,-1)$. The compact hypersurface with anti-canonical class $-\sum_{i=1}^{8} D_i$ is the manifold M_2. It admits five triangulations just as the dP_2 base itself. In the following we will investigate two of them in more detail. The corresponding Calabi-Yau space will be denoted by $M_2^{(dP_9)^2}$ and $M_2^{(dP_8)^2}$. Here we indicate the type of the divisors D_7, D_8 as we will check below[20].

---

[20]We are grateful to Albrecht Klemm for help with the programs to perform the toric computations. The analysis of the divisors and their intersection ring was carried out by using the Maple code Schubert.

The geometry of $M_2^{(\mathrm{dP_9})^2}$

Let us first discuss the Calabi-Yau manifold $M_2^{(\mathrm{dP_9})^2}$. The data of the associated linear sigma model is the following. We have eight complex coordinates x_i. The divisors D_i are defined by the constraints $x_i = 0$. In addition there are four $U(1)$ symmetries. The corresponding charges are shown in (83). Note that we have chosen the charge vectors to correspond to the Mori cone generators for this triangulation.

	x_1	x_2	x_3	x_4	x_5	x_6	x_7	x_8	p
$\ell^{(1)}$	3	2	0	0	0	1	0	0	6
$\ell^{(2)}$	0	0	1	0	1	-1	0	-1	0
$\ell^{(3)}$	0	0	0	1	1	-1	-1	0	0
$\ell^{(4)}$	0	0	0	0	-1	-1	1	1	0

$$(83)$$

The Mori cone for this triangulation is generated by four holomorphic curves C^a which intersect the divisors D_i as $D_i \cdot C^a = \ell_i^{(a)}$. Hence, the $\ell^{(a)}$ are the coordinates of the C^a in the two-cycle basis dual to D_i. Since there are as many Mori generators as Kähler parameters $h^{1,1} = 4$, this Mori cone is simplicial. Using the Mori generators it is also straightforward to determine a basis K_i of four-cycles generating the Kähler cone. Expanding the Kähler form as $J = r^i [K_i]$ the condition that all physical volumes are positive translates into

$$\int_{C^a} J = r^i\, C^a \cdot K_i > 0. \tag{84}$$

This requires $r^i > 0$ for

$$
\begin{aligned}
K_1 &= 3D_5 + D_6 + 2D_7 + 2D_8 \,, & K_2 &= D_5 + D_7 \,, \\
K_3 &= D_5 + D_8 \,, & K_4 &= D_5 + D_7 + D_8 \,.
\end{aligned}
\tag{85}
$$

In this basis all triple intersections are positive, ensuring positivity of the divisor volumes and the total volume of Y. However, for our applications it is more useful to display the triple intersection numbers in the basis $\{D_5, D_6, D_7, D_8\}$ as

$$I_3 = D_6\big(7\,D_6^2 - D_5^2 - D_7^2 - D_8^2 - D_5\,D_6 - D_6\,D_7 - D_6\,D_8 + D_5\,D_7 + D_5\,D_8\big) \,. \tag{86}$$

Not surprisingly, there are both negative and positive intersections in this basis.

To determine the geometry of the different divisors D_i we now compute the Euler characteristic $\chi = \int_D c_2(T_D)$, as well as $\int_D c_1^2(T_D)$ for each divisor in $M_2^{(\mathrm{dP_9})^2}$. We

exemplify this for the divisor D_8 and restrict the intersection form (86) to this surface

$$I_{D_8} = -D_6^2 - D_6 D_8 + D_5 D_6 . \tag{87}$$

Using this intersection form one computes

$$\chi(D_8) = 12, \qquad \int_{D_8} c_1^2(T_{D_8}) = 0 . \tag{88}$$

From this we conclude that $D_8 = \pi^*(E_2)$ is a dP$_9$ surface. Analogously, we proceed for the remaining divisors D_i. We identify

$$\begin{array}{llll}
D_3 = \pi^*(l - E_2) & K3 , & D_4 = \pi^*(l - E_1) & K3 , \\
D_5 = \pi^*(l - E_1 - E_2) & dP_9 , & D_6 = \mathcal{B} & dP_2 , \\
D_7 = \pi^*(E_1) & dP_9 , & D_8 = \pi^*(E_2) & dP_9 .
\end{array} \tag{89}$$

Let us note that indeed the exceptional divisors D_7 and D_8 are dP$_9$ surfaces which justifies our notation $M_2^{(dP_9)^2}$. Finally, using (83) the divisor D_1 can be identified with

$$D_1 = 3\,\mathcal{B} + 9\,\pi^*(l - E_1 - E_2) + 6\,\pi^*(E_1) + 6\,\pi^*(E_2) = D_T, \tag{90}$$

that is, the tri-section D_T defined in (82) of the elliptic fibration over $\mathcal{B} = dP_2$. With these identifications one can check that the triple intersection form (86) is indeed the one generated by $\{\mathcal{B}, \pi^*(E_i), \pi^*(l - E_1 - E_2)\}$. All terms in (86) contain the base D_6 and the expression in the brackets corresponds to the intersection form of E_i and $l - E_1 - E_2$ as well as the self-intersection 7 of the anti-canonical class on dP$_2$.

Let us now specify an orientifold projection $\Omega_p \sigma (-1)^{F_L}$. As a simple example consider the involution

$$\sigma : x_3 \to -x_3 \tag{91}$$

and analyse the fixed point set. In order to do that we first note that the coordinates obey some scaling relations dictated by the $U(1)$ weights $\ell^{(k)}$ displayed in (83). This implies that in order to determine the fix-point set of (91), the coordinates x_i need only to agree up to scaling such that

$$x_j = \pm \prod_{k=1}^{4} \lambda_k^{\ell_j^{(k)}} x_j , \tag{92}$$

where $\lambda_k \in \mathbb{C}^*$, and the minus sign should be used for x_3 while the plus sign holds for all other coordinates. The value of the complex scalars λ_k is restricted by the

Stanley-Reisner ideal of the toric ambient space. More precisely, this ideal contains the information which coordinates x_i are not allowed to vanish simultaneously. For the case at hand it reads

$$SR = \{x_3\,x_5,\ x_3\,x_7,\ x_4\,x_5,\ x_4\,x_8,\ x_7\,x_8,\ x_1\,x_2\,x_6\}\ . \tag{93}$$

For example, since $x_1 x_5$ is in the Stanley-Reisner ideal, the subspace $x_1 = x_5 = 0$ is not in the toric variety. Combining these conditions with the scalings eq. (92) fixes the λ_i to specific values and allows us to determine the fix-point locus[21].

Let us apply this strategy explicitly to our example. The divisors $D_3 = \{x_3 = 0\}$ and $D_7 = \{x_7 = 0\}$ are fixed under σ consistent with the scalings (83). As mentioned, D_3 is a $K3$ surface with $\chi = 24$ and D_7 is a dP$_9$ with $\chi = 12$. However, this is not the end of the story, as there exist also fixed points which give the location of $O3$-planes. Using the projective identifications, we first get the two candidate fixed points

$$p_1 = \{x_4 = x_5 = x_6 = 0\}, \qquad p_2 = \{x_5 = x_6 = x_8 = 0\}, \tag{94}$$

where however, the first one p_1 is part of the Stanley-Reisner ideal and therefore discarded. In addition there exist two fixed loci

$$p_3 = \{x_1 = x_4 = x_5 = 0\}, \qquad p_4 = \{x_1 = x_5 = x_8 = 0\}, \tag{95}$$

where again the first is discarded and the second actually consists of 3 fixed points, which is essentially the space $\mathbb{P}_{1,2}[6]$. Note that this is precisely the situation discussed in Subsection 4.2. From eq. (94) one infers that the involution eq. (91) admits one isolated fix-point in the base D_6. σ acts on the smooth torus fibre over this point as inversion, such that three fix-points eq. (95) arise in the tri-section D_1.

To summarise, the fixed points locus consists of two non-intersecting $O7$ planes and four $O3$ planes. Therefore, the right-hand side of the $D7$-brane tadpole cancellation condition (13) reads

$$8[D_{O7}] = 8\,\pi^*(l - E_2) + 8\,\pi^*(E_1) \tag{96}$$

and the right-hand side of the $D3$ brane tadpole condition (17) takes the form

$$\frac{\chi(K3) + \chi(\mathrm{dP}_9)}{6} + \frac{N_{O3}}{2} = 8. \tag{97}$$

---

[21]Note that in general, the determination of the fix-point set in the Calabi-Yau hypersurface can be more tricky. This is due to fact that it will in general be non-generic hypersurface to admit the involution σ. In our examples, this will not introduce any new subtleties.

Note that indeed we get a non-negative integer. In order to cancel the $D7$ brane tadpole we can only introduce branes wrapping entirely the fibre. Candidates are of course D_3 and D_7 which are point-wise invariant under the orientifold projection and therefore belong to class 3.) introduced in Subsection 2.1. A natural candidate of class 2.) is $D_5 = \pi^*(l - E_1 - E_2)$. This dP$_9$ is not point-wise invariant. In fact, using that D_5 intersects the O7-plane in a genus 1 curve and that all four O3 planes are inside D_5 one uses the Lefschetz fix-point formula [72] to compute for D_5 that $b_+^2 = 6$ and $b_-^2 = 4$. This involution indeed corresponds to a viable involution of dP$_9$.

Let us also consider the involution $x_1 \rightarrow -x_1$, which is nothing else than the reflection of the torus fibre. The fixed point locus can be determined as $D_{O7} = D_1 \cup D_6$, such that the right hand side of (13) reads

$$8[D_{O7}] = 32\,\mathcal{B} + 24\,\pi^*c_1(\mathcal{B})$$ (98)

and no fixed points. For the Euler characteristics we find $\chi(D_1) = 435$ and $\chi(D_6) = \chi(\mathrm{dP}_2) = 5$, such that the right hand side of (17) takes the form

$$\frac{\chi(D_{O7})}{6} + \frac{N_{O3}}{2} = \frac{220}{3}\,.$$ (99)

Finally, let us determine how this involution acts on $\pi^*(E_1) = \mathrm{dP}_9$. The divisor $\mathcal{B}$ intersects $\pi^*(E_1)$ of course over a sphere and from $\chi(D_1 \cap D_7) = D_1 \cdot D_7 \cdot (-D_1 - D_7) = -6$ we conclude that the Euler characteristic of the fix-point set in dP$_9$ is $\chi = -4$. This implies $b_+^2 = 2$ and $b_-^2 = 8$ and corresponds to the blow-up of the Bertini involution $(\mathcal{B}_8, \sigma_\mathrm{B})$ of Table 6 at one invariant point.

The geometry of $\mathrm{M}_2^{(\mathrm{dP_8})^2}$

Let us now consider the triangulation which corresponds to a Calabi-Yau manifold with two exceptional dP$_8$ divisors D_7 and D_8. Again we specify the data for the linear sigma-model such that the charge vectors correspond to the Mori cone generators for this triangulation.

	x_1	x_2	x_3	x_4	x_5	x_6	x_7	x_8	p
$\ell^{(1)}$	3	2	0	1	1	0	-1	0	6
$\ell^{(2)}$	3	2	1	0	1	0	0	-1	0
$\ell^{(3)}$	0	0	0	-1	-1	1	1	0	0
$\ell^{(4)}$	0	0	1	1	1	-3	0	0	0
$\ell^{(5)}$	0	0	-1	0	-1	1	0	1	0

(100)

Note that the Mori cone eq. (100) is generated by five holomorphic curves C^a in this triangulation. Since this is more than the $h^{1,1} = 4$ Kähler deformations the Mori cone is non-simplicial. Also for this case we have to determine the dual Kähler cone spanned by four-cycles. By definition the Kähler cone is generated by four-cycles D which satisfy $D \cdot C^a \geq 0$. For our purposes it will be convenient to determine the Kähler cone in coordinates r^i. We therefore chose to discard one of the 5 Mori vectors (100), namely, the last one $\ell^{(5)}$. As in the $M_2^{(\mathrm{dP}_9)^2}$ phase it is then straightforward to determine the Kähler cone generators

$$
\begin{aligned}
K_1 &= 3D_5 + D_6 + 2D_7 + 3D_8 , & K_2 &= -D_8, \\
K_3 &= 3D_5 + D_6 + 3D_7 + 3D_8 , & K_4 &= D_5 + D_7 + D_8 .
\end{aligned}
\tag{101}
$$

Note that for $J = r^i[K_i]$, the positivity of the curves $C^i, i = 1, ..., 4$ is ensured when $r^i > 0$. In order that the last curve is positive we have to additionally impose $\int_{C^5} J = r^i K_i \cdot C^5 = r^1 - r^2 + r^3 > 0$. Clearly, a similar analysis can be carried out when discarding one of the other $\ell^{(a)}$ which allows to define coordinates for the complete non-simplicial Kähler cone.

For convenience we again display the triple intersection numbers for $M_2^{(\mathrm{dP}_8)^2}$ in the basis $\{D_5, D_6, D_7, D_8\}$,

$$
I_3 = 9\, D_6^3 + D_7^3 + D_8^3 + D_5 \big(D_5\, D_6 + D_5\, D_7 + D_5\, D_8 - 2\, D_5^2 - 3\, D_6^2 - D_7^2 - D_8^2 \big) .
\tag{102}
$$

In particular, for the intersection form on the surface D_8 we get

$$
I_{D_8} = D_5^2 + D_8^2 - D_5\, D_8
\tag{103}
$$

so that

$$
\chi(D_8) = 11, \qquad \int_{D_8} c_1^2(T_{D_8}) = 1 ,
\tag{104}
$$

which we identify with the correct values for dP$_8$. For D_7 we find the same result. Comparing this result with (88) we note that in this cone of the complexified Kähler moduli space, one $\mathbb{P}^1$ in each $\pi^*(E_i)$ of $M_2^{(\mathrm{dP}_9)^2}$ has been flopped away so that dP$_9 \rightarrow$ dP$_8$. Indeed the two exceptional divisors E_i of the dP$_2$ base in $M_2^{(\mathrm{dP}_9)^2}$ are absent in $M_2^{(\mathrm{dP}_8)^2}$ since $\chi(D_6) = 3$, and $\int c_2(T_{D_6}) = 9$.

Having performed the flop transitions, the exceptional $\mathbb{P}^1$s have to reappear in other divisors. In fact, we compute

$$
\chi(D_3) = 25 , \quad \chi(D_5) = 14, \qquad \int c_1^2(T_{D_3}) = -1 , \quad \int c_1^2(T_{D_5}) = -2 .
\tag{105}
$$

52

Again, the divisor D_4 has the same topology as D_3. This implies that the divisor D_3, D_4 corresponding to the pull-back divisors $\pi^*(l - E_i)$ in $M_2^{(\mathrm{dP}_9)^2}$ now contain each one additional $\mathbb{P}^1$. The divisor D_5 corresponding to $\pi^*(l - E_1 - E_2)$ contains two additional $\mathbb{P}^1$s.

Let us now investigate the involutions on $M_2^{(\mathrm{dP}_8)^2}$. A simple involution exchanging the two dP$_8$ surfaces has been employed in [73]. However, since these two del Pezzo surfaces do not intersect, this involution will not be useful in constructing GUT models. We therefore consider again the involution $\sigma : x_3 \to -x_3$, which still has the non-intersecting O7 planes D_3 and D_7. There exist 4 fixed points so that the tadpole contribution is

$$\frac{\chi(D_{O7})}{6} + \frac{N_{O3}}{2} = 8 \ . \tag{106}$$

This condition is identical to the condition eq. (97) on $M_2^{(\mathrm{dP}_9)^2}$ since the topology change of the two O7 divisors precisely cancels. One checks that 3 fix-points are located on the del Pezzo 8 defined by $x_8 = 0$ which intersects the orientifold locus D_3 on a genus 1 curve. This implies using Table 6 that $b_+^2 = 5$, $b_-^2 = 4$ for the del Pezzo 8.

The involution defined by the reflection $x_1 \to -x_1$, again has the fixed point divisors $D_{O7} = D_1 \cup D_6$. For the Euler characteristics we find $\chi(D_1) = 435$ and $\chi(D_6) = 3$. However, this time the involution also has the two fixed points $p_1 = \{x_4 = x_5 = x_7 = 0\}$ and $p_2 = \{x_3 = x_5 = x_8 = 0\}$. For the D3-tadpole contribution we therefore obtain

$$\frac{\chi(D_{O7})}{6} + \frac{N_{O3}}{2} = \frac{222}{3} \ . \tag{107}$$

Finally, let us determine how this involution acts on $D_7 = \mathrm{dP}_8$. The base $\mathcal{B} = D_6$ does not intersect D_7 after the flop transition, while D_1 intersects D_7 over curve with $\chi = -6$. Moreover, only the fixed point p_1 lies on D_7 , while p_2 lies on D_8. Therefore, the Euler-characteristic of the fixed point set in D_7 is $\chi = -5$ and we obtain $b_2^+ = 1$, $b_2^- = 8$. Comparing this result with Table 6 we conclude that the involution $x_1 \to -x_1$ acts on the dP$_8$ as the Bertini involution $(\mathcal{B}_8, \sigma_{\mathrm{B}})$.

4.4 Orientifold of An Elliptic Fibration Over dP$_3$

We can repeat the procedure just described also for the del Pezzo base dP$_3$. This remains to be rather simple, since this del Pezzo is still toric and represented by the
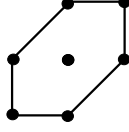
Figure 2: *The points of the polyhedron of the* dP$_3$ *base.*

points $(1,0)$, $(0,1)$, $(-1,0)$, $(0,-1)$, $(-1,-1)$ and $(1,1)$ as shown in Figure 2. In this case there are in fact 18 triangulations of the dP$_3$ base. The toric ambient space for the corresponding Calabi-Yau hypersurface M_3 is obtained by adding the point $v_9^* = (3, 2, 1, 1)$ to the polyhedron of M_2 above. This polyhedron has 18 triangulations which yield different phases of the Calabi-Yau hypersurface M_3. As determined by eqns. (80) and (79), each M_3 has the topological data $h^{1,1}(M_3) = 5$, $h^{2,1}(M_3) = 185$, and $\chi(M_3) = -360$. In the following we discuss one out of the 18 phases in more detail. Namely, the Weierstraß phases $M_3^{(\text{dP}_9)^3}$ where the divisors D_7, D_8, D_9 are dP$_9$ surfaces. A second phase, $M_3^{(\text{dP}_8)^3}$ will be of importance in Subsection 4.6 where we discuss the issue of moduli stabilisation for compactifications on M_n. On M_3 we will also be able to introduce interesting orientifold projections with a non-trivial split $h^{1,1} = h^{1,1}_+ + h^{1,1}_-$.

The geometry of $\mathbf{M_3^{(dP_9)^3}}$

Let us discuss the Weierstraß phase where all (-1)-curves lead to dP$_9$ surfaces. Using Table 4 we infer that dP$_3$ has six (-1)-curves which yield six dP$_9$ surfaces. The Mori cone associated to this phase is shown in eq. (108).

	x_1	x_2	x_3	x_4	x_5	x_6	x_7	x_8	x_9	p
$\ell^{(1)}$	3	2	0	0	0	1	0	0	0	6
$\ell^{(2)}$	0	0	0	1	1	-1	-1	0	0	0
$\ell^{(3)}$	0	0	0	0	-1	-1	1	1	0	0
$\ell^{(4)}$	0	0	1	1	0	-1	0	0	-1	0
$\ell^{(5)}$	0	0	0	-1	0	-1	1	0	1	0
$\ell^{(6)}$	0	0	1	0	1	-1	0	-1	0	0
$\ell^{(7)}$	0	0	-1	0	0	-1	0	1	1	0

(108)

Using the data for the Mori cone, it is straightforward to evaluate the associated Kähler cone. However, we again display the triple intersection numbers in the basis

$D_6, \ldots, D_9$

$$I_3 = D_6\left(6D_6^2 - D_5^2 - D_7^2 - D_8^2 - D_9^2 - D_6(D_5 + D_7 + D_8 + D_9) + D_5 D_8 + D_7 D_5\right) . \quad (109)$$

In a similar spirit as in the previous section we can also check that the divisors

$$\begin{aligned}
D_3 &= \pi^*(l - E_1 - E_3) , & D_4 &= \pi^*(l - E_2 - E_3) , & D_5 &= \pi^*(l - E_1 - E_2) , \\
D_7 &= \pi^*(E_2) , & D_8 &= \pi^*(E_1) , & D_9 &= \pi^*(E_3) . \quad (110)
\end{aligned}$$

are the six dP$_9$ surfaces, while the dP$_3$ base is the divisor D_6.

Let us now turn to the definition of the involution on $M_3^{(\text{dP}_9)^3}$. Using Table 6, we find four candidate involutions on the dP$_3$ base. Our prime focus will be on the exchange involution $(\mathcal{B}_3, \sigma_3)$, which admits the rational curve $2l - E_1 - E_2$ as fix-point divisor. Lifted to the elliptically fibred threefold, this involution descends to

$$\sigma : \quad x_7 \leftrightarrow x_3 , \qquad x_8 \leftrightarrow x_4 , \qquad x_9 \leftrightarrow x_5 . \quad (111)$$

We can thus evaluate the action of σ^* on the cohomology $H^2(M_3)$ spanned by $[D_5, D_6, D_7, D_8, D_9]$ to show that

$$h_+^{1,1} = 3 , \qquad h_-^{1,1} = 2 . \quad (112)$$

This implies that by using (1) this orientifold compactification will admit three Kähler moduli T_I and two B-field moduli G^i.

Again, we can determine the fixpoint set of σ using toric geometry. Taking into account the scaling relations (108) and the corresponding constraints from the Stanley-Reisner ideal, one finds the fix-point divisor

$$x_5 x_8 x_3 x_9 - x_4 x_9 x_5 x_7 = 0 , \quad (113)$$

and no isolated fix-points meeting the hypersurface. The isolated fix-points and hence O3-planes can also be directly inferred from the fact that there are no fix-points on the dP$_3$ base for this involution. In accord with the general arguments presented in Subsection 4.2, the locus eq. (113) corresponds to an O7-plane on the divisor class $D_{O7} = D_4 + D_9 + D_5 + D_7 = \pi^*(2l - E_1 - E_2)$ and induces a tadpole

$$8[D_{O7}] = 8\pi^*(2l - E_1 - E_2) . \quad (114)$$

For this O7-plane one computes $\chi(D_{O7}) = 48$, such that the induced D3-tadpole is $\chi(D_{O7})/6 = 8$.

4.5 The Swiss-Cheese Property

Though we will deliver some more comments in Section 8, in this paper we do not yet intend to combine the GUT model search with a complete analysis of moduli stabilisation. However, we would like to point out that some of the manifolds discussed so far provide new examples of so-called swiss-cheese type Calabi-Yau manifolds. Here we understand this term in the strong sense that the volume $\mathcal{V}$ of the Calabi-Yau can be expressed as[22]

$$\mathcal{V} = \frac{\sqrt{8}}{6}\left[\frac{1}{\sqrt{3^5}}(\tau_0)^{\frac{3}{2}} - \frac{1}{3}(\tau_{\mathcal{B}})^{\frac{3}{2}} - \sum_{i=1}^{h^{1,1}-2}(\tau_i)^{\frac{3}{2}}\right], \tag{115}$$

where the numerical coefficients are chosen for later convenience and τ_B, τ_i are volumes of a basis of four-cycles $\Gamma_0, \Gamma_{\mathcal{B}}, \Gamma_i$ given by

$$\tau_0 = \frac{1}{2}\int_{\Gamma_0} J \wedge J \ , \qquad \tau_{\mathcal{B}} = \frac{1}{2}\int_{\Gamma_{\mathcal{B}}} J \wedge J \ , \qquad \tau_i = \frac{1}{2}\int_{\Gamma_i} J \wedge J \ . \tag{116}$$

Our aim is to show that for the manifolds $M_n^{(\mathrm{dP}8)^n}$ one can always find such a basis $\Gamma_0, \Gamma_{\mathcal{B}}, \Gamma_i$ such that $\mathcal{V}$ is of the form (115).

Swiss-Cheese property of $\mathbf{M_2^{(dP_8)^2}}$ and $\mathbf{M_3^{(dP_8)^3}}$

We first consider the manifold $M_2^{(\mathrm{dP}8)^2}$. Recall that this Calabi-Yau is connected via a flop transition to the corresponding Weierstraß model, which is an elliptic fibration over the dP_2 base. In fact, the two exceptional two cycles $E_{1,2}$ in the base dP_2 have been flopped away. We will use the same notation as in Sections 4.3 and 4.4. The triple intersection form on $M_2^{(\mathrm{dP}8)^2}$ in the basis D_i was given in eq. (102). Expanding the Kähler form as $J = r_5 D_5 + r_6 D_6 + r_7 D_7 + r_8 D_8$ and defining

$$\Gamma_{\mathcal{B}} = D_6 \ , \qquad \Gamma_1 = D_7 \ , \qquad \Gamma_2 = D_8 \ , \tag{117}$$

we compute the τ_i in (116) as

$$\tau_{\mathcal{B}} = \tfrac{1}{2}(r_5 - 3\,r_6)^2 \ , \qquad \tau_1 = \tfrac{1}{2}(r_5 - r_7)^2 \ , \qquad \tau_2 = \tfrac{1}{2}(r_5 - r_8)^2 \ . \tag{118}$$

---

[22]It has been shown [65] that a much weaker condition is already sufficient to make the LARGE volume scenario work.

Now, let us define the following divisor, which obviously is related to the former tri-section D_1 in the Weierstraß phase

$$\Gamma_0 = D_1 + 3\,D_7 + 3\,D_8 = 3\,(3\,D_5 + D_6 + 3\,D_7 + 3\,D_8)\ . \tag{119}$$

The volume of this divisor is given by $\tau_0 = \frac{3}{2}r_5^2$. We have found four divisors whose volumes can be written as perfect squares and it is now a simple calculation to show that the total volume of the Calabi-Yau can be written as in (115), showing the swiss cheese structure. Note that indeed the three small cycles are of the type $\Gamma_{\mathcal{B}} = \mathbb{P}_2$, $\Gamma_{1,2} = \mathrm{dP}_8$ and therefore all are shrinkable to a point.

Along the same lines also the swiss cheese structure of the Calabi-Yau $M_3^{(\mathrm{dP}_8)^3}$ can be shown. This manifold is related to the Weierstraß model over dP_3. For completeness, let us list the relevant data. The intersection form reads

$$\begin{aligned}
I_3 &= -2\,D_5^3 + 9\,D_6^3 + D_7^3 + D_8^3 + D_9^3 + D_5^2\,D_6 - 3\,D_5\,D_6^2 + D_5^2\,D_7 - D_5\,D_7^2 \\
&\quad + D_5^2\,D_8 - D_5\,D_8^2\ . \tag{120}
\end{aligned}$$

For the volumes of the del Pezzo type divisors $\Gamma_{\mathcal{B}} = D_6$, $\Gamma_i = D_{i+6}$ we get

$$\tau_{\mathcal{B}} = \tfrac{1}{2}(r_5 - 3\,r_6)^2\ ,\quad \tau_1 = \tfrac{1}{2}(r_5 - r_7)^2\ ,\quad \tau_2 = \tfrac{1}{2}(r_5 - r_8)^2\ ,\quad \tau_3 = \tfrac{1}{2}r_9^2\ , \tag{121}$$

and with

$$\Gamma_0 = D_1 + 3\,D_7 + 3\,D_8 + 3\,D_9 = 3\,(3\,D_5 + D_6 + 3\,D_7 + 3\,D_8)\ . \tag{122}$$

and $\tau_0 = \frac{3}{2}r_5^2$ the total volume of the Calabi-Yau can again be written as eq. (115).

Proof of Swiss-Cheese property for $\mathbf{M_n^{(dP_8)^n}}$

What we have concretely confirmed for the latter two examples of Calabi-Yau three-folds is, in fact, more generally true. Starting with the Weierstraß phase of an elliptic fibration over a dP_n, $n = 0, \ldots, 8$ base, the phase related to this one by flopping away all n $\mathbb{P}^1$-cycles in the base, is of the swiss-cheese type. To prove this, we show that we can define $n + 2$ divisors such that the triple intersection form is diagonal. Before the flop transition we have the pull-back divisors $\pi^*(E_i) = \mathrm{dP}_9$. After the flop transition, these lose the $\mathbb{P}^1$ given by $\mathcal{B} \cap \pi^*(E_i)$ and we get $\Gamma_i := \pi^*(E_i)_{\mathrm{flop}} = \mathrm{dP}_8$ for $i = 1, \ldots, n$. Clearly, these divisors satisfy

$$\Gamma_i^3 = 1\ ,\qquad \Gamma_i \cap \Gamma_j = 0\quad \text{for } i \neq j\ . \tag{123}$$

The former base $\mathcal{B} = \mathrm{dP}_n$ is now just $\mathbb{P}^2$ so that we define $\Gamma_\mathcal{B} := \mathcal{B}_{\mathrm{flop}} = \mathbb{P}^2$. Since we have flopped away the intersection locus with the $\pi^*(E_i)$, we can write

$$\Gamma_\mathcal{B}^3 = \mathcal{B}_{\mathrm{flop}}^3 = c_1^2(\mathbb{P}^2)\,\mathcal{B}_{\mathrm{flop}} = 9, \qquad \Gamma_\mathcal{B} \cap \Gamma_i = 0 . \tag{124}$$

For the remaining divisor we start with the former tri-section $3(\mathcal{B}+3\pi^*(l)-\sum_i \pi^*(E_i))$ and realise that, after the flop transition, this divisors gains an extra of $3n$ $\mathbb{P}^1$s. Therefore, this divisor cannot be diagonal to the ones introduced so far. However, we can define the new divisor

$$\begin{aligned}
\Gamma_0 &= 3(\mathcal{B} + 3\pi^*(l) - \sum_i \pi^*(E_i))_{\mathrm{flop}} + 3\sum_i \pi^*(E_i)_{\mathrm{flop}} \\
&= 3(\mathcal{B}_{\mathrm{flop}} + 3\pi^*(l)),
\end{aligned} \tag{125}$$

which satisfies

$$\Gamma_0^3 = 243, \qquad \Gamma_0 \cap \Gamma_i = 0, \qquad \Gamma_0 \cap \Gamma_\mathcal{B} = 0 . \tag{126}$$

Therefore, we have found a basis of $(n+2)$ divisors which diagonalise the triple intersection form. Taking into account that except Γ_0 all four-cycles are shrinkable to a point, we expect that inside the Kähler cone, we can write the volume of the Calabi-Yau in the swiss cheese form eq. (115). Apparently, the two former toric Calabi-Yau manifolds are only two specific examples.

For realising the LARGE volume scenario it is not necessary to have a Calabi-Yau having the strong swiss-cheese type property [65] as in (115). Therefore, one can also discuss the case that from the n initial $\pi^*(E_i)$ divisors of the type dP_9 only r have been flopped to the dP_8 phase. Since dP_9 is not shrinkable to a point, one does not expect a swiss-cheese type structure for them, but along the same lines as above one can still write the volume as

$$\mathcal{V} = \mathcal{V}\left(M_{n-r}^{(\mathrm{dP}_9)^{n-r}}\right) - \sum_{i=1}^{r} (\tau_i)^{\frac{3}{2}} . \tag{127}$$

where $M_{n-r}^{(\mathrm{dP}_9)^{n-r}}$ denotes the Weierstraß phase of the elliptic fibration over dP_{n-r}.

4.6 D-Term Conditions For D7-Branes on Del Pezzo Surfaces

In this section we have introduced a specific class of manifolds which admit shrinkable del Pezzo surfaces as divisors. In the following we like to address the question

whether we can wrap D7-branes on these surfaces and stabilise their volume at sizes significantly larger than the string scale by demanding a vanishing D-term, eq. (39).

Let us denote the del Pezzo surface with a wrapped D7-brane by (D_{dP}, L_{dP}) and its orientifold image by (D'_{dP}, L'_{dP}). In the following discussion it is crucial to again distinguish the three cases defined at the beginning of Subsection 2.1, page 11. We will focus on the cases 2 and 3 where D_{dP} and D'_{dP} are in the same homology class. This implies that D_{dP} cannot support B_- moduli and the D-term arises entirely from the gauging X_{aI} given in (37). The precise form of X_{aI} depends on the choice of four-cycles to define the coordinates T_I. Let us focus on the swiss-cheese examples of Subsection 4.5. We have argued in eqns. (123)–(126) that one can choose a four-cycle basis $\Gamma_0, \Gamma_{\mathcal{B}}, \Gamma_i$ of $H_4(Y)$ such that the triple intersection form reads

$$I_3 = 243\,\Gamma_0^3 + 9\,\Gamma_{\mathcal{B}}^3 + \sum_i \Gamma_i^3 \; . \tag{128}$$

The $\Gamma_{\mathcal{B}}$ and Γ_i are del Pezzo surfaces, and hence are the candidate D_{dP} for an appropriate orientifold projection. We use this basis in the expansion of the Kähler form $J = -r_{dP}[D_{dP}] + \ldots$, where $r_{dP} > 0$ in the Kähler cone. The coordinate T_{dP} associated to D_{dP} is then given by

$$\mathrm{Re}\,T_{dP} = \frac{1}{2}e^{-\phi}\int_{D_{dP}} J \wedge J \; \sim \; r_{dP}^2 \; , \tag{129}$$

and the Kähler potential for the fields G^i, T_I takes the form

$$K = -2\ln(\mathcal{V}_{\mathrm{red}} - (T_{dP} + \bar{T}_{dP})^{\frac{3}{2}}) \; , \tag{130}$$

where we have used eq. (115). The important point is that $\mathcal{V}_{\mathrm{red}}$ is independent of the moduli T_{dP} and only depends on the remaining G^i, T_I. We can also evaluate the Killing vector in the basis $\Gamma_0, \Gamma_{\mathcal{B}}, \Gamma_i$ and find that it diagonalises in the T_{dP} direction with the only non-trivial contribution

$$X_{dP} = \int_{D_{dP}} [D_{dP}] \wedge c_1(\widetilde{L}_{dP}) \; . \tag{131}$$

Using these equations it is straightforward to evaluate the D-term

$$\xi_{dP} \; \sim \; r_{dP} \; , \tag{132}$$

which thus has to vanish for a supersymmetric vacuum $\xi_{dP} = 0$. This implies that we are taken to the point $r_{dP} \to 0$, where the size of the del Pezzo surface becomes of order string scale.

59

Entering a small volume regime implies that our classical analysis is no longer valid and additional corrections need to be included. In particular, as in the underlying $\mathcal{N} = 2$ theory, world-sheet instantons will correct the expressions. However, these corrections will not alter the fact that $\partial_{T_{dP}} K \sim r_{dP}$ but rather correct the definition of the $\mathcal{N} = 1$ coordinate T_{dP} [62]. Thus, if one still uses the eq. (131) for the Killing vector one is unavoidably driven to the point where r_{dP} is small. This is precisely the regime, where for the local building the techniques of quiver gauge theories on dP_r singularities are relevant [74, 75, 29, 30, 76]. Thus, the global models we presented provide a concrete embedding of these local constructions.

The question now is how general our findings are. One might naively think that whenever one has shrinkable dP_r, $r \leq 8$ surfaces the triple intersection form has the swiss-cheese form eq. (127) so that for GUT branes on these cycles, one is driven to the quiver locus. In Section 7 we will present another class of del Pezzo transitions, based on the Quintic, in which we will instead find mutually intersecting dP_r surfaces, which therefore do *not* diagonalise the triple intersection form. Therefore, it is not the shrink-ability of the del Pezzo surfaces but rather the swiss-cheese form of the triple intersection form which is responsible for the D-term minimisation at the quiver locus.

5   A GUT Model on $\mathbf{M}_2^{(\mathrm{dP_9})^2}$

In this section we investigate whether the simple geometries with orientifold involutions introduced in the last section are already sufficient to construct realistic, globally consistent intersecting D7-brane GUT models. We work out one toy example in some detail which exemplifies the necessary steps to build a realistic model. This will illustrate the important role played by the structure of the manifold to satisfy the constraints from Table 3. The discussion of this section also serves as a preparation for the construction of two three-generation GUT models in Section 6 on related geometries.

Concretely, we consider the Calabi-Yau manifold $M_2^{(\mathrm{dP_9})^2}$ of Subsection 4.3 and choose as the orientifold involution $\Omega\sigma(-1)^{F_L}$ with $\sigma : x_3 \to -x_3$. As discussed previously, the fixed point locus consists of the disjoint divisors $\pi^*(E_1)$ and $\pi^*(l - E_2)$ and four additional fixed points. To cancel the D7-brane tadpole eq. (13), we introduce D7-branes on the divisors

$$D_a = \pi^*(E_1), \qquad D_b = \pi^*(l - E_1 - E_2), \qquad D_c = \pi^*(l - E_2), \qquad (133)$$

and denote the corresponding embeddings $\iota_j : D_j \hookrightarrow Y$. Recall from Subsection 4.3 that D_a, D_b are dP$_9$ surfaces while D_c is a K3 surface. The O7-tadpole $8\big(\pi^*(l - E_2) + \pi^*(E_1)\big)$ is cancelled by three stacks of D7-branes with multiplicities

$$N \times D_a + (N - 4) \times D_b + (8 - N) \times D_c, \qquad N = 4, 5, 6, 7, 8 \tag{134}$$

together with their orientifold images wrapping the same divisors. The resulting gauge group is $SO(2N) \times SP(2N - 8) \times SO(16 - 2N)$. Note that the last stack has vanishing intersection with the first two stacks, and will be hidden from the visible sector. The next step is to break the first two gauge groups by turning on non-trivial line-bundles in $U(N) \times U(N - 4)$.

5.1 The Chiral Model

For now, let us first focus on the chiral sector of the theory and solely compute chiral indices. The computation of the entire cohomology classes is postponed to Subsection 5.4. As our initial Ansatz for the line bundles on the divisors, we will pick all three to be restrictions of global line bundles,

$$
\begin{aligned}
L_a &= \iota_a^* \, \mathcal{O}_Y\Big(k\mathcal{B} + \pi^*(\widetilde{\eta}_a)\Big), \\
L_b &= \iota_b^* \, \mathcal{O}_Y\Big(k\mathcal{B} + \pi^*(\widetilde{\eta}_b)\Big), \\
L_c &= \iota_c^* \, \mathcal{O}_Y\Big(m\mathcal{B} + \pi^*(\eta_c)\Big).
\end{aligned}
\tag{135}
$$

In the following, we will be forced to modify this Ansatz by line bundles that are trivial in $H^2(Y, \mathbb{Z})$. However, this changes only the vector-like pairs but not the chiral spectrum.

Since D_a and D_b are not *Spin*, it is convenient to explicitly split off a factor $\sqrt{K}$ from $\widetilde{\eta}_{a,b}$. Note that one can rewrite

$$\sqrt{K_{D_a}} = \sqrt{\mathcal{O}_{D_a}(-f)} = \iota_a^*\sqrt{\mathcal{O}_Y(-D_a)} = \iota_a^* \, \mathcal{O}_Y\big(-\tfrac{1}{2}\pi^*(E_1)\big) \tag{136}$$

and similarly for D_b. Hence, let us set

$$\widetilde{\eta}_a = \eta_a - \frac{1}{2}E_1, \quad \widetilde{\eta}_b = \eta_b - \frac{1}{2}(l - E_1 - E_2). \tag{137}$$

With these definitions, we have parametrised the line bundles by

$$k, l, m \in \tfrac{1}{2}\mathbb{Z}, \quad \eta_a \in H_2\big(D_a, \tfrac{1}{2}\mathbb{Z}\big), \quad \eta_b \in H_2\big(D_b, \tfrac{1}{2}\mathbb{Z}\big), \quad \eta_c \in H_2\big(D_c, \tfrac{1}{2}\mathbb{Z}\big). \tag{138}$$

Moreover, for vanishing B_+-field all have to be integral. For non-zero discrete B_+-flux, they have to satisfy the quantisation condition eq. (8).

In view of the rules form Table 1 it is straightforward to compute the resulting chiral spectrum, and we list it in Table 7. Let us make a couple of remarks concerning

number	$U(N)$	$U(N-4)$	$U(8-N)$
$-2k$	$\boxminus_{(2)}$	1	1
$-2k$	1	$\square\square_{(2)}$	1
$-2k$	$\overline{\square}_{(-1)}$	$\overline{\square}_{(-1)}$	1

Table 7: *Chiral spectrum for intersecting D7-brane model. The indices denote the $U(1)$ charges.*

this spectrum: The third stack does not carry any chiral modes and is completely hidden from the first two. Moreover, the cubic $SU(N)$ and $SU(N-4)$ anomalies are indeed cancelled. Analysing the Abelian and mixed Abelian–non-Abelian anomalies, we find that the linear combination $U(1)_X = \frac{1}{N}U(1)_a + \frac{1}{N-4}U(1)_b$ is anomaly-free. However, due to the Green-Schwarz mass terms, it can nevertheless receive a mass by mixing with an axionic mode. In fact, this is the case as long as the first Chern classes of the line bundles are independent as elements in $H^2(Y)$ [54], and there is no massless $U(1)$ prior to breaking $SU(5)$ to the Standard Model. Intriguingly, for $N = 5$ we get an $SU(5)$ model with $N_{\text{gen}} = -2k$ generations of Standard Model particles. The $2k$ states in the symmetric representation of $U(1)_b$ carry the quantum numbers of right-handed neutrinos. So far we have not required D-term supersymmetry of the configuration. For this, one has to ensure that one can choose the Kähler moduli inside the Kähler cone. We will come to this in Subsection 5.3.

5.2 D3-Brane Tadpole and K-Theory Constraints

In this subsection, we now investigate the D3-brane tadpole cancellation condition in some more detail. As we have seen, this condition plays no role for the cancellation of the non-Abelian anomalies. In absence of three-form flux the general equation (22) is evaluated to be

$$N_{D3} + N_{\text{gauge}} = 10, \tag{139}$$

where the contribution from the $U(1)$ fluxes on the D7-branes

$$
\begin{aligned}
N_{\text{gauge}} &= -\frac{1}{2} \sum_i N_i \int_{D_i} c_1^2(L_i) \\
&= k\Big[(N-2)\,k - N\,E_1 \cdot \widetilde{\eta}_a - (N-4)\,(l - E_1 - E_2) \cdot \widetilde{\eta}_b\Big] \\
&\quad + m\Big[(8-N)\,m - (8-N)\,(l - E_2) \cdot \eta_c\Big]
\end{aligned}
\tag{140}
$$

Clearly, for half-integer k, m and pull-back classes $\pi^*(\eta_{a,b,c})$, this is not always an integer. In this case we simply cannot cancel this tadpole by introducing an integer number of filler D3-branes. Only models with $N_{\text{gauge}} \in \mathbb{Z}$ can be tad-pole free.

Let us now turn to the K-theory constraints. As discussed, these can be determined by the SP-probe brane argument and cancellation of the Witten anomaly. In general, the identification of all potential SP-branes is not an easy task and it is often hard to decide if one has not missed a $\mathbb{Z}_2$ constraint. As pointed out previously, since we do not have a CFT description, it not straightforward to decide whether a invariant four-cycle supports SO or SP Chan-Paton factors. Our strategy is to start from the branes on the O-planes, that is, $\pi^*(E_1)$ and $\pi^*(l - E_2)$, from which we know that they carry SO Chan-Paton factors. A four-cycle with locally four Neumann-Dirichlet boundary conditions relative to the O-planes is expected to carry SP Chan-Paton factors. Consider the divisor $\pi^*(l - E_1 - E_2)$, which wraps the toroidal fibre and intersects $\pi^*(E_1)$ in a point in the four-dimensional base $\mathcal{B}$. There, we expect that a brane wrapped on $\pi^*(l - E_1 - E_2)$ carries SP Chan-Paton factors. This identification is further supported by the chiral spectrum in Table 7, where the $a'a$ sector leads to fields in the anti-symmetric representation, whereas the $b'b$ sector leads to symmetric ones.

This line of reasoning identifies three 4-cycles supporting symplectic Chan-Paton factors, namely

$$
\mathcal{B}, \qquad \pi^*(E_2), \qquad \pi^*(l - E_1 - E_2).
\tag{141}
$$

All of these divisors are not *Spin* and, therefore, they have to carry a half-integral bundle to comply with the Freed-Witten quantisation condition. As usual, under the action of Ω the field strength gets reflected, in which case the candidates in eq. (141) actually carry $U(N)$ Chan-Paton factors. However, by turning on quantised B-flux through some cycles in $H_2(Y, \mathbb{Z})$, the quantisation conditions on the divisors can change, in which case vanishing gauge flux is allowed resulting in a non-trivial $\mathbb{Z}_2$ K-theory constraint.

5.3 D-Flatness

According to the general discussion in Subsection 2.4, the FI-terms for $U(1)_a$ and $U(1)_b$ are given by

$$
\begin{aligned}
\xi_a &\sim k(r_1 - r_\mathcal{B}) + r_\mathcal{B}\, E_1 \cdot \widetilde{\eta}_a, \\
\xi_b &\sim k(r_l - r_1 - r_2 - r_\mathcal{B}) + r_\mathcal{B}\,(l - E_1 - E_2) \cdot \widetilde{\eta}_b, \\
\xi_c &\sim m(r_l - r_2 - 2\,r_\mathcal{B}) + r_\mathcal{B}\,(l - E_2) \cdot \eta_c,
\end{aligned}
\tag{142}
$$

where we have expanded

$$
J = r_\mathcal{B}\,\mathcal{B} + r_l\,\pi^*(l) - r_1\,\pi^*(E_1) - r_2\,\pi^*(E_2).
\tag{143}
$$

Since we do not want to give VEVs to Standard Model fields charged under $U(1)_a$ respectively $U(1)_b$, we have to require that the two FI-terms eq. (142) vanish. We have to make sure that the resulting constraints define a plane inside the Kähler cone of this triangulation

$$
r_\mathcal{B} > 0, \qquad r_1 - r_\mathcal{B} > 0, \qquad r_2 - r_\mathcal{B} > 0, \qquad r_l - r_1 - r_2 - r_\mathcal{B} > 0.
\tag{144}
$$

However, we are actually interested in a slightly weaker condition. Since the top Yukawa coupling $\mathbf{10\,10\,5}_H$ is of order one, the coupling-generating instanton necessarily has to be in the non-perturbative regime. In fact, we would like to achieve vanishing (classical) volume of the 4-cycle wrapped by the instanton, corresponding to a particular boundary of the Kähler cone. Note that world-sheet instanton corrections are expected to eventually fix the size at the order of the string scale. Of course, for the model to make sense the gauge couplings of all space-time filling D7-branes should stay finite, which can be achieved in presence of non-trivial gauge flux.

Note that, even if one has satisfied the D7- and D5-brane tadpole cancellation conditions guaranteeing already cancellation of non-Abelian anomalies, the extra conditions of

- integer D3-brane tadpole contribution of the gauge fluxes on the D7-branes,

- a number of $\mathbb{Z}_2$ K-theory constraints, and

- satisfying the D-flatness conditions inside or at most on the boundary of the Kähler cone

provide further strong constraints. On the Calabi-Yau threefold $M_2^{(\mathrm{dP}_9)^2}$, we have not succeeded in realising a $SU(5)$ GUT model with an odd number of generations. One either does not satisfy the first condition above or lands on an unacceptable boundary of the Kähler cone in the sense that the volume of the Calabi-Yau manifold vanishes. The best example we have found by our manual search on $M_2^{(\mathrm{dP}_9)^2}$ will be detailed in the next section. Having said this, we will resolve the described problems for concrete examples on the related manifold $M_2^{(\mathrm{dP}_8)^2}$ in Section 6.

5.4 Globally Consistent Model

We now fix[23] $N = 5$, leading to a gauge group $U(5) \times U(1) \times SO(6)$. For an odd number of generations we would have to consider an orientifold without vector structure but with discrete NS-NS two-form flux $\int_F B = \frac{1}{2}$. As mentioned, in this case we did not succeed in satisfying integer D3-brane tadpole contribution of the gauge flux and D-flatness inside the Kähler cone. Therefore, we will settle for a model with an even number of generations and choose

$$c_1(B) = \frac{1}{2}\pi^*(E_1). \tag{145}$$

In particular, this satisfies $\int_F B = 0$ and, therefore, $k \in \mathbb{Z}$ must be integral.

Now we choose the line bundles on the three stacks of D7-branes to be

$$
\begin{aligned}
L_a &= \iota_a^* \, \mathcal{O}_Y\Big(-\mathcal{B} - \pi^*(E_1) \Big), \\
L_b &= \iota_b^* \, \mathcal{O}_Y\Big(-\mathcal{B} \Big), \\
L_c &= \iota_c^* \, \mathcal{O}_Y.
\end{aligned}
\tag{146}
$$

For explicitness, let us check the quantisation eq. (8). On the dP$_9$ surfaces, we will use the standard basis

$$H_2\big(\mathrm{dP}_9, \mathbb{Z}\big) = \mathrm{span}_\mathbb{Z}\big\{l, e_1, \ldots, e_9\big\}. \tag{147}$$

Each such surface D_a, D_b is elliptically fibred with fibre class $f = 3l - \sum e_i$ and zero-section

$$\mathcal{B} \cap D_a = e_9 \in H_2\big(D_a, \mathbb{Z}\big), \quad \mathcal{B} \cap D_b = e_9 \in H_2\big(D_b, \mathbb{Z}\big). \tag{148}$$

---

[23]That is, $N_a = 5$, $N_b = 1$, and $N_c = 3$.

Noting that the B-flux eq. (145) restricts trivially on the four-cycle D_c, one finds that

$$
\begin{array}{ccccccc}
D_j: & c_1(L_j) & - & B|_{D_j} & + & \tfrac{1}{2}c_1(K_{D_j}) & \in H_2(D_j, \mathbb{Z}) \\
\hline
D_a = \pi^*(E_1): & -e_9 + f & - & (-\tfrac{1}{2}f) & + & \tfrac{1}{2}(-f) & \in H_2(D_a, \mathbb{Z}) \\
D_b = \pi^*(l - E_1 - E_2): & -e_9 & - & \tfrac{1}{2}f & + & \tfrac{1}{2}(-f) & \in H_2(D_b, \mathbb{Z}) \\
D_c = \pi^*(l - E_2): & 0 & - & 0 & + & 0 & \in H_2(D_c, \mathbb{Z}),
\end{array}
\tag{149}
$$

and the bundles are, indeed, correctly quantised. For this choice, the contribution to the D3-brane tadpole is

$$
N_{\text{gauge}} = -\frac{1}{2} \sum_i N_i \int_{D_i} c_1^2(L_i) = 8 \tag{150}
$$

and we can cancel this tadpole, for example, by two dynamical D3-brane carrying $SP(4)$ gauge group. However, according to eq. (59), this cannot be the final answer as we will get an additional contribution from the $U(1)_Y$ flux.

A D7-brane wrapping the divisor $\pi^*(l - E_1 - E_2)$ now carries integer quantised gauge flux. Therefore, the gauge bundle can be chosen to be trivial leading to an SP-brane. For such a probe brane we get a Witten anomaly respectively expect a K-theory constraint. It is easy to see that the above choice of branes and line bundles gives indeed a even number of fundamental SP-representations. The B-flux eq. (145) does not restrict to the other candidate SP cycles, $\mathcal{B}$ and $\pi^*(E_2)$ so that a trivial line bundle does not exist. Consequently no further conditions arise.

The supersymmetry conditions become

$$
\xi_a = r_1 - 2\,r_\sigma = 0, \quad \xi_b = r_l - r_1 - r_2 - r_\sigma = 0. \tag{151}
$$

The first condition can be satisfied inside the Kähler cone whereas the second condition lies on the boundary of the Kähler cone where the 2-cycle $C = l - E_1 - E_2$ inside dP$_2$ has zero size. As we will explain in detail in the following, this is exactly as desired, and there exists a D3-instanton wrapping $\pi^*(l - E_1 - E_2)$ and generating the top-Yukawa couplings. Due to the non-trivial line bundle on the brane D_b, we find for the $U(1)$ gauge coupling on this brane

$$
\frac{1}{g_b^2} \sim -\int_{D_b} c_1^2(L_b) = O(1), \tag{152}
$$

which stays finite but, thankfully, leaves the perturbative regime.

Non-chiral SU(5) spectrum

We now move forward and compute the vector-like matter spectrum as well. First, we turn to the GUT brane. To compute the relevant bundle cohomology groups, we first evaluate the pull-back in the definition of the line bundles eq. (146). One obtains

$$
\begin{aligned}
L_a &= \iota_a^* \, \mathcal{O}_Y\Big(-\mathcal{B} - \pi^*(E_1)\Big) = \mathcal{O}_{D_a}\Big(\big(-\mathcal{B} - \pi^*(E_1)\big) \cap D_a\Big) \\
&= \mathcal{O}_{D_a}\big(-e_9 + f\big), \\
L_b &= \mathcal{O}_{D_b}\big(-e_9\big), \\
L_c &= \mathcal{O}_{D_c}.
\end{aligned}
\tag{153}
$$

For the $SU(5)$ matter, we now have to compute the cohomology of powers of L_a. Using Appendix C, we easily find

$$
H^*\Big(\mathrm{dP}_9, L_a^\vee \otimes L_a^\vee\Big) = (0,4,0), \qquad H^*\Big(\mathrm{dP}_9, L_a \otimes L_a\Big) = (0,6,0).
\tag{154}
$$

Thus we get two chiral and four vector-like pairs of matter fields in the anti-symmetric representation **10** of $SU(5)$.

Next, let us consider the states in the symmetric representation **1** of $U(1)$, that is, the right-handed neutrinos. Since the bundle $(L_b^\vee)^2$ has sections, we get unwelcome non-trivial elements in $\mathrm{Ext}^0(\iota_* L_b^\vee, \iota_* L_b)$ which would render the theory inconsistent. In order to get rid of these, we now use the freedom to twist this pull-back bundle by a bundle R_b whose push-forward is trivial in Y. In particular, we pick

$$
R_a = \mathcal{O}_{D_a}, \quad R_b = \mathcal{O}_{D_b}(-e_1 + e_2), \quad R_c = \mathcal{O}_{D_c}
\tag{155}
$$

and replace the bundle on D_i, $i = \{a, b, c\}$, with the tensor product

$$
L_i \longrightarrow \widetilde{L}_i = L_i \otimes R_i.
\tag{156}
$$

As explained previously, this modification does not change the chiral matter content. However, the twisting with R_b yields an extra contribution to the D3-tadpole eq. (150), which is now

$$
N_{\mathrm{gauge}} = -\sum_i N_i \int_{D_i} \mathrm{ch}_2\big(L_i \otimes R_i\big) = 9.
\tag{157}
$$

The spectrum is, now,

$$
H^*\Big(\mathrm{dP}_9, (L_b^\vee)^2 \otimes (R_b^\vee)^2\Big) = (0,4,0), \qquad H^*\Big(\mathrm{dP}_9, (L_a)^2 \otimes (R_b)^2\Big) = (0,6,0),
\tag{158}
$$

yielding two chiral and two vector-like pairs.

Finally, consider the matter fields in the $\overline{\mathbf{5}}$ representation, which are localised on the curve

$$D_a \cap D_b = F, \tag{159}$$

that is, on an elliptic fibre $\mathbb{P}_{1,2,3}[6] \subset Y$. We first need to pull-back the bundles via the inclusion $\iota_F : F \to D_a$ and D_b, respectively. Note that the specific fibre F is, viewed as a curve in D_a or D_b, in the fibre class f. In order to label its intersection points with the sections $e_1, \ldots, e_9$, let us define

$$\begin{aligned}
p_1 &= \iota_a(e_1) \cap F, \quad p_2 = \iota_a(e_2) \cap F, \quad \ldots, \quad p_8 = \iota_a(e_8) \cap F, \\
p_1' &= \iota_b(e_1) \cap F, \quad p_2' = \iota_b(e_2) \cap F, \quad \ldots, \quad p_8' = \iota_b(e_8) \cap F, \\
0 &= \iota_a(e_9) \cap F = \iota_b(e_9) \cap F = \mathcal{B} \cap F.
\end{aligned} \tag{160}$$

Here we have implicitly fixed some of the complex structure moduli of the manifold such that indeed the sections of D_a and D_b intersect F in the same points. Using this notation, we obtain

$$\begin{aligned}
L_a|_F &= \iota_F^* L_a = \mathcal{O}_F\Big(\big(-e_9 + f\big) \cap F\Big) = \mathcal{O}_F\big(-0\big), \\
\big(L_b \otimes R_b\big)|_F &= \mathcal{O}_F(-0 - p_1' + p_2').
\end{aligned} \tag{161}$$

With $K_F = \mathcal{O}_F$ we can easily compute the $\overline{\mathbf{5}}$-spectrum, and obtain

$$\begin{aligned}
H^*\Big(F, \iota_F^*\big(L_a^\vee \otimes (L_b \otimes R_b)^\vee\big)\Big) &= H^*\Big(F, \mathcal{O}_F(0 + 0 + p_1' - p_2')\Big) \\
&= H^*\Big(F, \mathcal{O}_F(2\text{pts.})\Big) = (2, 0).
\end{aligned} \tag{162}$$

Hence, we get precisely 2 chiral fields in the anti-fundamental representation. The Higgs $\mathbf{5}_H + \overline{\mathbf{5}}_H$-spectrum, on the other hand, is determined by

$$H^*\Big(F, \iota_F^*\big(L_a^\vee \otimes (L_b \otimes R_b)\big)\Big) = H^*\Big(F, \mathcal{O}_F(-p_1' + p_2')\Big) = (0, 0). \tag{163}$$

One might worry that there is no candidate $\mathbf{5}_H - \overline{\mathbf{5}}_H$ pair giving rise to the Higgs after symmetry breaking; However, as we will see in the following, turning on a suitable L_Y flux will generate one vector-like pair as desired.

Instanton effects

A Euclidean D3-brane wrapping the divisor $\pi^*(l - E_1 - E_2)$ with trivial line bundle is of $O(1)$ type and clearly rigid. Therefore, this instanton is a candidate to generate

the $\mathbf{10}\,\mathbf{10}\,\mathbf{5_H}$ Yukawa couplings. For the chiral charged matter zero modes, we indeed get $I_{a,\text{inst}} = 1$ and $I_{b,\text{inst}} = -1$. Therefore, the necessary condition eq. (45) for the generation of the top Yukawa coupling is satisfied. Moreover, the line bundle on the divisor $D_b = \pi^*(l - E_1 - E_2)$ has first Chern class $c_1(L_b \otimes R_b) = -e_9 - e_1 + e_2$, and therefore

$$H^*\big(D_b, L_b \otimes R_b\big) = (0, 1, 0), \quad H^*\big(D_b, L_b^\vee \otimes R_b^\vee\big) = (0, 0, 0). \tag{164}$$

This implies $\text{Ext}^*(L_b \otimes R_b, \mathcal{O}_{D_b}) = (0, 1, 0, 0)$ and shows that there exists precisely one chiral zero mode λ_b without any additional vector-like pairs. Since the instanton intersects the brane D_a over the fibre curve, we find exactly one chiral zero mode λ_a. Moreover, the D-term constraint for the brane D_b has fixed the Kähler moduli such that the instanton action goes to zero; it follows that leaving (locally) the perturbative regime, the top Yukawa couplings are really of order one.

To generate Majorana neutrino masses, one needs an $O(1)$ instanton intersecting only the brane stack D_b. A candidate would be a Euclidean D3-brane wrapping the divisor $\pi^*(E_2)$. However, since this divisor is not *Spin*, it is not of $O(1)$ but $U(1)$ type.

Non-chiral $\mathbf{SU(3)} \times \mathbf{SU(2)} \times \mathbf{U(1)_Y}$ spectrum

Finally, let us break the $SU(5)$ gauge symmetry to the Standard Model. To do so, we will turn on $U(1)_Y$ gauge flux supported on a curve in $H_2(D_a, \mathbb{Z})$ which is a boundary on Y. In particular, we pick

$$\mathcal{L}_a = L_a, \quad \mathcal{L}_Y = \mathcal{O}_{D_a}(-e_1 + e_2). \tag{165}$$

The $\mathcal{L}_Y$ bundle has vanishing cohomology classes on $D_a = \text{dP}_9$, and, therefore, no exotics are introduced. The contribution to the D3-tadpole from this flux is

$$N_{\text{gauge}}^Y = -\int_{D_a} c_1^2(\mathcal{L}_Y) = 2. \tag{166}$$

The combined gauge flux contribution to the D3 tadpole is $N_{\text{gauge}} = 9 + 2 = 11$, overshooting by one unit. Therefore, to cancel this tadpole, one needs to introduce one dynamical anti–D3-brane.

The relevant cohomology classes for the descendants of the antisymmetric representation $\mathbf{10}$ of $SU(5)$ are listed in Table 8. Note that, of course, the chiral matter

GUT	SM Field	Cohomology		chiral	vector
10	$(\overline{\mathbf{3}}, \mathbf{1})_{-4_Y}$	$H^*(D_a, (\mathcal{L}_a^\vee)^2)$	$= (0, 4, 0)$	2	4+4
		$H^*(D_a, \mathcal{L}_a^2)$	$= (0, 6, 0)$		
	$(\mathbf{3}, \mathbf{2})_{1_Y}$	$H^*(D_a, (\mathcal{L}_a^\vee)^2 \otimes \mathcal{L}_Y^{-1})$	$= (0, 5, 0)$	2	5+5
		$H^*(D_a, \mathcal{L}_a^2 \otimes \mathcal{L}_Y)$	$= (0, 7, 0)$		
	$(\mathbf{1}, \mathbf{1})_{6_Y}$	$H^*(D_a, (\mathcal{L}_a^\vee)^2 \otimes \mathcal{L}_Y^{-2})$	$= (0, 8, 0)$	2	8+8
		$H^*(D_a, \mathcal{L}_a^2 \otimes \mathcal{L}_Y^2)$	$= (0, 10, 0)$		
1	$(\mathbf{1}, \mathbf{1})_{0_Y}$	$H^*(D_b, (L_b^\vee \otimes R_b^\vee)^2)$	$= (0, 4, 0)$	2	4+4
		$H^*(D_b, L_b^2 \otimes R_b^2)$	$= (0, 6, 0)$		
$\overline{\mathbf{5}}$	$(\overline{\mathbf{3}}, \mathbf{1})_{2_Y}$	eq. (168a)	$= (2, 0)$	2	0
	$(\mathbf{1}, \mathbf{2})_{-3_Y}$	eq. (168b)	$= (2, 0)$	2	0
$\mathbf{5}_H + \overline{\mathbf{5}}_H$	$(\mathbf{3}, \mathbf{1})_{-2_Y}$	$H^*(F, \mathcal{O}_F(-p_1' + p_2'))$	$= (0, 0)$	0	0
	$(\mathbf{1}, \mathbf{2})_{3_Y}$	$H^*(F, \mathcal{O}_F)$	$= (1, 1)$	0	1+1

Table 8: *Spectrum for the orientifold model in Section 5. The indices denote the $U(1)$ charges.*

does not change; only extra vector-like pairs of matter fields appear. We now turn toward the matter fields in the anti-fundamental representation $\overline{\mathbf{5}}$ as well as the Higgs, both of which are localised on the intersection curve F. In addition to eq. (161), we have

$$\iota_F^* \mathcal{L}_Y = \mathcal{L}_Y|_F = \mathcal{O}_F\big(-p_1 + p_2\big). \tag{167}$$

First, note that the $\overline{\mathbf{5}}$-spectrum is unchanged since

$$H^*\Big(F, \iota_F^*\big(\mathcal{L}_a^\vee \otimes L_b^\vee \otimes R_b^\vee\big)\Big) = H^*\Big(\mathcal{O}_F(0 + 0 + p_1' - p_2')\Big) = (2, 0), \tag{168a}$$

$$H^*\Big(F, \iota_F^*\big(\mathcal{L}_a^\vee \otimes L_b^\vee \otimes R_b^\vee \otimes \mathcal{L}_Y^\vee\big)\Big) = H^*\Big(\mathcal{O}_F(2 \cdot 0 + p_1 + p_1' - p_2 - p_2')\Big) = (2, 0). \tag{168b}$$

More interesting is the Higgs spectrum, which is determined by

$$\iota_F^*\big(\mathcal{L}_a^\vee \otimes (L_b \otimes R_b) \otimes \mathcal{L}_Y^\vee\big) = \mathcal{O}_F(p_1 - p_1' + p_2 - p_2') = \mathcal{O}_F(0 - q) \tag{169}$$

for some point $q \in F$. The precise point can be computed using the group law on the elliptic curve F, and will depend on the complex structure of D_a, D_b (and, therefore, Y). We assume that $q = 0$, which happens on a locus of codimension one in the complex structure moduli space; See also the discussion around eq. (160). In this case,

$$H^*\Big(F, \iota_F^*\big(\mathcal{L}_a^\vee \otimes (L_b \otimes R_b) \otimes \mathcal{L}_Y^\vee\big)\Big) = H^*\Big(F, \mathcal{O}_F\Big) = (1, 1). \tag{170}$$

As desired, we then obtain one pair of Higgs-conjugate Higgs fields. Moreover, the Higgs doublet is, in fact, split from the dangerous colour triplet. The latter is still absent, thanks to

$$H^*\Big(F, \iota_F^*\big(\mathcal{L}_a^\vee \otimes (L_b \otimes R_b)\big)\Big) = H^*\Big(F, \mathcal{O}_F(-p_1' + p_2')\Big) = (0, 0). \tag{171}$$

To summarise, we have defined a simple involution on $M_2^{(\mathrm{dP}_9)^2}$ which allows for the introduction of a three-stack intersecting D7-brane configuration cancelling the D7-, D5- and D3-brane tadpoles, the latter at the cost of introducing one anti D3-brane, as well as the K-theory tadpoles. We have found an $SU(5)$ GUT-like model with two chiral generations of Standard Model particles and one Higgs-conjugate Higgs pair. Moreover, we have been able to realise the $U(1)_Y$ flux gauge symmetry breaking and computed the resulting chiral and non-chiral matter spectrum. The inevitable appearance of the latter is one of the shortcomings of this example. It can be traced back to the fact that our involution acts trivially on the cohomology $H^2(Y, \mathbb{Z})$. As a

consequence, antisymmetric matter is localised not on a curve but on a whole divisor, widening the sources of contributions to the cohomology. By contrast, matter and Higgs are localised on the elliptic fibre of Y. Since the Higgs H_u and H_d are localised on the same curve, we cannot suppress dimension-five proton decay operators. The D-term supersymmetry conditions can be satisfied on the boundary of Kähler moduli space such that a D3-brane instanton realises $\mathbf{10\,10\,5}$ Yukawa couplings of order 1. In Table 9 we summarise phenomenologically desirable features of this simple model.

property	mechanism	status
globally consistent	tadpoles + K-theory	$\checkmark^{*,**}$
D-term susy	vanishing FI-terms inside Kähler cone	$\checkmark^{***}$
gauge group $SU(5)$	$U(5) \times U(1)$ stacks	$\checkmark$
3 chiral generations	choice of line bundles	$-$
no vector-like matter	localisation on curves	$-$
1 vector-like of Higgs	choice of line bundles	$\checkmark^{****}$
no adjoints	rigid 4-cycles, del Pezzo	$\checkmark$
GUT breaking	$U(1)_Y$ flux on trivial 2-cycles	$\checkmark$
3-2 splitting	Wilson lines on $g = 1$ curve	$\checkmark$
3-2 split + no dim=5 p-decay	local. of H_u, H_d on disjoint comp.	$-$
$\mathbf{10\,\overline{5}\,\overline{5}}_H$ Yukawa	perturbative	$\checkmark$
$\mathbf{10\,10\,5}_H$ Yukawa	presence of appropriate D3-instanton	$\checkmark$
Majorana neutrino masses	presence of appropriate D3-instanton	$-^{*****}$

Table 9: *Summary of $SU(5)$ properties realised in the model of Section 5.*
* overshooting in D3-tadpole $\to$ 1 $\overline{D3}$ brane
** K-theory to the best of our ability to detect SP cycles
*** realised on acceptable boundary of Kähler moduli space
**** for special choice of complex structure moduli
***** at least not with O(1) instantons

6   GUT Model Search

The model presented in the previous section does not exhibit all properties desirable for a nice string GUT model. However, as for each single shortcoming it is quite clear how to improve on this. The non-trivial task is to achieve this in a globally consistent framework and without loosing the good features already realised. To this end a more systematic search is necessary and beyond the scope of this paper. In this section we provide a couple of manually found models which incorporate some other desirable properties from Table 3, but come short on already realised ones. The two features we focus on in this section are 3 chiral families and the absence of vector-like matter fields.

6.1   A 3-Generation GUT Model on $M_2^{(\mathrm{dP}_8)^2}$

We now present an example of a GUT model of the type described previously which indeed gives rise to 3 chiral families of Standard Model matter. To this end we consider the manifold $M_2^{(\mathrm{dP}_8)^2}$ introduced in Subsection 4.3. Since the intersection form eq. (102) differs considerably from the one of the un-flopped Weierstraß phase, eq. (86), it seems plausible that the no-go result for an odd number of generations can be evaded.

We closely follow the philosophy spelt out in Section 5 so that we can be brief. Concretely, consider again a 3-stack model based on the divisors $D_a = D_7$, $D_b = D_5$ and $D_c = D_5 + D_7$, wrapped by D7-branes with multiplicities

$$N \times D_7, \qquad (N-4) \times D_5, \qquad (8-N) \times (D_5 + D_7), \qquad (172)$$

plus their orientifold images, with $N = 5$ corresponding to the GUT model we are interested in. The above configuration satisfies the $D7$-brane tadpole constraint for any N.

Let us first define the chiral $SU(5)$ GUT model by parametrising the part of line bundles L_a, L_b and L_c descending from the Calabi-Yau Y as

$$L_a = \iota_a^* \mathcal{O}_Y \Big(a_1 D_5 + a_3 D_7 \Big), \quad L_b = \iota_b^* \mathcal{O}_Y \Big(\sum_{i=1}^4 b_i D_{i+4} \Big), \qquad (173)$$

$$L_c = \iota_c^* \mathcal{O}_Y \Big(c_1 D_1 + c_2 D_2 + c_4 D_4 \Big).$$

For the correct definition of the bundles it is essential to take into account that this time all three divisors are not *Spin*. According to the quantisation condition

73

eq. (7) for vanishing B-field the parameters b_1, a_3, c_1 are therefore half-integer while $a_1, b_2, b_3, b_4, c_2, c_4$ are integer.

As can be computed from the intersection form eq. (102), the divisors D_a and D_b still intersect along a genus 1 curve where the 5 and the $\mathbf{5}_H + \overline{\mathbf{5}}_H$ are localised. Note also that the divisors D_c and D_a do not intersect, while D_c and D_b now intersect along a genus 0 curve. Thus there exists no massless exotic matter in the $D_a - D_c$ sector, even at the vector-like level, while there might appear truly hidden sector matter fields from the $D_b - D_c$ intersection. This chiral matter is displayed in Table 10. Clearly all non-Abelian anomalies vanish due to cancellation of D7- and absence of D5-brane tadpoles. Note that for general bundles there exist both symmetric and anti-symmetric states under $U(N-4)$. In what follows we specialise to the case $N = 5$ corresponding to a GUT model with the first four lines representing the $\mathbf{10}$, $\overline{\mathbf{5}}$, $\mathbf{5_H} + \overline{\mathbf{5}}_\mathbf{H}$ and N_R^c.

chirality	$U(N)$	$U(N-4)$	$U(8-N)$
$-2a_1 + 2a_3$	$\boxminus_{(2)}$	1	1
$-(a_1 + b_1) + a_3 + b_3$	$\overline{\square}_{(-1)}$	$\overline{\square}_{(-1)}$	1
$-(a_1 - b_1) + (a_3 - b_3)$	$\overline{\square}_{(-1)}$	$\square_{(1)}$	1
$2(-b_1 + b_3)$	1	$\boxminus\!\boxminus_{(2)}$	1
$2(-b_1 + b_2 + b_4)$	1	$\boxminus_{(2)}$	1
$(b_1 - c_1) - (b_2 - c_2) - (b_4 - c_4)$	1	$\overline{\square}_{(-1)}$	$\square_{(1)}$
$(b_1 + c_1) - (b_2 + c_2) - (b_4 + c_4)$	1	$\overline{\square}_{(-1)}$	$\overline{\square}_{(-1)}$
$2(-c_1 + c_2 + c_4)$	1	1	$\boxminus_{(2)}$

Table 10: *Chiral spectrum for intersecting D7-brane model. The indices denote the $U(1)$ charges.*

Global consistency conditions

The D3-brane tadpole condition is

$$N_{D3} + N_{\text{gauge}} = 10, \tag{174}$$

with N_{gauge} given by

$$
\begin{aligned}
-\frac{1}{2} \sum_a N_a \, c_1^2(L_a) \;=\;& -\frac{5}{2} \left(a_1^2 + a_3^2 - 2a_1 a_3 \right) - \frac{3}{2} \left(-c_1^2 + 2c_1 c_2 - 3c_2^2 + 2c_1 c_4 - c_4^2 \right) \\
& - \frac{1}{2} \left(-2b_1^2 + 2b_1 b_2 - 3b_2^2 + 2b_1 b_3 - b_3^2 + 2b_1 b_4 - b_4^2 \right).
\end{aligned} \tag{175}
$$

Note, however, that there will be additional contributions later on from the part of the line bundles trivial on the ambient space Y. As in the previous section, due to the simple structure of the orientifold action, the D5-brane tadpoles cancel automatically between the branes and their image.

On the other hand, there can arise K-theory constraints from the 3 invariant divisors D_6, D_8 and D_5 which may carry symplectic Chan-Paton factors. The divisor D_6 is the former basis dP_2 of the Weierstraß model $M_2^{(\text{dP}_9)^2}$ with the two $\mathbb{P}^1$s removed. As such it is the surface $\mathbb{P}^2$ with $K_{D6} = \mathcal{O}_{D6}(3)$ and obviously not *Spin*. This means that, according to eq. (7), the chiral part of a line bundle on D_6

$$
L_{D_6} = \iota^* \mathcal{O}_Y \left(x_1 D_5 + x_2 D_6 \right) \tag{176}
$$

can be trivial only for $B = 0 \times D_5 + \frac{1}{2} D_6 + \ldots$. Otherwise the cycle does not carry symplectic gauge factors and therefore no K-theory constraint arises from D_6.

The K-theory constraint from D_6 therefore reads

$$
b_1 + 3c_1 - 3(b_2 + 3c_2) \in 2\mathbb{Z} \quad \text{if} \quad B = 0 \times D_5 + \frac{1}{2} D_6. \tag{177}
$$

A similar analysis for D_8 and D_5 yields the two additional constraints

$$
b_1 + 3c_1 - (b_4 + 3c_4) \in 2\mathbb{Z} \quad \text{if} \quad B = 0 \times D_5 + \frac{1}{2} D_8,
$$
$$
5a_1 - 5a_3 - 2(b_1 + 3c_1) + (b_2 + 3c_2) + b_3 + (b_4 + 3c_4) + 3c_1 \in 2\mathbb{Z} \tag{178}
$$
$$
\text{if} \quad B = \frac{1}{2} D_5 + 0 \times (D_6 + D_7 + D_8).
$$

In all other cases the K-theory constraints from these three divisors are trivial.

D-term supersymmetry constraints

To determine the D-term supersymmetry conditions we have to expand the Kähler form J in terms of the generators of the full Kähler cone and evaluate the Fayet-Iliopoulos terms. For our purposes it will be sufficient to restrict our attention to

the Kähler subcone corresponding to the vectors K_i displayed in eq. (101) and take

$$J = \sum_i r_i K_i, \qquad r_i \in \mathbb{R}_+. \tag{179}$$

As discussed around eq. (101), it suffices to check if the associated FI-terms

$$
\begin{aligned}
\xi_a &\simeq (a_1 - a_3)r_1, \\
\xi_b &\simeq b_2 r_4 + b_3 r_1 - b_1 r_2 + b_4 r_2 + b_1 r_3, \\
\xi_c &\simeq c_2 r_4 + c_4 r_2 + c_1 (r_1 - r_2 + r_3)
\end{aligned} \tag{180}
$$

vanish for some values of $r_i > 0$ for which in addition $r_1 - r_2 + r_3 > 0$.

A 3-generation GUT model

As a quick search reveals it is indeed possible to find globally consistent supersymmetric models with 3 chiral generations of SU(5) GUT matter. As one example out of the O(100) models we found we present the configuration with non-vanishing B-field

$$B = \frac{1}{2}D_5 + \frac{1}{2}D_7 \tag{181}$$

and line bundles

$$
\begin{aligned}
L_a &= \iota_a^* \mathcal{O}_Y \Big(-\frac{7}{2}D_5 - 2D_7 \Big), \\
L_b &= \iota_b^* \mathcal{O}_Y \Big(-D_5 - D_6 + \frac{1}{2}D_7 \Big), \\
L_c &= \iota_c^* \mathcal{O}_Y \Big(-D_5 \Big).
\end{aligned} \tag{182}
$$

According to Table 10 this choice yields precisely 3 chiral GUT families of $\mathbf{10}$, $\overline{\mathbf{5}}$ and N_R^c with no chiral exotics. In addition there is chiral hidden matter as summarised in Table 11.

The contributions to the D3-brane tadpole of this GUT model is

$$N_{\text{gauge}} = -\frac{5}{2} \cdot \frac{9}{4} + \frac{1}{2} \cdot \frac{17}{4} + \frac{3}{2} \cdot \frac{4}{4} = -2 \tag{183}$$

so that at this stage we would need to add $N_{D3} = 12$ dynamical D3-branes. Note that it is suspicious that the contribution of the gauge flux on the $SU(5)$ brane to

76

chirality	$U(5)$	$U(1)$	$U(3)$
3	$\yng(1,1)_{(2)}$	1	1
3	$\overline{\square}_{(-1)}$	$\overline{\square}_{(-1)}$	1
3	1	$\yng(2)_{(2)}$	1
1	1	$\overline{\square}_{(-1)}$	$\square_{(1)}$
1	1	$\square_{(1)}$	$\square_{(1)}$
2	1	1	$\yng(1,1)_{(2)}$

Table 11: *Chiral spectrum for intersecting D7-brane model with indices denoting the $U(1)$ charges. The last three lines are completely hidden chiral matter.*

the D3-brane tadpole is negative. Indeed, we will see in a moment that this bundle leads to ghosts. We will avoid this conclusion by twisting it by an additional bundle R_a which is trivial on Y.

For the above choice of B-field the K-theory constraints from D_5, D_6, D_8 are vacuous. As expected from the general consideration in Subsection 4.6, the D-term constraint for D_a drives us to the boundary of Kähler moduli space in that it requires $r_1 = 0$. The general solution of the three D-term equations for the Kähler moduli is

$$r_1 = 0, \quad r_2 = x, \quad r_3 = x, \quad r_4 = 0. \tag{184}$$

For positive x this solution lies on the boundary of Kähler moduli space in that besides $r_1 = 0$ and $r_4 = 0$ also the volume of the generator C^5 of the Mori cone vanishes. In this regime the classical volume of the divisor D_7 vanishes, while all other brane volumes and the total volume of the Calabi-Yau are positive. Note that for this model the classical value of the GUT gauge coupling is $\alpha_{GUT}^{-1} \simeq -c_1^2(L_a) < 0$, which we have just seen to be negative. This is another indication that the model is pathological in its present form and will be rectified momentarily by twisting L_a further.

GUT breaking and SU(3) × SU(2) × U(1) spectrum

To break the GUT symmetry to $SU(3) \times SU(2) \times U(1)_Y$ and to compute the vector-like MSSM spectrum we need the explicit pushforward and pullback maps ι_* and ι^* between the second (co)homology of D_7 and the ambient space Y. Recall that D_7 is a dP$_8$ surface with $H_2(D_7, \mathbb{Z})$ spanned by $h, e_1, \ldots e_8$. The pushforward $\iota_* : H_2(D_7, \mathbb{Z}) \to H_2(Y, \mathbb{Z})$ follows immediately once one takes into account that relative to $\pi^*(E_1) = \mathrm{dP}_9$ the curve $\mathcal{B}E_1$ is flopped away in the present phase. Explicitly,

$$\iota_*(e_i) = f, \quad i = 1, \ldots 8, \qquad \iota_*(h) = 3f, \tag{185}$$

where $-f \in H_2(Y, \mathbb{Z})$ now denotes the class of the curve $D_7 \cap D_7$ in Y. This in turn follows from $\iota^* D_7 = K_{D_7} = -3h + \sum e_i$ together with the identity $\iota_* \iota^* = 1$. Finally one completes the pullback map to

$$\iota^* D_7 = -3h + \sum_{i=1}^{8} e_i, \qquad \iota^* D_5 = 3h - \sum_{i=1}^{8} e_i \tag{186}$$

and all others vanishing. Therefore, one finds for the pullback of $c_1(L_a)$ to D_7

$$c_1(L_a) = -\frac{3}{2} \left(3h - \sum_{i=1}^{8} e_i \right). \tag{187}$$

For this bundle we can now compute

$$H^* \big(\mathrm{dP}_8, L_a^\vee \otimes L_a^\vee \big) = (7, 0, 0), \qquad H^* \big(\mathrm{dP}_8, L_a \otimes L_a \big) = (0, 0, 4), \tag{188}$$

which implies $\mathrm{Ext}^*(\iota_* L_a^\vee, \iota_* L_a) = (7, 4, 0, 0)$. Therefore, this line bundle on the $SU(5)$ stack leads to ghosts in the spectrum. Since the Kähler form is on the boundary of the Kähler cone this is not in contradiction with the no-ghost theorem from Subsection 2.4. However, we still have the freedom to tensor L_a with a line bundle R_a which is trivial on the ambient space Y. This does not change the chiral spectrum but the non-chiral one.

This freedom can be used to choose the bundles $\mathcal{L}_a = L_a \otimes R_a$ and $\mathcal{L}_Y$ as

$$c_1(\mathcal{L}_a) = \frac{1}{2} \left(-h + \sum_{i=1}^{4} e_i - \sum_{i=5}^{8} e_i \right), \qquad c_1(\mathcal{L}_Y) = -e_1 + e_5. \tag{189}$$

This configuration leads to the multiplicities displayed in Table 12 for the decomposition of the **10** into MSSM states. For its computation see Appendix B. Note the appearance of only two extra vector-like states.

repr.	extension	spectrum
$(\overline{\mathbf{3}}, \mathbf{1})_{-4_Y}$	$\mathrm{Ext}^*(\mathcal{L}_a^\vee, \mathcal{L}_a)$	$(0, 1, 4, 0)$
$(\mathbf{3}, \mathbf{2})_{1_Y}$	$\mathrm{Ext}^*(\mathcal{L}_a^\vee \otimes \mathcal{L}_Y^{-1}, \mathcal{L}_a)$	$(0, 0, 3, 0)$
$(\mathbf{1}, \mathbf{1})_{6_Y}$	$\mathrm{Ext}^*(\mathcal{L}_a^\vee \otimes \mathcal{L}_Y^{-2}, \mathcal{L}_a)$	$(0, 1, 4, 0)$

Table 12: *Multiplicities of MSSM descendants from the SU(5)* **10**.

To compute the MSSM descendants of the $\overline{\mathbf{5}}$ we recall that the divisors D_7 and D_5 intersect again along a genus 1 curve F with $c_1(\mathcal{L}_Y|_F) = 0$. We will make use of our freedom to twist also L_b by a line bundle R_b which is trivial on the Calabi-Yau Y and define

$$\mathcal{L}_b = L_b \otimes R_b. \tag{190}$$

Since R_b is trivial on Y this does not change the chiral spectrum. Irrespective of its form we find $c_1\left(\mathcal{L}_a^\vee \otimes \mathcal{L}_b^\vee|_{D_5 \cap D_7}\right) = 3$, leading to precisely 3 multiplets of $(\overline{\mathbf{3}}, \mathbf{1})_{2Y}$ and $(\mathbf{1}, \mathbf{2})_{-3Y}$ and no extra vector-like states.

On the other hand we will choose R_b such that the Wilson lines for the bundles $\mathcal{L}_a^\vee \otimes \mathcal{L}_b|_{D_5 \cap D_7}$ and $\mathcal{L}_a^\vee \otimes \mathcal{L}_Y^\vee \otimes \mathcal{L}_b|_{D_5 \cap D_7}$ give rise to precisely one pair of Higgs doublets and no Higgs triplet. To this end we recall that D_5 is a $\mathbb{P}^2$ surface with 11 points blown up to a $\mathbb{P}^1$, and in analogy with the notation for del Pezzo surfaces $H^2(D_5, \mathbb{Z})$ is spanned by $h, e_1, \ldots e_9, E_{10}, E_{11}$. Here E_{10} and E_{11} denote the extra two $\mathbb{P}^1$ which have been flopped into D_5 in the present phase. For a special choice of complex structure moduli the elliptic curve $D_5 \cap D_7$ intersects $h, e_1, \ldots e_8$ in the same points as the classes[24] $h, e_1, \ldots e_8$ in $H^2(D_7)$. It is then clear that, given the choice eq. (189) for $\mathcal{L}_a$ and $\mathcal{L}_Y$, we have to pick

$$R_b = \mathcal{O}(4h - 2e_1 - e_2 - e_3 - e_4 - e_5 - 2e_6 - 2e_7 - 2e_8) \tag{191}$$

on D_5 to comply with the requirement stated in equation (65).

The twist with the bundles R_a, R_b and the addition of the bundle $\mathcal{L}_Y$ change the overall contributions of the gauge fluxes to the D3-brane tadpole. These now read

$$N_{\text{gauge}} = \frac{5}{2} \cdot \frac{7}{4} + \frac{1}{2} \cdot \left(\frac{17}{4} + 4\right) + \frac{3}{2} = 10. \tag{192}$$

---

[24]This is actually more than we need since we only have to ensure that the sum of the Wilson lines add up to zero to engineer one Higgs pair.

This time N_{gauge} precisely equals the D3-brane charge of the orientifold planes, and cancellation of the full D3-brane tadpole is possible in a supersymmetric manner without introducing further $D3$-branes. Moreover, note that despite the vanishing volume of the GUT divisor $D_7 = \text{dP}_8$, the gauge coupling now comes out positive.

Finally, one might wonder about the existence of ghosts on the $U(1)$ and $U(3)$ branes since we have not been able to satisfy all three D-term supersymmetry conditions inside the Kähler cone. On the other hand, one can convince oneself that it is possible to satisfy the supersymmetry conditions inside the Kähler cone for each of the line bundles L_b and L_c separately. This is already enough for our lemma in Subsection 2.4 to guarantee absence of states in Ext^0 and Ext^3.

Instanton effects

The existence of a model with three chiral generations of MSSM matter rested upon the choice eq. (181) for the B-field. The downside of this choice is that none of the invariant divisors D_5, D_6, D_8 allows for trivial line bundles. As a consequence there exist no divisors that would give rise to symplectic gauge groups for spacetime-filling branes, and thus no $O(1)$ instantons. To decide if neutrino Majorana masses or the $\mathbf{10\,10\,5_H}$ coupling are generated non-perturbatively we would therefore have to study the effects of D3-brane instantons wrapping non-invariant cycles, for example along the lines of [77]. This, however, is beyond the scope of the present work.

We conclude this section by summarising the key phenomenological properties of our model in Table 13.

6.2 A GUT Model on $\mathbf{M}_3^{(\text{dP}_9)^3}$

In this section we investigate whether we can build a GUT model, where the $\mathbf{10}$ representation is also localised on a curve. This is expected to avoid the appearance of extra vector-like states.

Concretely, we consider the elliptic fibration over the dP$_3$ base in the Weierstraß phase with the section $\mathcal{B} = \text{dP}_3$ and the six dP$_9$ pull-back divisors $\pi^*(E_1)$, $\pi^*(E_2)$, $\pi^*(E_3)$, $\pi^*(l - E_1 - E_2)$, $\pi^*(l - E_1 - E_3)$ and $\pi^*(l - E_2 - E_3)$. Moreover, we choose

property	mechanism	status
globally consistent	tadpoles + K-theory	✓*
D-term susy	vanishing FI-terms inside Kähler cone	✓**
gauge group $SU(5)$	$U(5) \times U(1)$ stacks	✓
3 chiral generations	choice of line bundles	✓
no vector-like matter	localisation on $\mathbb{P}^1$ curves	−
1 vector-like of Higgs	choice of line bundles	✓***
no adjoints	rigid 4-cycles, del Pezzo	✓
GUT breaking	$U(1)_Y$ flux on trivial 2-cycles	✓
3-2 splitting	Wilson lines on $g = 1$ curve	✓
3-2 split + no dim=5 p-decay	local. of H_u, H_d on disjoint comp.	−
$\mathbf{10\,\overline{5}\,\overline{5}_H}$ Yukawa	perturbative	✓
$\mathbf{10\,10\,5_H}$ Yukawa	presence of appropriate D3-instanton	−****
Majorana neutrino masses	presence of appropriate D3-instanton	−****

Table 13: *Summary of $SU(5)$ properties realised in the model of Subsection 6.1.*
* K-theory to the best of our ability to detect SP cycles
** realised on acceptable boundary of Kähler cone
*** for special choice of complex structure moduli
**** at least not with O(1) instantons

the involution acting as

$$
\begin{pmatrix} l \\ E_1 \\ E_2 \\ E_3 \end{pmatrix} \mapsto \begin{pmatrix} 2l - E_1 - E_2 - E_3 \\ l - E_1 - E_3 \\ l - E_2 - E_3 \\ l - E_1 - E_2 \end{pmatrix}
\tag{193}
$$

on the dP$_3$. The orientifold $O7$-plane wraps the divisor

$$
D_{O7} = \pi^*(2l - E_1 - E_2)
\tag{194}
$$

which has $\chi(D_{O7}) = 48$. Since there are no fixed points for this involution, there are no O3-planes. and the contribution of the curvature terms to the $D3$ tadpole condition is $N_{D3} + N_{flux} = 12$.

Kähler cone

Expanding the Kähler form as

$$
J = r_\mathcal{B}\,\mathcal{B} + r_l\,\pi^*(l) - r_1\,\pi^*(E_1) - r_2\,\pi^*(E_2) - r_3\,\pi^*(E_3)\;.
\tag{195}
$$

the Kähler cone is simply

$$
r_\mathcal{B} > 0, \quad r_i - r_\mathcal{B} > 0, \quad r_l - r_i - r_j - r_\mathcal{B} > 0, \qquad i < j \in \{1,2,3\}\;.
\tag{196}
$$

However, the involution σ has $h_-^{1,1} = 2$, so that we expect that two of these five Kähler moduli are fixed. Indeed, requiring that J is invariant under σ yields the two relations

$$
r_1 = r_2, \qquad r_l = 2\,r_2 + r_3\;.
\tag{197}
$$

We are only left with three dynamical Kähler moduli.

In addition, in this case we have two B_- moduli. With the general Ansatz

$$
B_- = b_\mathcal{B}\,\mathcal{B} + b_l\,\pi^*(l) - b_1\,\pi^*(E_1) - b_2\,\pi^*(E_2) - b_3\,\pi^*(E_3)
\tag{198}
$$

subject to $\sigma(B_-) = -B_-$ we obtain the three constraints

$$
b_\mathcal{B} = 0, \qquad b_l = b_3 \qquad b_1 = 2\,b_3 - b_2\;.
\tag{199}
$$

Tadpole cancellation

To cancel the D7-brane tadpole eq. (13) we introduce three stacks of D7-branes on the divisors

$$
\begin{aligned}
D_a &= \pi^*(E_2) , & D_a' &= \pi^*(l - E_2 - E_3), \\
D_b &= \pi^*(l - E_1) , & D_b' &= \pi^*(l - E_2), \\
D_c &= \pi^*(E_3) , & D_c' &= \pi^*(l - E_1 - E_2).
\end{aligned}
\tag{200}
$$

As for the line bundles it is convenient to split off the continuous B_--moduli by writing $c_1(\widetilde{L}) = c_1(L) - B_-$. Choosing the $\mathcal{B}$ part of the line bundles on these divisors as

$$
c_1(\widetilde{L}_a) = 3k\mathcal{B} + \pi^*(\eta_a), \quad c_1(\widetilde{L}_b) = -5k\mathcal{B} + \pi^*(\eta_b), \quad c_1(\widetilde{L}_c) = -3k\mathcal{B} + \pi^*(\eta_c), \tag{201}
$$

cancels also the D5-brane tadpole. The resulting chiral spectrum is listed in Table 14.

number	$U(5)$	$U(3)$	$U(5)$
$6k$	$\boxbar_{(2)}$	1	1
$2k$	$\overline{\square}_{(-1)}$	$\overline{\square}_{(-1)}$	1
$10k$	1	$\overline{\boxbar}_{(-2)}$	1

Table 14: *Chiral spectrum for intersecting D7-brane model. The indices denote the $U(1)$ charges.*

Some remarks are in order concerning this spectrum: One gets precisely $6k$ generations of $\overline{\mathbf{10}}$ and, taking into account the extra multiplicities due to the $U(3)$ stack, $2k \times 3$ generations of $\overline{\mathbf{5}}$, but without right-handed neutrinos. In fact we found that none of the pull-back divisors carries symplectic Chan-Paton factors. In this model the flavour group is gauged. Moreover, since E_2 and $l - E_1$ do not intersect there are *no massless Higgs fields in the* (ab) *sector*. However in the (ac') sector, vanishing Wilson-lines along the elliptic fibre imply that we obtain one vector-like matter field in the $(\mathbf{5}, \mathbf{1}, \mathbf{5}) + (\overline{\mathbf{5}}, \mathbf{1}, \overline{\mathbf{5}})$ representation. These carry the GUT quantum numbers to be identified with five pairs of Higgs fields. As mentioned in Subsection 3.1,

since the Higgs and $\overline{\mathbf{5}}$ matter fields are charged under different U(1) groups also the bottom-type Yukawa couplings need to be realised by D3-brane instantons. Clearly, this is not a completely realistic model, but some rough features are realised and in particular the massless matter states in the anti-symmetric representation of $SU(5)$ are localised on the fibre F of the elliptic fibration. The minimal choice $k = \frac{1}{2}$ gives already three generations.

Three generation model

Taking now the quantisation conditions for the gauge fluxes into account and turning on half-integer B-field flux through the fibre, that is, $c_1(B) = \frac{1}{2}\mathcal{B}$, we choose

$$
\begin{aligned}
c_1(\widetilde{L}_a) &= \frac{3}{2}\mathcal{B} + \frac{3}{2}\pi^*(E_2), \quad c_1(\widetilde{L}_b) = -\frac{5}{2}\mathcal{B} + 5\,\pi^*(E_1), \\
c_1(\widetilde{L}_c) &= -\frac{3}{2}\mathcal{B} - \frac{3}{2}\pi^*(E_3)
\end{aligned}
\tag{202}
$$

for the line bundles.

The D-term constraints

$$
\int_{D_a} J \wedge \left(c_1(\widetilde{L}_a) + B_- \right) = 0
\tag{203}
$$

for all three brane stacks give three constraints which can all be solved inside the Kähler cone provided

$$
r_{\mathcal{B}} > 0 \qquad -\frac{3}{2} < b_2 < \frac{3}{2} \ .
\tag{204}
$$

The contributions of each of the three stacks to the D3-tadpole condition are positive and add up as

$$
N_{\mathrm{gauge}} = \frac{3 \cdot 45}{8} + \frac{3 \cdot 75}{4} + \frac{3 \cdot 45}{8} = 90 \gg 12 \ .
\tag{205}
$$

Here we see explicitly that eventually the B_- field drops out so that one ends up really with an integer contribution. Clearly this is a massive overshooting and requires the introduction of anti D3-branes. Finally, for $c_1(B) = \frac{1}{2}\mathcal{B}$ the divisor $\mathcal{B}$ can carry a trivial line bundle and is expected to have SP Chan-Paton factors. The resulting global Witten anomaly (K-theory) constraint is satisfied.

Non-chiral spectrum and GUT breaking

Nevertheless, the purpose was to demonstrate that by choosing non-diagonal involutions, it is (in principle) possible to have also the matter in the antisymmetric representation of $SU(5)$ localised on a curve. In fact here all matter is localised in the fibre elliptic curve $C = F$ with trivial canonical line-bundle. From that it immediately follows that there is no vector-like matter in the $\mathbf{10} + \overline{\mathbf{5}}$ representation. Since the $U(5)$ stack is a rigid dP_9 surface, we can break the $SU(5)$ GUT gauge symmetry to the Standard Model gauge group by turning on $U(1)_Y$ flux of the form $\mathcal{L}_Y = \mathcal{O}(e_1 - e_2)$. In contrast to the first two examples we presented, this does not give any new vector-like matter. As for the Higgs sector, we are now in the favourable situation that the bundles $\tilde{L}_a$ and $\tilde{L}_b$ are both pullbacks from the ambient space. According to the discussion around eq. (66) it therefore suffices to twist $\tilde{L}_a$ by $R_a = \mathcal{L}_Y^{-1}$ to arrange for precisely one Higgs doublet and no Higgs triplet *without* further adjusting any complex structure moduli. Adding $\mathcal{L}_Y$ and R_a results in an additional 3 units of D3-brane charge in the D3-tadpole equation.

Summary of features

Let us summarise in Table 15 which of the desired features we were able to realise in this simple model.

7 GUTs on Del Pezzo Transitions of the Quintic

So far we have studied GUT models on descendants of the elliptic fibration Calabi-Yau $\mathbb{P}_{1,1,1,6,9}[18]$. We have gone a long way to eventually arrive at GUT like examples featuring many of the desired properties. One of the general aspects of these models was that for the $SU(5)$ GUT stack localised on a shrinkable dP_8 surface the D-term conditions in conjunction with the swiss-cheese property of the triple intersection form force the GUT four-cycle to collapse to string scale size, that is, to the quiver locus. If this were a generic feature of all Calabi-Yau orientifolds containing shrinkable surfaces, it would clearly have strong implications for model building.

The clarification of this point is one of our motivations for studying another class of Calabi-Yau manifolds containing del Pezzo surfaces. Instead of starting with the elliptic fibration $\mathbb{P}_{1,1,1,6,9}[18]$, we take the simple Quintic $\mathbb{P}_{1,1,1,1,1}[5]$ and perform del Pezzo transitions. The mathematics of this construction is collected in Subsection 7.1

property	mechanism	status
globally consistent	tadpoles + K-theory	$\checkmark^{*,**}$
D-term susy	vanishing FI-terms inside Kähler cone	$\checkmark$
gauge group $SU(5)$	$U(5) \times U(3)$ stacks	$\checkmark$
3 chiral generations	choice of line bundles	$\checkmark$
no vector-like matter	localisation on g=1 curves	$\checkmark$
5 vector-like Higgs	choice of line bundles	$\checkmark$
no adjoints	rigid 4-cycles, del Pezzo	$\checkmark$
GUT breaking	$U(1)_Y$ flux on trivial 2-cycles	$\checkmark$
3-2 splitting	Wilson lines on $g=1$ curve	$\checkmark$
3-2 split + no dim=5 p-decay	local. of H_u, H_d on disjoint comp.	$-$
$\mathbf{10\,\overline{5}\,\overline{5}_H}$ Yukawa	presence of appropriate D3-instanton	$-^{***}$
$\mathbf{10\,10\,5_H}$ Yukawa	presence of appropriate D3-instanton	$-^{***}$
Majorana neutrino masses	presence of appropriate D3-instanton	$-^{***}$

Table 15: *Summary of $SU(5)$ properties realised in the model of Subsection 6.2.*
* overshooting in D3-tadpole $\rightarrow \overline{D}$3-branes
** K-theory to the best of our ability to detect SP cycles
*** at least not with $O(1)$ instantons

with the result that here we can get intersecting dP_r, $r \leq 8$ surfaces, so that the triple intersection forms do not have the diagonal swiss-cheese type structure. In Subsection 7.2 we provide one more example of a GUT model, for which all Standard Model matter is really localised on curves of genus zero and one, respectively.

7.1 Del Pezzo Transitions of the Quintic

In this section we introduce a class of compact Calabi-Yau manifolds which can be obtained from the quintic hypersurface by performing del Pezzo transitions. Again these spaces will be realised as hypersurfaces in an ambient toric manifold. It will turn out that the del Pezzo surfaces arising after the transitions can intersect and thus are ideal candidates for supporting intersecting D7-branes.

The toric data and intersection forms

Let us first give the points in the polyhedron for the toric ambient spaces. The hypersurface is then determined to have the anti-canonical class given by the sum of all toric divisors as in Subsection 4.2. The quintic hypersurface has the points $v_1^* = (-1, 0, 0, 0)$, $v_2^* = (0, -1, 0, 0)$ $v_3^* = (0, 0, -1, 0)$, $v_4^* = (0, 0, 0, -1)$ and $v_5^* = (1, 1, 1, 1)$. Its Hodge numbers are $h^{1,1} = 1$ and $h^{2,1} = 101$. By arranging some of the $h^{2,1}$ complex structure deformations in the hypersurface constraint one can generate del Pezzo singularities and blow up del Pezzo surfaces. This process increases $h^{1,1}$ by the number of Kähler moduli of the del Pezzo four-cycles and lowers $h^{2,1}$ since one has to fix a certain number of the complex structure moduli to generate a singularity.

As a first transition we can blow up a dP_6 surface by adding the point $v_6^* = (1, 0, 0, 0)$ to the polyhedron and consider the resulting hypersurface Q^{dP_6}. In fact, the new Calabi-Yau manifold has $h^{1,1} = 2$ and $h^{2,1} = 90$. There is only one triangulation for the ambient toric space. Using the same methods as in Subsection 4.2 one can explicitly check that the divisor D_6 is a dP_6 del Pezzo surface. The intersection form is simply

$$I_3 = 3D_6^3 + 3D_5^2 D_6 - 3D_6^2 D_5 + 2D_5^3 \ . \tag{206}$$

This Calabi-Yau is also of the strong swiss-cheese type, since the intersection form diagonalises for the transformation $(\tilde{D}_5 = D_6 - D_5, \ \tilde{D}_6 = D_6)$. This is also consistent with the fact that the dP_6 surface in this manifold is generic which can be inferred from the fact that in this transition $\Delta \chi = 24$. For generic transitions, as the ones in

Subsection 4.2 with Euler numbers eq. (79), one has $\Delta\chi = 2C_{(n)}$, where $C_{(n)}$ is the dual Coxeter number of the exceptional groups associated to dP_n.

To generate a second del Pezzo surface we add the point $v_7^* = (0,1,0,0)$ to the polyhedron. This blows up a point on the dP_6 surface D_6 to a $\mathbb{P}^1$ such that $\mathrm{dP}_6 \to \mathrm{dP}_7 \cong D_6$ and generates a second dP_7 surface D_7. The ambient toric space has one Calabi-Yau triangulation and the hypersurface, denoted by $Q^{(\mathrm{dP}_7)^2}$, has Hodge numbers $h^{1,1} = 3$ and $h^{2,1} = 79$. One can then check that the two dP_7 surfaces D_6, D_7 intersect on a $\mathbb{P}^1$. To do that one computes the triple intersection form

$$I_3 = 2D_7^3 + 2D_6^3 + 2D_5^2(D_7 + D_6) - D_7^2(2D_5 + D_6) - D_6^2(2D_5 + D_7) + D_5D_6D_7 \ . \quad (207)$$

This intersection form cannot be diagonalised due to the intersection of D_6 and D_7. In other words, the two dP_7 surfaces are not generic, but share a common $\mathbb{P}^1$. This can be also inferred from the fact that $\Delta\chi = 2 \times 24$ with respect to the quintic hypersurface. This change is expected for a transition with two generic dP_6 surfaces and corresponds to the fact that the E_6 sublattices on the two dP_7 surfaces are still trivial in the Calabi-Yau threefold. For two generic dP_7 surfaces one would find $\Delta\chi = 2 \times 36$. That only an E_6 sublattice is trivial in the Calabi-Yau can also be inferred by computing the BPS-instantons as suggested in [41]. One finds that the representations of E_7 appearing for a generic dP_7 transition are split into E_6 representations for our intersecting divisors D_6 and D_7.

We can perform a third transition by adding the point $v_8^* = (0,0,1,0)$ to the polyhedron and denote the corresponding hypersurface by $Q^{(\mathrm{dP}_8)^3}$. In this case one additional $\mathbb{P}^1$ is blown up on each dP_7 surface D_6, D_7 such that $\mathrm{dP}_7 \to \mathrm{dP}_8$. The two dP_8 surfaces D_6, D_7 intersect a new dP_8 surface D_8 in the blown-up $\mathbb{P}^1$ curves. The new toric ambient space has one triangulation, and the corresponding Calabi-Yau hypersurface has Hodge numbers $h^{1,1} = 4$ and $h^{2,1} = 68$. The intersection form is given by

$$\begin{aligned}
I_3 = {} & D_6^3 + D_7^3 + D_8^3 - D_5^3 + D_5^2(D_6 + D_7 + D_8) \\
& - D_6^2(D_5 + D_7 + D_8) - D_7^2(D_5 + D_6 + D_8) - D_8^2(D_5 + D_6 + D_7) \\
& + D_5(D_6D_8 + D_7D_8 + D_7D_6). \quad (208)
\end{aligned}$$

Once again we note that the dP_8 surfaces are non-generic, since they intersect over $\mathbb{P}^1$ curve. This is an accord with the fact that $\Delta\chi = 3 \times 24$ with respect to the quintic. In fact, one concludes that in each del Pezzo 8 surface and E_6 sublattice is trivial in the Calabi-Yau space.

Finally, we can add the point $v_9^* = (0, 0, 0, 1)$ to the polyhedron and denote the corresponding hypersurface by $Q^{(\mathrm{dP}_9)^4}$. In fact, the new Calabi-Yau space has $h^{1,1} = 5$ and $h^{2,1} = 57$ and one checks that the toric divisors D_6, D_7, D_8, D_9 are dP_9 surfaces. Clearly, this space cannot be obtained by resolving a del Pezzo singularity, since dP_9 can be only shrunk to a curve and not to a point. Nevertheless it is a viable Calabi-Yau background with intersection form

$$
\begin{aligned}
I_3 = D_5(D_6 D_8 &+ D_8 D_9 + D_6 D_9 + D_6 D_7 + D_7 D_8 + D_7 D_9) \\
&- D_6^2(D_7 + D_8 + D_9) - D_7^2(D_6 + D_8 + D_9) - D_8^2(D_6 + D_7 + D_8) \\
&- D_9^2(D_6 + D_7 + D_8) - D_5^3. \quad (209)
\end{aligned}
$$

One can check that each of the dP_9 divisors intersects the other three in a $\mathbb{P}^1$. Schematically the intersecting del Pezzo surfaces in the four manifolds Q^{dP_6}, $Q^{(\mathrm{dP}_7)^2}$, $Q^{(\mathrm{dP}_8)^3}$ and $Q^{(\mathrm{dP}_9^4)}$ are shown in Figure 3. The Euler number has changed again by 24, such that $\Delta \chi = 4 \times 24$ with respect to the quintic hypersurface. Again, this corresponds to the fact that there are four E_6 lattices on the dP_9 surfaces which are trivial in $Q^{(\mathrm{dP}_9)^4}$.

Q^{dP_6} $\qquad\qquad$ $Q^{(\mathrm{dP}_7)^2}$ $\qquad\qquad$ $Q^{(\mathrm{dP}_8)^3}$ $\qquad\qquad$ $Q^{(\mathrm{dP}_9)^4}$
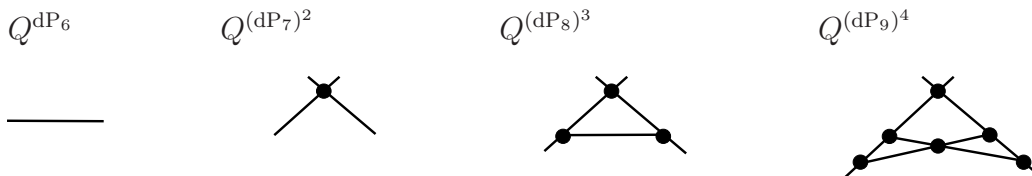
Figure 3: *Schematics of the intersecting del Pezzo surfaces on transitions of the quintic. Each intersection is a $\mathbb{P}^1$.*

Kähler cone and orientifold involution

In Sections 7.2 and 7.3 we will construct GUT models on $Q^{(\mathrm{dP}_8)^3}$ and $Q^{(\mathrm{dP}_9)^4}$ with matter and Higgs localised on curves. However, in order to determine the spectrum and check the supersymmetry conditions, we first need to calculate the Kähler cone and the orientifold involution acting on it.

Let us begin by analysing the hypersurface $Q^{(\mathrm{dP}_8)^3}$. The Mori cone is simplicial

for this Calabi-Yau phase, and generated by the vectors

	x_1	x_2	x_3	x_4	x_5	x_6	x_7	x_8	p
$\ell^{(1)}$	1	0	0	1	1	0	−1	−1	−1
$\ell^{(2)}$	0	0	0	−1	−1	1	1	1	−1
$\ell^{(3)}$	0	0	1	1	1	−1	−1	0	−1
$\ell^{(4)}$	0	1	0	1	1	−1	0	−1	−1

(210)

Its dual, the Kähler cone, is therefore again simplicial and generated by

$$
\begin{aligned}
K_1 &= 2D_5 + D_6 + D_7 + D_8, & K_2 &= D_5 + D_6, \\
K_3 &= D_5 + D_7, & K_4 &= D_5 + D_8.
\end{aligned}
$$

(211)

As before, the Kähler cone is needed in order to evaluate the D-terms in the physical region of the moduli space.

We next specify an orientifold involution σ on $Q^{(\text{dP}_8)^3}$. Explicitly, σ is given by the exchange of coordinates

$$
\sigma: \quad x_2 \leftrightarrow x_3, \quad x_7 \leftrightarrow x_8.
$$

(212)

This leads to a split $h_+^{1,1} = 3$ and $h_-^{1,1} = 1$, yielding a four-dimensional theory with 3 Kähler moduli T_I and one B_--modulus G as defined in eq. (1). The fixed point locus of this involution contains one O7-plane wrapping the four-cycle

$$
D_{O7} = D_5 + D_7 + D_8
$$

(213)

and one fixed point, $N_{O3} = 1$. Note that $\chi(D_{O7}) = 47$, and, therefore, $\chi(D_{O7}) + N_{O3}$ is indeed divisible by four.

Turning to the other Calabi-Yau phase $Q^{(\text{dP}_9)^4}$, the Mori cone is now non-simplicial

90

and generated by the vectors

	x_1	x_2	x_3	x_4	x_5	x_6	x_7	x_8	x_9	p
$\ell^{(1)}$	0	0	-1	0	-1	1	1	0	1	-1
$\ell^{(2)}$	0	1	0	1	1	-1	0	-1	0	-1
$\ell^{(3)}$	1	0	0	1	1	0	-1	-1	0	-1
$\ell^{(4)}$	-1	0	0	0	-1	0	1	1	1	-1
$\ell^{(5)}$	0	1	1	0	1	-1	0	0	-1	-1
$\ell^{(6)}$	0	0	0	-1	-1	1	1	1	0	-1
$\ell^{(7)}$	0	0	1	1	1	-1	-1	0	0	-1
$\ell^{(8)}$	1	1	0	0	1	0	0	-1	-1	-1
$\ell^{(9)}$	1	0	1	0	1	0	-1	0	-1	-1
$\ell^{(10)}$	0	-1	0	0	-1	1	0	1	1	-1

$$(214)$$

In order to define coordinates for the Kähler cone, we first discard the $\ell^{(\kappa)}$, $\kappa = 3, 4, 6, 7, 8$ and determine the dual basis of four-cycles

$$
\begin{aligned}
K_1 &= D_5 + D_6 + D_7, & K_2 &= D_5 + D_8 + D_9, \\
K_3 &= D_5 + D_6, & K_4 &= D_5 + D_7 + D_8, \\
K_5 &= D_5 + D_9.
\end{aligned}
\qquad (215)
$$

Expanding $J = \sum_i r_i K_i$ we have to take $r_i \geq 0$ in the Kähler cone. However, we note that the discarded $\ell^{(\kappa)}$ impose the additional conditions

$$
\begin{aligned}
r_3 - r_4 + r_5 \geq 0, & \qquad r_2 - r_3 + r_4 \geq 0, & \qquad r_1 + r_4 - r_5 \geq 0, \\
r_2 - r_1 + r_5 \geq 0, & \qquad r_1 - r_2 + r_3 \geq 0.
\end{aligned}
\qquad (216)
$$

We have to ensure that these conditions are satisfied when evaluating the D-terms in coordinates r_i.

Let us finally specify the involution on $Q^{(\mathrm{dP_9})^4}$. It is simply given by the exchange of $x_2 \leftrightarrow x_3$ and $x_7 \leftrightarrow x_8$, the same as in eq. (212). This leads to a split $h_+^{1,1} = 4$ and $h_-^{1,1} = 1$ and, hence, four T_I Kähler moduli and one B_--modulus G. The fixed point locus of this involution contains one O7-plane, wrapping the same linear combination as in eq. (213) and three fixed points, $N_{O3} = 3$. Note that now $\chi(D_{O7}) = 37$, and, therefore, $\chi(D_{O7}) + N_{O3}$ is again divisible by four.

7.2 A GUT Model Without Vector-Like Matter

In this section we present a $SU(5)$ GUT model with all matter realised on curves. One of our motivations to discuss this example is to illustrate that the GUT brane can indeed wrap a shrinkable dP_r, $r \leq 8$ without being driven to the quiver locus by the D-terms. Our starting point is the Calabi-Yau $Q^{(dP_8)^3}$, which contains three intersecting dP_8 surfaces. Using the notation from the previous section, we choose the involution eq. (212), which leads to an O7-plane eq. (213) and one O3-plane. In the following we will specify the D7-branes which define a GUT model with two chiral generations.

Two generation model

To cancel the D7-brane tadpole (13) we introduce three stacks of D7-branes on the divisors

$$
\begin{aligned}
U(5): \quad & D_a = D_7, & D_a' = D_8, & \quad \chi(D_a) = 11, \\
U(1): \quad & D_b = D_5, & D_b' = D_5, & \quad \chi(D_b) = 25, \\
SO(6): \quad & D_c = D_5 + D_7, & D_c' = D_5 + D_8, & \quad \chi(D_c) = 36.
\end{aligned}
\tag{217}
$$

Here we note that $D_2 = D_5 + D_7$ and $D_3 = D_5 + D_8$ are toric divisors. Then the contribution of the curvature terms to the D3-brane tadpole cancellation condition reads

$$
\frac{N_{O3}}{4} + \frac{\chi(D_{O7})}{12} + \sum_a N_a \frac{\chi_o(D_a)}{24} = \frac{1}{4} + \frac{47}{12} + \frac{5 \cdot 11 + 1 \cdot 25 + 3 \cdot 36}{24} = 12 .
\tag{218}
$$

Next, we choose $c_1(B) = \frac{1}{2}D_5$ and split off the continuous B_--moduli by writing $c_1(\widetilde{L}) = c_1(L) - B_-$. Taking into account the Freed-Witten quantisation conditions, the following choice of line bundles

$$
c_1(\widetilde{L}_a) = \frac{1}{2}D_5 + \frac{1}{2}D_7 - D_8, \quad c_1(\widetilde{L}_b) = D_5, \quad c_1(\widetilde{L}_c) = 0
\tag{219}
$$

cancels the D5-brane tadpole as well. Here we used the fact that D_7 restricts trivially to $D_c = D_5 + D_7$. The resulting chiral spectrum is listed in Table 16.

Let us make a couple of remarks concerning this spectrum: One obtains precisely two generations of MSSM particles including the right-handed neutrinos. Moreover, the states transforming in the **10** representation of $SU(5)$ are localised on the curve $D_7 \cap D_8 = \mathbb{P}^1$, so that there are no additional vector-like states. Similarly, the

number	$U(5)$	$U(1)$	$SO(6)$
2	$\Box\!\Box_{(2)}$	1	1
2	$\overline{\square}_{(-1)}$	$\square_{(1)}$	1
2	1	$\square\square_{(-2)}$	1

Table 16: *Chiral spectrum for intersecting D7-brane model. The indices denote the $U(1)$ charges.*

matter states in the $\overline{\mathbf{5}}$ representation are localised on the curve $D_7 \cap D_5 = T^2$ so that there are no vector-like states either. Moreover, as in the examples before from the $(a'b)$ sector we will get one vector-like pair of Higgs fields $\mathbf{5}_H + \overline{\mathbf{5}}_H$ by twisting L_b appropriately, see discussion at the end of this subsection. Only the right-handed neutrinos are localised on a surface, namely on D_5.

A D7-brane wrapped upon D_5 can carry a trivial line bundle so that this brane is expected to carry symplectic Chan-Paton factors. The resulting K-theory constraint

$$\int_Y [D_5] \wedge [D_7] \wedge c_1(L_a) + \int_Y [D_7] \wedge [D_5] \wedge c_1(L_b) \in 2\mathbb{Z} \tag{220}$$

is indeed satisfied for our model. The D3-tadpoles induced by each single brane stack are positive and add up as

$$N_{\text{gauge}} = \frac{5 \cdot 1}{2} + \frac{1 \cdot 1}{2} = 3 \ . \tag{221}$$

Let us next evaluate the D-term constraints. The generators K_i of the Kähler cone are given in (211). We use these to expand the Kähler form as $J = \sum_i r_i K_i$ with $r_i > 0$. Note that due to the orientifold action for the last two Kähler cone generators we have $r_3 = r_4$. In addition there exists one B_- modulus

$$B_- = b \left(D_7 - D_8 \right) \ . \tag{222}$$

The D-term constraints

$$\int_{D_i} J \wedge \left(c_1(\widetilde{L}_i) + B_- \right) = 0 \tag{223}$$

93

for all three brane stacks $i = a, b, c$ yield three conditions, which are solved on the boundary of the Kähler cone by

$$r_1 = 0, \quad r_2 = 0, \quad b = 0. \tag{224}$$

However, the volumes of the three branes involved and the overall volume are finite

$$\tau_7 = \frac{1}{2} \int_{D_7} J \wedge J = r_3^2, \qquad \tau_5 = \frac{1}{2} \int_{D_5} J \wedge J = 2\, r_3^2,$$

$$\text{Vol}(Y) = \frac{1}{6} \int_Y J \wedge J \wedge J = 2\, r_3^3, \tag{225}$$

so that we still have parametric control over the α' expansion in the brane sector.

Finally, to break the $SU(5)$ GUT group to the MSSM, we turn on the trivial line bundle $\mathcal{L}_Y$. On $D_a = D_7 = \mathrm{dP}_8$ there are now three non-trivial two-cycles. They include the two genus zero curves $\mathbb{P}^1$s from the intersection $D_7 \cap D_6$ and $D_7 \cap D_8$. In addition there exists the genus one curve $D_7 \cap D_5$ which is identical to $-D_7 \cap D_7$. Identifying $D_7 \cap D_6 = e_7$ and $D_7 \cap D_6 = e_8$ and $D_7 \cap D_5 = 3h - \sum_{i=1}^8 e_i$, we realise that the two-cycles on dP_8 trivial in Y are the ones from dP_6 orthogonal to K. By definition this is the E_6 sublattice of $H_2(\mathrm{dP}_6, \mathbb{Z})$. Therefore, choosing for instance $c_1(\mathcal{L}_Y) = e_1 - e_2$ breaks the $SU(5)$ gauge group to the Standard Model gauge group and contributes additional two units to the D3-brane tadpole. To generate one pair of Higgs doublets and project out the triplet on the elliptic curve $C = D_5 \cap D_7$ we twist $\widetilde{L}_a$ by the bundle $R_a = \mathcal{L}_Y^{-1}$ on D_7. In essence this yields yet another unit of D3-brane charge in the D3-tadpole equation and we need six dynamical D3-branes to saturate it. Since $\mathcal{L}_Y$ restricts trivially to e_7 and e_8, there are precisely two generations of charged quark and leptons without any vector like states.

As already mentioned a D7-brane on D_5 carries SP Chan-Paton factors, so that an Euclidean D3-brane instanton on the same cycle is of type $O(1)$. Indeed, such an instanton carries the right chiral zero modes $I_{a,\mathrm{inst}} = 1$ and[25] $I_{b,\mathrm{inst}} = 1$ to generate the top-Yukawa couplings. However, since the surface D_5 has $h^{(2,0)}(D_5) = 1$, it is not rigid and there can be additional vector-like zero modes from the intersection of the instanton with the D7-brane wrapping $D_b = D_5$.

We summarise in Table 17 which of the desired features we were able to realise in this simple model.

---

[25]There is a change of sign compared to (45) as here the Higgs originates from the sector $(a'b)$ instead of (ab).

property	mechanism	status
globally consistent	tadpoles + K-theory	$\checkmark^*$
D-term susy	vanishing FI-terms inside Kähler cone	$\checkmark^{**}$
gauge group $SU(5)$	$U(5) \times U(1)$ stacks	$\checkmark$
3 chiral generations	choice of line bundles	−
no vector-like matter	localisation on $g = 0, 1$ curves	$\checkmark$
5 vector-like Higgs	choice of line bundles	$\checkmark$
no adjoints	rigid 4-cycles, del Pezzo	$\checkmark$
GUT breaking	$U(1)_Y$ flux on trivial 2-cycles	$\checkmark$
3-2 splitting	Wilson lines on $g = 1$ curve	$\checkmark$
3-2 split + no dim=5 p-decay	local. of H_u, H_d on disjoint comp.	−
$10\,\overline{5}\,\overline{5}_\mathbf{H}$ Yukawa	perturbative	$\checkmark$
$10\,10\,5_\mathbf{H}$ Yukawa	presence of appropriate D3-instanton	$\checkmark^{***}$
Majorana neutrino masses	presence of appropriate D3-instanton	−****

Table 17: *SU*(5) *properties realised in the model of Subsection 7.2.*
   * *K-theory to the best of our ability to detect SP-cycles*
   ** *realised on acceptable boundary of Kähler moduli space*
   *** *up to absorption of additional vector-like zero modes*
   **** *at least not with O*(1) *instantons*

7.3 A Three-Generation Model With Localised Matter on $Q^{(\mathrm{dP_9})^4}$

While in on $Q^{(\mathrm{dP_8})^3}$ global consistency conditions are in conflict with the construction of three-generation models, on its cousin $Q^{(\mathrm{dP_9})^4}$ it turns out possible to find GUT models with three generations and all GUT matter realised on matter curves, but without running into half-integer D3 tadpoles. The construction of these models is almost identical to the two-generation example of the previous subsection, and we can be quite brief.

We again cancel the D7-brane tadpole (13) by introducing three stacks of D7-branes on the divisors

$$
\begin{array}{llll}
U(5): & D_a = D_7, & D'_a = D_8, & \chi(D_7) = 12, \\
U(1): & D_b = D_5, & D'_b = D_5, & \chi(D_5) = 13, \\
U(3): & D_c, = D_5 + D_7, & D'_c = D_5 + D_8 & \chi(D_5 + D_7) = 25.
\end{array}
$$

We consider the non-trivial B_+-flux

$$
c_1(B) = \frac{1}{2}(D_7 + D_8 + D_9), \tag{226}
$$

which allows us to introduce the well-defined bundles

$$
\begin{aligned}
c_1(\widetilde{L}_a) &= 3D_5 + 2D_7 - \frac{1}{2}D_8 + \frac{1}{2}D_9, \\
c_1(\widetilde{L}_b) &= \frac{5}{2}D_5 + D_6 - \frac{1}{2}D_7 + \frac{5}{2}D_8 - \frac{1}{2}D_9, \\
c_1(\widetilde{L}_c) &= \frac{1}{2}D_5 + \frac{3}{2}D_8 - \frac{1}{2}D_9.
\end{aligned} \tag{227}
$$

This configuration cancels the D5-tadpole and achieves a pure three-generation spectrum as summarised in Table 18. All phenomenological considerations detailed in the previous section regarding the spectrum of this model apply also for the present three-generation model since the intersection pattern of the divisors D_a, D_b and D_c is unchanged.

The only differences occur when analysing the global consistency and supersymmetry conditions, as we next discuss. Prior to breaking $SU(5)$ via $U(1)_Y$ flux the D3-brane tadpole

$$
N_{D3} + N_{\mathrm{gauge}} = 10 \tag{228}
$$

number	$U(5)$	$U(1)$	$U(3)$
3	$\boxed{\boxed{}}_{(2)}$	1	1
3	$\overline{\square}_{(-1)}$	$\square_{(1)}$	1
3	1	$\overline{\square\square}_{(-2)}$	1
2	1	1	$\overline{\boxed{\boxed{}}}_{(-2)}$
2	1	$\overline{\square}_{(-1)}$	$\overline{\square}_{(-1)}$

Table 18: *Chiral spectrum for intersecting D7-brane model. The indices denote the $U(1)$ charges.*

is just satisfied without room for extra $D3$-branes, as we verify by computing

$$N_{\text{gauge}} = \frac{5}{2} \cdot \frac{1}{2} + \frac{1}{2} \cdot \frac{31}{4} + \frac{3}{2} \cdot \frac{13}{4} = 10. \tag{229}$$

Next we parametrise the Kähler form $J = \sum_{i=1}^{5} K_i$ in terms of the five generators of the Kähler cone introduced previously, where compatibility with the orientifold action fixes $r_1 = r_2$. One easily finds that the general solution to the D-term supersymmetry conditions relates the so-defined Kähler r_1, r_2 as well as the B_--modulus $B_- = b\,(D_7 - D_8)$ to r_4, r_5 as

$$r_1 = \frac{2}{3}r_4 - r_5, \quad r_3 = \frac{13}{6}r_4 - 2r_5, \quad B_- = \frac{34r_4 - 27r_5}{38r_4 - 30r_5}. \tag{230}$$

Remarkably any such choice of Kähler form lies inside the Kähler cone as long as $r_5 > 0$ and $\frac{3}{2}r_5 \leq r_4 \leq 2\,r_5$. The existence of solutions inside the Kähler cone is, together with the appearance of exactly three generations of Standard Model matter, one of the motivations to present this example.

However, two caveats require further attention. As the reader is by now very familiar with, we break $SU(5)$ further to the Standard Model gauge group by turning on the line bundle $\mathcal{L}_Y$ on D_a that is trivial on the ambient Calabi-Yau space. As before the E_6 sublattice within $H^2(D_a)$ of the dP$_9$ surface D_a is trivial on the Calabi-Yau, and the minimal choice for $\mathcal{L}_Y$ that avoids extra vector-like states is, for example, $\mathcal{L}_Y = \mathcal{O}(e_1 - e_2)$. This, however, leads to an extra contribution of $+2$ in N_{gauge} appearing in the D3-brane tadpole equation (228). In addition, the by now

familiar twist of L_a by $R_a = \mathcal{L}_Y^{-1}$ required to engineer one Higgs doublet and to project out the triplet contributes with $+1$ on the left-hand side of equation (228). In conclusion, there is a total overshooting by three units in the D3-brane tadpole equation, which requires the introduction of three anti-D_3 branes.

A second subtlety is associated with cancellation of K-theory charge. Applying our probe argument we note that the only invariant candidate cycles for SP Chan-Paton factors are D_1, D_4, D_5, D_6 and D_9, each of which is non-Spin. In view of the B_+-flux eq. (226) none of them can carry an invariant line bundle in agreement with the Freed-Witten quantisation condition *except* D_9. In fact, any line bundle of the form $L_9^{(n)} = \frac{n}{2}(D_7 - D_8)$ with n odd is a liable and invariant gauge field configuration. As stressed several times by now, in absence of unambiguous CFT techniques to establish the orientifold action in the invariant sector it is hard to decide if $(D_9, L_9^{(n)})$ carries SP or rather SO Chan-Paton factors. In the first case, its worldvolume theory would suffer from a global Witten anomaly in our three-generation model, as can be verified by computing that the number of fundamental representations under the symplectic gauge group is odd. In this case, the probe argument would suggest that model would not be globally consistent due to the non-cancellation of K-theory charge. We do not attempt to settle this issue at this stage but rather leave this model in the limbo of phenomenologically highly appealing configurations whose liability as a genuine string vacuum hinges upon as subtle and innocent a condition as the cancellation of torsion K-theory charge. With this warning in mind we conclude our model building adventures with a summary of the phenomenological properties of this model in Table 19.

8   Comments on Moduli Stabilisation

So far we have focused our attention on the construction of realistic $SU(5)$ GUT models on intersecting D7-branes in Type IIB orientifold models. Eventually, to obtain a truly predictive framework we have to address the central question of moduli stabilisation. Luckily, just for this kind of models very powerful techniques for moduli stabilisation have been developed during the last years. First to mention is the possibility of freezing the complex structure moduli and the dilaton via three-form fluxes inducing a Gukov-Vafa-Witten type superpotential. Combining this with D3-instanton induced contributions depending on the Kähler moduli very predictive scenarios with in principle all moduli stabilised have been proposed. These include in particular the original KKLT scenario [6] with supersymmetry breaking via an

property	mechanism	status
globally consistent	tadpoles + K-theory	✓[*,**]
D-term susy	vanishing FI-terms inside Kähler cone	✓
gauge group $SU(5)$	$U(5) \times U(1)$ stacks	✓
3 chiral generations	choice of line bundles	✓
no vector-like matter	localisation on $g = 0, 1$ curves	✓
5 vector-like Higgs	choice of line bundles	✓
no adjoints	rigid 4-cycles, del Pezzo	✓
GUT breaking	$U(1)_Y$ flux on trivial 2-cycles	✓
3-2 splitting	Wilson lines on $g = 1$ curve	✓
3-2 split + no dim=5 p-decay	local. of H_u, H_d on disjoint comp.	−
$\mathbf{10}\,\overline{\mathbf{5}}\,\overline{\mathbf{5}}_{\mathbf{H}}$ Yukawa	perturbative	✓
$\mathbf{10}\,\mathbf{10}\,\mathbf{5}_{\mathbf{H}}$ Yukawa	presence of appropriate D3-instanton	−[***]
Majorana neutrino masses	presence of appropriate D3-instanton	−[***]

Table 19: *Summary of $SU(5)$ properties realised in the model of Subsection 7.3.*
[*] overshooting in D3-tadpole → 3 $\overline{D3}$-branes
[**] K-theory to the best of our ability to detect SP-cycles and modulo the possible issue of $(D_9, L_9^{(n)})$
[***] at least not with $O(1)$ instantons

uplift potential[26]. In some respects even better controlled is the LARGE volume scenario with Kähler moduli dominated supersymmetry breaking [7,8].

In this latter scenario it is essential to have a Calabi-Yau with negative Euler characteristic (that is, $h^{2,1} > h^{1,1}$) and shrinkable, rigid four-cycles supporting D3-brane instantons contributing to the superpotential. Such cycles are given by del Pezzo surfaces dP_n with $n \leq 8$. Therefore, gauge coupling unification with $SU(5)$ breaking via $U(1)_Y$ fluxes and controllable moduli stabilisation with natural supersymmetry breaking both lead us to the class of Type IIB orientifolds (with some four-cycles $T_{Yuk} \to 0$) on Calabi-Yau manifolds which contain dP_n surfaces supporting two-cycles which are trivial in the Calabi-Yau manifold.

We have already discussed in Subsection 4.5 that the $M_n^{(dP_8)^n}$ manifolds exhibit the swiss-cheese structure of the volume form. Thus, the class of Calabi-Yau manifolds studied in Sections 4, 5, and 6 as promising candidates for GUT model building likewise exhibits some attractive features for LARGE volume moduli stabilisation. For the $M_n^{(dP_8)^n}$ manifolds we have also shown that placing the $SU(5)$ GUT on a shrinkable dP_8 cycle, the D-terms force this cycle to shrink to string scale size. If one is not deterred by the appearance of quantum corrections, one can consider this either as a global embedding of local quiver theories[27]. If one tries to avoid such corrections the above observation can alternatively serve as a motivation to place the GUT branes on del Pezzo dP_9 or other non-shrinkable rigid surfaces instead. In this latter case, the D-term constraints can be solved in the large radius regime. This results in a scenario where the GUT branes are localised on dP_9 surfaces while instantons on dP_8 or lower del Pezzo surfaces can generate the superpotential contributions realising the LARGE volume scenario. At this stage we also point out that for consistency in a GUT model the string scale must be fixed not below the GUT scale, of course. Thus in our context the original LARGE volume scenario, if applied, has to be modified anyway as to stabilise the volume of the manifold at not too LARGE values $\mathcal{V} \simeq 10^4$. For a scenario leading to $M_s = M_{GUT}$ along these lines see [10].

The arrangement just described also resolves the constraints pointed out in [60] for the coexistence of a chiral MSSM or GUT like intersecting D7-brane sector on the one hand and of a D3-brane instanton sector contributing to the uncharged superpotential on the other. Since here the phenomenologically relevant sizes of

---

[26]In this sense the presence of anti-D3 branes in some of our models might turn out to be some use.

[27]While this work was in its final stages the authors of [76] proposed a very similar scenario.

the D7-brane cycles are fixed by the D-term constraints instead of the F-terms, the resulting soft-terms and low-energy signatures are expected to be different from the ones computed so far in the literature for the LARGE volume scenario [8, 78, 9, 10]. There, it was mostly assumed that the string scale is in the intermediate regime and that the MSSM supporting D7-branes wrap the same cycle as the D3-brane instanton.

Very similar conclusions follow from the analysis of the quintic descendants. In contrast to the models derived from $\mathbb{P}_{1,1,1,6,9}[18]$, here we have found intersecting dP_n, $n \leq 8$ surfaces, which therefore do not show a swiss cheese structure and allow the D-terms to freeze the Kähler moduli such that the volumes of these del Pezzo remain finite. To arrange for the LARGE or rather GUT volume scenario for this class of models additional points at generic positions have to be blown up, presumably resulting in additional del Pezzo divisors, which are orthogonal to ones supporting D7-branes.

The next logical step is to combine fluxes, instanton effects and GUT D7-brane sectors such that a completely realistic and predictive model arises. For this purpose, one first needs to study the coexistence of three-form fluxes and D7-branes on the same Calabi-Yau, for which additional consistency conditions arise. Here to mention is both the Freed-Witten condition $H_3|_D = 0$ and a possible change for the quantisation of the gauge fluxes due to the presence of F_3 form flux [79]. Moreover, also the coexistence of Euclidean D3-brane instanton contributions to the superpotential and the desired presence of a chiral GUT D7-brane sector implies additional constraints [60]. All this to be evaluated and taken into account carefully to claim to have realised the MSSM or a variation therefore, from a string compactification.

This is a formidable task, but not out of reach in the not too far future. We think the results reported in this paper on GUT realisations in Type IIB orientifolds provide an encouraging step towards achieving this goal.

9 Conclusions

In this paper we have started to systematically analyse the construction of Georgi-Glashow like $SU(5)$ GUTs from Type IIB orientifolds with D7- and D3-branes. First, we formulated the quite restrictive global model building rules. Beyond the common tadpole and K-theory constraints, there arise a couple of additional subtle but quite restrictive constraints. These include the delicate quantisation rules for the gauge

flux on the D7-branes wrapping rigid del Pezzo surfaces, which derive from the fact that del Pezzo surfaces are not *Spin*. In addition these gauge fluxes have to be chosen such that the D-term constraints can be satisfied inside the Kähler cone of the Calabi-Yau threefold. Applied to $SU(5)$ GUT models, in particular the quantisation conditions cannot be satisfied with only the GUT breaking line bundle $\mathcal{L}_Y$ supported on the $SU(5)$ stack. The presence of a second bundle $\mathcal{L}_a$ embedded into the diagonal $U(1) \subset U(5)$ is essential. It would be interesting to study the precise lift of the consistency conditions to the F-theory description of these models. While some details are known, we think it is fair to say that the general picture is still not fully understood.

After outlining the general structure, we have provided a class of concrete Calabi-Yau threefolds containing del Pezzo surfaces. Though the construction is more general, we first considered examples descending from the Calabi-Yau manifold $\mathbb{P}_{1,1,1,6,9}[18]$ via del Pezzo transitions. The resulting Calabi-Yau threefolds feature various phases (triangulations) related via flop-transitions of curves in the del Pezzo base. To define orientifolds of Type IIB on these manifolds, we have classified all their involutions resulting from involutions of the del Pezzo base. This provides already a large set of models, which deserves a more systematic (statistical) investigation than we could provide in this paper. Clearly, there exist more general involutions which also act on the elliptic fibre. The prototype example is just the $y \to -y$ involution of the elliptic fibre. It would be interesting to study these more general orientifolds, as well. Another natural route to pursue is to start with the related torus fibred Calabi-Yau manifolds $\mathbb{P}_{1,1,1,3,6}[12]$ and $\mathbb{P}_{1,1,1,3,3}[9]$. More generally, one could study systematically which Calabi-Yau manifolds in the known class of hypersurfaces in toric varieties allow for similar del Pezzo transitions.

Equipped with the general structure and appropriate concrete Calabi-Yau manifolds, we have manually searched for globally consistent examples. We have presented three models in detail, each realising around 60-70% of the desired GUT features, with almost every property being realised in at least one example. Therefore, we do not see any conceptual obstacle to finding GUT models exhibiting all features in a single configuration.

We have also introduced a second class of suitable Calabi-Yau manifolds defined via del Pezzo transitions of the simple quintic hypersurface in $\mathbb{P}_4$. In particular, these manifolds contain intersecting shrinkable del Pezzo surfaces, a property the first class based on $\mathbb{P}_{1,1,1,6,9}[18]$ was lacking due to the swiss-cheese structure of the triple intersection form. Finally, we have presented two GUT models with all matter

fields localised on curves and therefore without any additional vector-like matter, the second of which realises just three families of Standard Model matter plus a Higgs pair. Clearly, it would be interesting to generalise the here presented techniques for constructing (toric) Calabi-Yau manifolds containing del Pezzo surfaces.

Our emphasis has been on the global string consistency conditions, which in a first attempt seem to be easier to analyse in the IIB orientifold framework than for F-theory compactifications on compact elliptically fibred Calabi-Yau fourfolds. The price one has to pay for working in the orientifold phase is that some couplings such as top-Yukawa couplings and Majorana neutrino masses are non-perturbatively generated by D3-brane instantons. With the recent understanding of such instanton effects we have however been able to formulate a criterion respectively constraint for their presence in concrete set-ups. The realistic corner in the moduli space of these models is clearly where the 4-cycles wrapped by these instantons go to zero size. In this respect it would be very important to better understand the relation of the orientifold construction to the F-theory uplift on Calabi-Yau fourfolds.

Eventually, we have briefly discussed the issue of moduli stabilisation for these models. We have shown that the manifolds $M_n^{(\mathrm{dP_8})^n}$ indeed feature a swiss-cheese structure, which is a prerequisite for realising the LARGE volume scenario. We think it is striking that both from the viewpoint of realising GUTs and from the viewpoint of phenomenologically acceptable moduli stabilisation one is led to the same class of string constructions, namely Type IIB orientifolds (F-theory) on Calabi-Yau threefolds with shrinkable four-cycles, that is, del Pezzo surfaces.

Acknowledgements

Appendices

A Involutions on Del Pezzo Surfaces

A.1 Del Pezzo Surfaces of High Degree

This appendix is the completion and continuation of Subsection 4.1. We start with a more detailed examination of the del Pezzo surfaces of high degree ≥ 6. In the Subsections A.2–A.6 we will consider each such del Pezzo surface individually and classify their involutions[28]. However, before we go into the details of the different involutions let us recall Table 20

A.2 Involutions on the Projective Plane

Let us start with the simplest del Pezzo surface, $\mathbb{P}^2$. There are no (-1)-curves. Up to coordinate transformations, the unique involution acts on the homogeneous coordinates as

$$\sigma : \mathbb{P}^2 \to \mathbb{P}^2, \quad [z_0 : z_1 : z_2] \mapsto [-z_0 : z_1 : z_2]. \tag{231}$$

The fixed point set of the involution σ is

$$\left(\mathbb{P}^2\right)^\sigma = \left\{[0 : * : *]\right\} \cup \left\{[1 : 0 : 0]\right\} \simeq \mathbb{P}^1 \cup \{\text{pt}\}, \tag{232}$$

and its homology class is $l \in H_2(\mathbb{P}^2, \mathbb{Z})$.

The projective plane is a toric variety, determined by the 2-dimensional polytope shown in Figure 4 as follows. Associate one complex-valued variable to each point of the polytope. Here, we label them x_0, x_1, and x_2. Whenever there are two points that are not connected by a line, the two variables are not allowed to vanish simultaneously. This does not happen here, but will be important later on. Finally, for each linear relation amongst the points we impose an equivalence under "homogeneous" rescaling. For example, the single linear relation

$$\overbrace{(0,1)}^{x_1} + \overbrace{(-1,-1)}^{x_0} + \overbrace{(1,0)}^{x_2} = 0$$
$$\Rightarrow \quad [x_0 : x_1 : x_2] = [\lambda x_0 : \lambda x_1 : \lambda x_2] \quad \forall \lambda \in \mathbb{C}^\times \tag{233}$$

---

[28]That is, the different connected components of the moduli space of involutions.

S	$\deg(S)$	case	action	fixed point set S^σ	$[S^\sigma] \in H_2$	action on $H_2(S,\mathbb{Z})$
$\mathbb{P}^2$	9	1	eq. (231)	$[0:*:*] \cup [1:0:0] \simeq \mathbb{P}^1 \cup \{\text{pt.}\}$	l	$\begin{pmatrix} 1 \end{pmatrix}$
$\mathbb{P}^1 \times \mathbb{P}^1$	8	1	eq. (237a)	$[1:1|*:*] \cup [-1:1|*:*]$	$(l_2) + (l_2)$	$\begin{pmatrix} 1 & 0 \\ 0 & 1 \end{pmatrix}$
$\mathbb{P}^1 \times \mathbb{P}^1$	8	2	eq. (237b)	$[\pm 1:1| \pm 1:1] \simeq 4 \text{ points}$	0	$\begin{pmatrix} 1 & 0 \\ 0 & 1 \end{pmatrix}$
$\mathbb{P}^1 \times \mathbb{P}^1$	8	3	eq. (237c)	diagonal $\mathbb{P}^1$	$l_1 + l_2$	$\begin{pmatrix} 0 & 1 \\ 1 & 0 \end{pmatrix}$
$\mathcal{B}_1$	8	1	eq. (241a)	$\pi^{-1}([0:*:*]) \cup e_1 \simeq 2\mathbb{P}^1$	$(l) + (e_1)$	$\begin{pmatrix} 1 & 0 \\ 0 & 1 \end{pmatrix}$
$\mathcal{B}_1$	8	2	eq. (241b)	$\mathbb{P}^1 \cup \{2 \text{ pts.}\}$	$l - e_1$	$\begin{pmatrix} 1 & 0 \\ 0 & 1 \end{pmatrix}$
$\mathcal{B}_2$	7	1	eq. (248)	$2\mathbb{P}^1 \cup \{\text{pt.}\}$	$(l - e_1) + (e_2)$	$\begin{smallmatrix} 1 & 0 & 0 \\ 0 & 1 & 0 \\ 0 & 0 & 1 \end{smallmatrix}$
$\mathcal{B}_2$	7	2	eq. (251)	$\mathbb{P}^1 \cup \{3 \text{ pts.}\}$	$l - e_1 - e_2$	$\begin{smallmatrix} 1 & 0 & 0 \\ 0 & 1 & 0 \\ 0 & 0 & 1 \end{smallmatrix}$
$\mathcal{B}_2$	7	3	eq. (252)	$\mathbb{P}^1 \cup \{\text{pt.}\}$	l	$\begin{smallmatrix} 1 & 0 & 0 \\ 0 & 0 & 1 \\ 0 & 1 & 0 \end{smallmatrix}$
$\mathcal{B}_3$	6	1	eq. (255)	$2\mathbb{P}^1 \cup \{2 \text{ pts.}\}$	$(e_1) + (l - e_2 - e_3)$	$\begin{smallmatrix} 1 & 0 & 0 & 0 \\ 0 & 1 & 0 & 0 \\ 0 & 0 & 1 & 0 \\ 0 & 0 & 0 & 1 \end{smallmatrix}$
$\mathcal{B}_3$	6	2	eq. (258)	$\mathbb{P}^1 \cup \{2 \text{ pts.}\}$	$l - e_3$	$\begin{smallmatrix} 1 & 0 & 0 & 0 \\ 0 & 0 & 1 & 0 \\ 0 & 1 & 0 & 0 \\ 0 & 0 & 0 & 1 \end{smallmatrix}$
$\mathcal{B}_3$	6	3	eq. (259)	$\mathbb{P}^1$	$2l - e_1 - e_2$	$\begin{smallmatrix} 2 & 1 & 1 & 1 \\ -1 & -1 & 0 & -1 \\ -1 & 0 & -1 & -1 \\ -1 & -1 & -1 & 0 \end{smallmatrix}$
$\mathcal{B}_3$	6	4	eq. (261)	4 points	0	$\begin{smallmatrix} 2 & 1 & 1 & 1 \\ -1 & 0 & -1 & -1 \\ -1 & -1 & 0 & -1 \\ -1 & -1 & -1 & 0 \end{smallmatrix}$

Table 20: *Involutions on del Pezzo surfaces of degree ≥ 6.*

corresponds to the usual rescaling of the homogeneous coordinates. Hence, the toric description of the projective plane is

$$\frac{\mathbb{C}^3 - \{\}}{\mathbb{C}^\times} = \mathbb{P}^2. \tag{234}$$

By construction, the "algebraic torus" $\left(\mathbb{C}^\times\right)^3$ acts[29] multiplicatively on the 3 homogeneous variables of $\mathbb{P}^2$, hence the name toric variety. Any subgroup of this action is called a toric group action. In particular, the involution eq. (231) is a toric $\mathbb{Z}_2$ action.

Alternatively, the involution can be seen as a symmetry of the polytope. The reflection symmetry shown in Figure 4 generates the involution
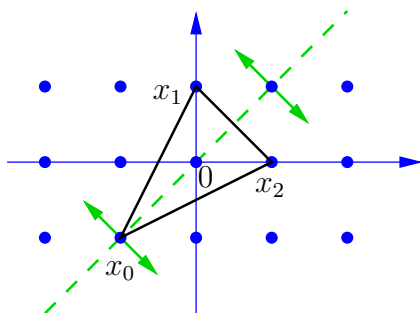
Figure 4: *Symmetry of the toric polytope defining $\mathbb{P}^2$.*

$$\sigma : \frac{\mathbb{C}^3}{\mathbb{C}^\times} \to \frac{\mathbb{C}^3}{\mathbb{C}^\times}, \quad [x_0 : x_1 : x_2] \mapsto [x_0 : x_2 : x_1]. \tag{235}$$

This is the same group action as in eq. (231), only written in different coordinates[30].

A.3 Involutions on the Product of Lines

There is only one non-trivial involution on $\mathbb{P}^1$ acting as $[z_0 : z_1] \mapsto [-z_0 : z_1]$, which can act on each factor of $\mathbb{P}^1 \times \mathbb{P}^1$. Together with the exchange of the two factors, this

---

[29]Clearly, the diagonal $\mathbb{C}^*$ is already modded out and acts trivially.

[30]For future reference, we note that the fixed point set in the coordinates eq. (235) is

$$\left(\mathbb{P}^2\right)^\sigma = \left\{[t_0 : t_1 : t_1] \big| [t_0 : t_1] \in \mathbb{P}^1\right\} \cup \left\{[0 : 1 : -1]\right\} \simeq \mathbb{P}^1 \cup \{\text{pt}\}. \tag{236}$$

generates all possible holomorphic involutions on $\mathbb{P}^1 \times \mathbb{P}^1$. All of these involutions arise from symmetries of the toric polytope, see Figure 5. The symmetry group of
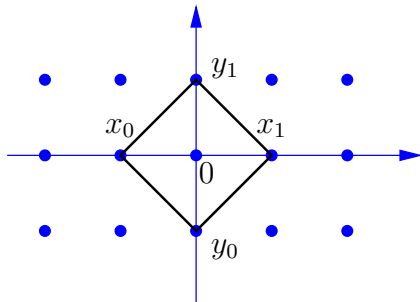
Figure 5: *The toric polytope defining $\mathbb{P}^1 \times \mathbb{P}^1$.*

the toric polytope is D_8, the dihedral group with 8 elements. It has three conjugacy classes of $\mathbb{Z}_2$ subgroups, namely:

1. Mirroring at vertical axis. In homogeneous coordinates, the induced action on $\mathbb{P}^1 \times \mathbb{P}^1$ is

$$\sigma_1 : \mathbb{P}^1 \times \mathbb{P}^1 \to \mathbb{P}^1 \times \mathbb{P}^1, \quad [x_0 : x_1 | y_0 : y_1] \mapsto [x_1 : x_0 | y_0 : y_1]. \tag{237a}$$

2. Rotating by π, with induced action

$$\sigma_2 : \mathbb{P}^1 \times \mathbb{P}^1 \to \mathbb{P}^1 \times \mathbb{P}^1, \quad [x_0 : x_1 | y_0 : y_1] \mapsto [x_1 : x_0 | y_1 : y_0]. \tag{237b}$$

3. Mirroring at diagonal axis = Rotate by $\frac{\pi}{2}$ and mirror at vertical axis. The induced action is

$$\sigma_3 : \mathbb{P}^1 \times \mathbb{P}^1 \to \mathbb{P}^1 \times \mathbb{P}^1, \quad [x_0 : x_1 | y_0 : y_1] \mapsto [y_0 : y_1 | x_0 : x_1]. \tag{237c}$$

According to the Künneth theorem, the homology group $H_2(\mathbb{P}^1 \times \mathbb{P}^1) = \mathbb{Z}^2$ is generated by the classes of the two factors, which we call l_1 and l_2. The fixed point sets and their homology classes are straightforward and listed in Table 20.

A.4 Blow-up of the Projective Plane

We now come to the first case with a (-1)-curve, namely the blow-up $\mathcal{B}_1$ of $\mathbb{P}^2$ at one point. One possible realisation is the hypersurface

$$\mathcal{B}_1 = \left\{ x_0 \cdot 0 + x_1 t_0 + x_2 t_1 = 0 \right\} \subset \mathbb{P}^2_{[x_0:x_1:x_2]} \times \mathbb{P}^1_{[t_0:t_1]}. \tag{238}$$

The obvious projection $\pi : \mathcal{B}_1 \to \mathbb{P}^2$, $[x_0 : x_1 : x_2 | t_0 : t_1] \mapsto [x_0 : x_1 : x_2]$ is, in fact, the corresponding blow-down map. To see this, consider the preimage:

- If $[x_0 : x_1 : x_2] \neq [1 : 0 : 0]$, then the preimage is the single point

$$\pi^{-1}\Big([x_0 : x_1 : x_2]\Big) = [x_0 : x_1 : x_2 | x_2 : -x_1] \tag{239}$$

- If $[x_0 : x_1 : x_2] = [1 : 0 : 0]$, then the preimage is

$$\pi^{-1}\Big([1 : 0 : 0]\Big) = \Big\{ [1 : 0 : 0 | t_0 : t_1] \,\Big|\, [t_0 : t_1] \in \mathbb{P}^1 \Big\} \simeq \mathbb{P}^1 \tag{240}$$

In other words, the hypersurface eq. (238) is the blow-up at $[1 : 0 : 0] \in \mathbb{P}^2$.

We now consider involutions of the hypersurface induced from the ambient space $\mathbb{P}^2 \times \mathbb{P}^1$. In fact, up to coordinate changes there are two distinct possibilities, namely

$$\sigma_1 : \mathcal{B}_1 \to \mathcal{B}_1, \quad \big[x_0 : x_1 : x_2 \big| t_0 : t_1\big] \mapsto \big[-x_0 : x_1 : x_2 \big| t_0 : t_1\big] \tag{241a}$$

and

$$\sigma_2 : \mathcal{B}_1 \to \mathcal{B}_1, \quad \big[x_0 : x_1 : x_2 \big| t_0 : t_1\big] \mapsto \big[x_0 : x_2 : x_1 \big| t_1 : t_0\big]. \tag{241b}$$

In terms of the blown-up $\mathbb{P}^2$, the two involutions can be understood as follows. Recall from Subsection A.2 that the fixed-point set on $\mathbb{P}^2$ is the disjoint union of a line and a point.

1. The first involution, eq. (241a), is the blow-up of the isolated fixed point on $\mathbb{P}^2$. The corresponding fixed-point set in $\mathcal{B}_1$ is the whole exceptional $\mathbb{P}^1$ as well as the fixed line in $\mathbb{P}^1$. This $\mathbb{Z}_2$ group action is toric.

2. The second involution, eq. (236), is the blow-up at a point on the fixed line on $\mathbb{P}^2$. The exceptional $\mathbb{P}^1$ is mapped to itself, but it is not point-wise fixed. Rather, the involution acts as a rotation by π on this $\mathbb{P}^1 \simeq S^2$ and the north and south pole of the sphere end up being fixed. Looking at the whole $\mathcal{B}_1$, the proper transform of the fixed line in $\mathbb{P}^2$ passes through one of the fixed points in the exceptional curve. Hence, the fixed point set consists of this proper transform[31] $\tilde{l} \simeq \mathbb{P}^1$ together with the remaining fixed point in the exceptional curve and the isolated fixed point that was already in $\mathbb{P}^2$.

   In terms of toric geometry, this involution is induced from the reflection symmetry of the polyhedron shown in Figure 6

---

[31] The σ_2-fixed line l_2 in $\mathbb{P}^2$ has the parametrisation

$$\xi \mapsto l_2(\xi) = [1 : \xi : \xi], \quad \xi \in \mathbb{C} \cup \{\infty\} \simeq \mathbb{P}^1. \tag{242}$$
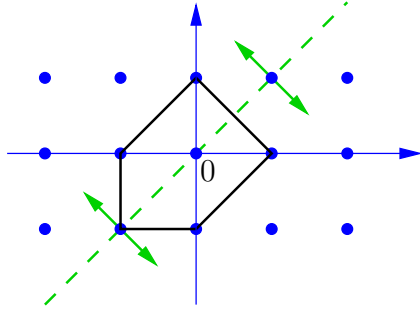
Figure 6: *Symmetry of the toric polytope defining $\mathcal{B}_1$.*

More abstractly, we can understand the two involutions from the (-1)-curves. Since there is precisely one such curve, namely e_1, this curve must necessarily be mapped to itself under any involution. But whenever there is an *invariant*[32] exceptional curve on $\mathcal{B}_n$, then we can blow down this curve and obtain a involution on $\mathcal{B}_{n-1}$ (or $\mathbb{P}^1 \times \mathbb{P}^1$ if $n = 2$). This is why every involution on $\mathcal{B}_1$ is simply the (unique) involution on $\mathbb{P}^2$ blown up at a fixed point. There are two connected components to the fixed point set, and the choice of blow-up point coincides with the two different ways that $e_1 \simeq \mathbb{P}^1$ can be mapped to itself:

1. If one blows up the isolated fixed point on $\mathbb{P}^2$, then e_1 is point-wise fixed under the induced involution on $\mathcal{B}_1$.

2. If one blows up one point in the fixed line on $\mathbb{P}^2$, then the induced involution on $\mathcal{B}_1$ acts on $e_1 \simeq S^2$ as rotation by π.

A.5 Blow-up of the Projective Plane at Two Points

The blow-up of $\mathbb{P}^2$ at two points, $\mathcal{B}_2$, is the first case with an interesting pattern of (-1)-curves. Clearly, there are the exceptional divisors e_1 and e_2. But there is also

---

It passes through the point $l_2(0) = [1 : 0 : 0]$, which we are about to blow up. By definition, the proper transform is the curve

$$\tilde{l} = \pi^{-1} \circ l_2\Big(\mathbb{P}^1 - \{0\}\Big) \ \cup \ \lim_{\xi \to 0}\Big(\pi^{-1} \circ l_2(\xi)\Big) \quad \subset \quad \mathcal{B}_1. \tag{243}$$

Since $\tilde{l} \cdot l = 1 = \tilde{l} \cdot e_1$, the homology class of the proper transform must be $[\tilde{l}] = l - e_1$.

[32]One can of course blow down any (-1)-curve and obtain a smooth surface, but the involution is lost (or, rather, becomes a birational map) if the (-1)-curve was not invariant.

a third rigid curve, namely the line on $\mathbb{P}^2$ through the two blow-up points. As we reviewed in Footnote 31, this line defines a curve on the blow-up $\mathcal{B}_2$. This so-called proper transform has homology class

$$\tilde{l} = l - e_1 - e_2. \tag{244}$$

One can easily check that $\tilde{l}^2 = -1$, as expected for a rigid curve. We draw the intersection pattern of the three lines in Figure 7. In the following, we will always
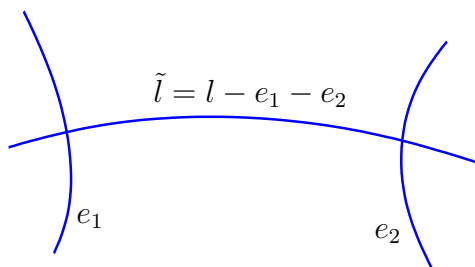
Figure 7: *On the left, intersection pattern of the three (-1)-curves on $\mathcal{B}_2$. The dual graph is shown on the right.*

use the dual graph of the (-1)-curves (and, by abuse of notation, drop the "dual"). By definition, this is the graph with

- One node for each (-1)-curve, and

- One connecting line whenever two curves intersect.

There are two different kinds of nodes, one of valence 2 and two of valence 1. Blowing down the middle node yields $\mathbb{P}^1 \times \mathbb{P}^1$, while blowing down one of the nodes at the end yields $\mathcal{B}_1$.

Clearly, the automorphism group of the graph is $\mathbb{Z}_2$ and the middle node is always fixed. Hence, the easiest way to describe all involutions is as blow-up of $\mathbb{P}^1 \times \mathbb{P}^1$, where there were three distinct involutions. Just an in eq. (238), we will realise the blow-up at the point $[\xi_0 : \xi_1 | \eta_0 : \eta_1] \in \mathbb{P}^1 \times \mathbb{P}^1$ as a degree-$(1,1,1)$ hypersurface

$$\mathcal{B}_2 = \left\{ (\xi_1 x_0 - \xi_0 x_1) t_0 + (\eta_1 y_0 - \eta_0 y_1) t_1 = 0 \right\} \subset \mathbb{P}^1_{[x_0:x_1]} \times \mathbb{P}^1_{[y_0:y_1]} \times \mathbb{P}^1_{[t_0:t_1]}. \tag{245}$$

Using this construction, we can characterise the three different involutions on $\mathcal{B}_2$ as follows:

1. First, let us start by blowing up $(\mathbb{P}^1 \times \mathbb{P}^1, \sigma_1)$ at a σ_1-fixed point. The fixed point set consists of two disjoint $\mathbb{P}^1$, so one might think that there is a discrete choice. However, the two $\mathbb{P}^1$ are exchanged by a remaining symmetry of $\mathbb{P}^1 \times \mathbb{P}^1$, so they cannot be distinguished. Henceforth, we will pick the fixed point

$$p = [1:1|0:1] \in \mathbb{P}^1 \times \mathbb{P}^1 \tag{246}$$

and define

$$\mathcal{B}_2 = \left\{ (x_0 - x_1)t_0 + y_0 t_1 = 0 \right\} \subset \mathbb{P}^1_{[x_0:x_1]} \times \mathbb{P}^1_{[y_0:y_1]} \times \mathbb{P}^1_{[t_0:t_1]}. \tag{247}$$

In order to make the hypersurface equation invariant under the involution, we must extend eq. (237a) to

$$\sigma_1 : \mathcal{B}_2 \to \mathcal{B}_2, \quad [x_0 : x_1 | y_0 : y_1 | t_0 : t_1] \mapsto [x_1 : x_0 | y_0 : y_1 | -t_0 : t_1]. \tag{248}$$

2. Now we blow up one of the 4 fixed points of $(\mathbb{P}^1 \times \mathbb{P}^1, \sigma_2)$. Again, the fixed points are exchanged by residual symmetries, and cannot be distinguished. Hence, there is essentially only one choice which we take to be

$$p = [1:1|1:1] \in \mathbb{P}^1 \times \mathbb{P}^1. \tag{249}$$

The blow-up with the induced involution is then

$$\mathcal{B}_2 = \left\{ (x_0 - x_1)t_0 + (y_0 - y_1)t_1 = 0 \right\} \subset \mathbb{P}^1_{[x_0:x_1]} \times \mathbb{P}^1_{[y_0:y_1]} \times \mathbb{P}^1_{[t_0:t_1]}, \tag{250}$$

$$\sigma_2 : \mathcal{B}_2 \to \mathcal{B}_2, \quad [x_0 : x_1 | y_0 : y_1 | t_0 : t_1] \mapsto [x_1 : x_0 | y_1 : y_0 | t_0 : t_1]. \tag{251}$$

3. Finally, we can blow-up one point on the fixed (diagonal) $\mathbb{P}^1$ in $(\mathbb{P}^1 \times \mathbb{P}^1, \sigma_3)$. For concreteness, let us take the point in eq. (249), which is also fixed under σ_3. Hence, the hypersurface equation is the same as in eq. (250). However, the induced involution has to extend a different involution on $\mathbb{P}^1 \times \mathbb{P}^1$, and must be

$$\sigma_3 : \mathcal{B}_2 \to \mathcal{B}_2, \quad [x_0 : x_1 | y_0 : y_1 | t_0 : t_1] \mapsto [y_0 : y_1 | x_0 : x_1 | t_1 : t_0]. \tag{252}$$

Equivalently, the three involutions can be described as blow-ups of $\mathbb{P}^2$ at two points. Let us quickly go over this equivalent point of view.

1. The first two involutions correspond to the trivial automorphism of the graph of (-1)-curves. Hence, one must blow up two fixed points of $(\mathbb{P}^2, \sigma)$. The first possibility is to blow up the isolated fixed point and one point on the fixed line in $\mathbb{P}^2$. As we saw in Subsection A.4, blowing up a point on the fixed $\mathbb{P}^1$ leaves the proper transform $\tilde{l}$ (in the homology class $l - e_1$) and one isolated point fixed. Blowing up the fixed point leads to a point-wise fixed exceptional divisor e_2.

2. The second involution is the blow-up of two points on the fixed $\mathbb{P}^1$ of $(\mathbb{P}^2, \sigma)$. The fixed point set consists of

   - The proper transform of the fixed line. Its homology class is $l - e_1 - e_2$.
   - One isolated fixed point on e_1 and one on e_2.
   - The isolated fixed point that was already on $\mathbb{P}^2$.

3. The last involution corresponds to the non-trivial automorphism of the graph. There, the involution must exchange the two blow-up points. The fixed point set is the same as on $(\mathbb{P}^2, \sigma)$.

Clearly, the first two involutions act trivially on $H_2(\mathcal{B}_2, \mathbb{Z})$. The third involution exchanges $e_1 \leftrightarrow e_2$ while leaving l invariant.

A.6 Blow-up of the Projective Plane at Three Points

The del Pezzo surface $\mathcal{B}_3$ has 6 rigid lines, the 3 exceptional divisors together with the 3 lines connecting any pair of blow-up points. Their homology classes are

$$e_1, \ e_2, \ e_3, \ l - e_2 - e_3, \ l - e_1 - e_3, \ l - e_2 - e_3. \tag{253}$$

The graph of (-1)-curves is a hexagon, whose automorphism group is D_{12}, the dihedral group with 12 elements. It has 3 conjugacy classes of order 2, which are depicted in Figure 8. We now investigate which involutions on $\mathcal{B}_3$ give rise to each graph automorphism.

1. Let us start with the trivial action on the graph. This is necessarily the blow-up of $(\mathbb{P}^2, \sigma)$ at three fixed points. Note, however, that by construction no three point can lie on any one line and, in particular, not on the fixed line.
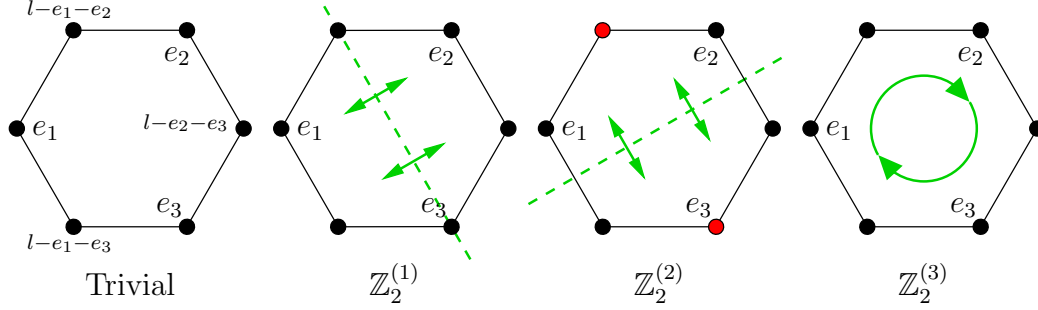
Figure 8: *The trivial and the three order-2 automorphisms of the graph of* (-1)*-curves on* $\mathcal{B}_3$.

Therefore, there is (up to coordinate changes) only one choice[33] of three fixed points to blow up. In the coordinates given by eq. (231), these three points can be chosen to be

$$p_1 = [1:0:0], \ p_2 = [0:1:0], \ p_3 = [0:0:1] \tag{254}$$

The first involution on $\mathcal{B}_3$ is the one defined through the blow-up,

$$\left(\mathcal{B}_3, \sigma_1\right) = \mathrm{Bl}_{\{p_1,p_2,p_3\}}\left(\mathbb{P}^2, \sigma\right). \tag{255}$$

We denote by e_i the exceptional divisor of the blow-up at p_i. With this notation, the fixed point set consists of the exceptional divisor e_1, the proper transform of the fixed $\mathbb{P}^1$, one isolated point on e_2, and one isolated point on e_3.

2. We now consider the first non-trivial involution on the graph of (-1)-lines, which is denoted $\mathbb{Z}_2^{(1)}$ in Figure 8. There are two fixed (-1)-curves, one of which we already labelled e_3. Blowing down this exceptional divisor e_3, we clearly obtain the surface $\mathcal{B}_2$ with the non-trivial action on its graph of (-1)-curves. There is only one such involution, namely $(\mathcal{B}_2, \sigma_3)$. Therefore, the desired involution on $\mathcal{B}_3$ is the blow-up of $(\mathcal{B}_2, \sigma_3)$ at a fixed point.

Recall that $(\mathcal{B}_2, \sigma_3)$ is the blow-up of $(\mathbb{P}^2, \sigma)$ at a point–image point pair. We can pick coordinates such that

$$\left(\mathcal{B}_2, \sigma_3\right) = \mathrm{Bl}_{\left\{[1:1:0],[-1:1:0]\right\}}\left(\mathbb{P}^2, \sigma\right). \tag{256}$$

---

[33]Namely the isolated fixed point and two points on the fixed line in $\mathbb{P}^2$.

The fixed point set of $(\mathcal{B}_2, \sigma_3)$ has two connected components, an isolated point $[1:0:0]$ and $[0: *: *] \simeq \mathbb{P}^1$. Note, however, that the isolated point is collinear with the previous blow-up points,

$$\big\{[1:1:0], [-1:1:0], [1:0:0]\big\} \in \Big\{[*:*:0]\Big\}. \tag{257}$$

Hence, we cannot blow up $(\mathcal{B}_2, \sigma_3)$ at the isolated fixed point. The only possibility is to pick a fixed point $q \neq [1:0:0]$. This point q must lie on the fixed $\mathbb{P}^1$ of $(\mathcal{B}_2, \sigma_3)$. Hence we obtain the involution

$$\big(\mathcal{B}_3, \sigma_2\big) = \mathrm{Bl}_q\big(\mathcal{B}_2, \sigma_3\big). \tag{258}$$

3. Now, consider the $\mathbb{Z}_2^{(2)}$-automorphism shown in Figure 8. There is no fixed (-1)-curve, so we cannot describe it in terms of a blown-up $\mathcal{B}_2$ del Pezzo. We can, however, blow down a pair of (-1)-curves that is exchanged by the involution *and* does not intersect. There is only one such pair, marked in red. Blowing down this pair yields a del Pezzo surface of degree 8 without any remaining (-1)-curves, that is, $\mathbb{P}^1 \times \mathbb{P}^1$.

   There are three choices for the involution on $\mathbb{P}^1 \times \mathbb{P}^1$. It turns out[34] that $(\mathbb{P}^1 \times \mathbb{P}^1, \sigma_3)$ gives rise to the right graph automorphism. Therefore, we set

$$\big(\mathcal{B}_3, \sigma_3\big) = \mathrm{Bl}_{\{p,q\}}\big(\mathbb{P}^1 \times \mathbb{P}^1, \sigma_3\big), \tag{259}$$

   where p, q is a generic point and its image on $(\mathbb{P}^1 \times \mathbb{P}^1, \sigma_3)$. The fixed point set $\mathcal{B}_3^{\sigma_4}$ is, by construction, the same as $(\mathbb{P}^1 \times \mathbb{P}^1)^{\sigma_3}$. Since the (-1)-curves span $H_2(\mathcal{B}_3, \mathbb{Z})$, the action on the curve homology classes can be read off from Figure 8. One obtains

$$\begin{pmatrix} l \\ e_1 \\ e_2 \\ e_3 \end{pmatrix} \mapsto \begin{pmatrix} 2l - e_1 - e_2 - e_3 \\ l - e_1 - e_3 \\ l - e_2 - e_3 \\ l - e1 - e_2 \end{pmatrix} \tag{260}$$

4. Finally, consider $\mathbb{Z}_2^{(3)}$. Again, there is no (-1)-curve, but we can blow down a pair of (-1)-curves and relate the involution to $\mathbb{P}^1 \times \mathbb{P}^1$. In fact, only one

---

[34]On $(\mathbb{P}^1 \times \mathbb{P}^1, \sigma_1)$ there is no suitable pair of non-fixed points to blow up into $\mathcal{B}_3$. The second involution, $(\mathbb{P}^1 \times \mathbb{P}^1, \sigma_3)$, will be used in Item 4.

involution on $\mathbb{P}^1 \times \mathbb{P}^1$ gives rise to the desired graph automorphism. Hence, we set

$$\left(\mathcal{B}_3, \sigma_4\right) = \mathrm{Bl}_{\{p,q\}}\left(\mathbb{P}^1 \times \mathbb{P}^1, \sigma_2\right), \tag{261}$$

where p, q is a generic point and its image on $(\mathbb{P}^1 \times \mathbb{P}^1, \sigma_2)$.

A.7   The Weyl Group and The Graph of Lines

Recall that, by definition, the degree of a curve is its intersection with the canonical class $K = -3l + \sum_i e_i$. As an alternative basis for the curve homology classes one
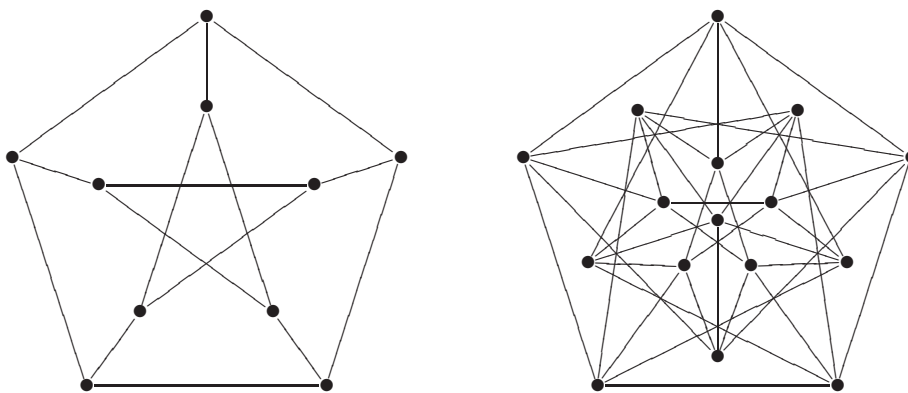
Figure 9: *The Petersen graph (left) and the Clebsch graph (right).*

can use the canonical class and the degree zero sublattice
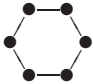
$$K^{\perp} \subset H_2(\mathcal{B}_n, \mathbb{Z}). \tag{262}$$

This sublattice contains a finite number of classes with self-intersection -2. One can show [80] that these classes span the root lattice[35] of a Lie algebra for $n \geq 2$. By this identification, we will call the (-2)-classes[36] of degree 0 roots, as well. Explicitly, the simple roots can be taken to be

$$\begin{aligned}
\alpha_i &= e_i - e_{i+1}, \quad i = 1, \ldots, n-1, \\
\alpha_n &= l - e_1 - e_2 - e_3.
\end{aligned} \tag{263}$$

---

[35]The lattice product on $K^{\perp}$ is *minus* the intersection product in homology.
[36]Note that such a (-2)-homology class cannot be represented by a holomorphic curve on a del Pezzo surface.

del Pezzo S	$\deg(S)$	# of roots	root lattice	Weyl group W	Order $|W|$	Number of $\mathbb{Z}_2$ conjugacy classes	graph
$\mathbb{P}^2$	9	0	{}	1	1	0	{}
$\mathbb{P}^1 \times \mathbb{P}^1$	8	0	{}	1	1	0	{}
$\mathcal{B}_1$	8	0	{}	1	1	0	
$\mathcal{B}_2$	7	2	A_1	$\mathbb{Z}_2$	2	1	
$\mathcal{B}_3$	6	8	$A_2 \oplus A_1$	$D_6 \times \mathbb{Z}_2 = D_{12}$	12	3	
$\mathcal{B}_4$	5	20	A_4	S_5	120	2	Petersen graph Figure 9
$\mathcal{B}_5$	5	40	D_5	Weyl(D_5)	1920	5	Clebsch graph Figure 9
$\mathcal{B}_6$	5	72	E_6	Weyl(E_6)	51840	4	27 nodes
$\mathcal{B}_7$	5	126	E_7	Weyl(E_7)	2903040	9	56 nodes
$\mathcal{B}_8$	5	240	E_8	Weyl(E_8)	696729600	9	240 nodes

Table 21: *The Weyl groups and the number of $\mathbb{Z}_2$ conjugacy classes. The Weyl group equals the automorphism group of the graph of (-1)-curves on each del Pezzo surfaces.*

The intersection matrix is given in terms of the Cartan matrix C_{ij} of the corresponding Lie algebra as

$$\alpha_i \cdot \alpha_j = -C_{ij}, \quad \alpha_i \cdot K = 0, \quad K^2 = 9 - n. \tag{264}$$

The root lattices for the del Pezzo surfaces are listed in Table 21 together with some information on the corresponding Weyl groups.

One of the advantages of working with this root lattice is the following characterisation of the symmetries of the graph of (-1)-curves on a del Pezzo surface:

Theorem 1 (Manin) *The Weyl group of the root lattice associated to a del Pezzo surface equals the automorphism group of the graph of (-1)-curves.*

In particular, we are interested in the conjugacy classes of involutions acting on the graph of (-1)-curves, which we can easily compute in terms of the conjugacy classes of $\mathbb{Z}_2$ subgroups in the corresponding Weyl group. It is now a simple (but tedious) computation to enumerate[37] all the Weyl group elements in each conjugacy class.

Note that, on del Pezzo surfaces of degree 6 and higher ($\mathcal{B}_n$ with $n \geq 3$), the canonical class and root lattice span the whole homology group[38] $H_2(\mathcal{B}_n, \mathbb{Q})$. From now on we will restrict ourselves to this case, where we now have three equivalent bases for the (rational) homology:

- The standard basis l, e_1, ..., e_n.

- The canonical class together with the n simple roots.

- Any maximal (that is, consisting of $n + 1$) linearly independent set of (-1)-curves.

The second basis is especially useful to determine the homology action of an involution on a del Pezzo surface. By definition, the canonical class is invariant under the action of a holomorphic map and the Weyl group acts on its orthogonal complement $K^\perp$. In Table 22, we use this to find the action on the homology of each possible involution of the graph of (-1)-curves. Note that conjugate involutions can have

---

[37]We list the sizes of the conjugacy classes in Table 22.

[38]In fact, $\text{span}\{K, \alpha_1, \ldots, \alpha_n\}$ is a finite-index sublattice of $H_2(\mathcal{B}_n, \mathbb{Z})$ for $n \geq 3$. However, since there is no torsion in the homology of del Pezzo surfaces this does not matter in the following.

Table 22: *The $\mathbb{Z}_2$ conjugacy classes in the Weyl groups associated to del Pezzo surfaces. These (together with the trivial group element) classify the possible actions on the degree-2 homology of the corresponding del Pezzo surface. Note that in some cases the potential action cannot be realised on a del Pezzo surface. The $d \times d$ identity matrix is denoted by $\mathbf{1}_d$, the 2×2 permutation matrix by $H = \left(\begin{smallmatrix} 0 & 1 \\ 1 & 0 \end{smallmatrix}\right)$.*

del Pezzo	Weyl group	Action on $H_2\big(\mathcal{B}_n, \mathbb{Z}\big) = \text{Span}\{l, e_1, \ldots, e_n\}$	(b_2^+, b_2^-)	Size of conj. class
$\mathcal{B}_3$	$A_2 \oplus A_1$	$I_{\mathcal{B}_3}^{(1)} = \mathbf{1}_2 \oplus H$	$(3,1)$	3
		$I_{\mathcal{B}_3}^{(2)} = \left(\begin{smallmatrix} 2 & 1 & 1 & 1 \\ -1 & -1 & 0 & -1 \\ -1 & 0 & -1 & -1 \\ -1 & -1 & -1 & 0 \end{smallmatrix}\right)$	$(2,2)$	3
		$I_{\mathcal{B}_3}^{(3)} = \left(\begin{smallmatrix} 2 & 1 & 1 & 1 \\ -1 & 0 & -1 & -1 \\ -1 & -1 & 0 & -1 \\ -1 & -1 & -1 & 0 \end{smallmatrix}\right)$	$(3,1)$	1
$\mathcal{B}_4$	A_4	$I_{\mathcal{B}_4}^{(1)} = \mathbf{1}_3 \oplus H$	$(4,1)$	10
		$I_{\mathcal{B}_4}^{(2)} = \mathbf{1}_1 \oplus 2H$	$(3,2)$	15
$\mathcal{B}_5$	D_5	$I_{\mathcal{B}_5}^{(1)} = \mathbf{1}_4 \oplus H$ No such $\mathcal{B}_5$ involution!	$(5,1)$	20
		$I_{\mathcal{B}_5}^{(2)} = \mathbf{1}_2 \oplus 2H$	$(4,2)$	60
		$I_{\mathcal{B}_5}^{(3)} = I_{\mathcal{B}_3}^{(2)} \oplus H$	$(3,3)$	60
		$I_{\mathcal{B}_5}^{(4)} = I_{\mathcal{B}_3}^{(3)} \oplus H$	$(4,2)$	10
		$I_{\mathcal{B}_5}^{(5)} = \left(\begin{smallmatrix} 3 & 2 & 1 & 1 & 1 & 1 \\ -2 & -1 & -1 & -1 & -1 & -1 \\ -1 & -1 & -1 & 0 & 0 & 0 \\ -1 & -1 & 0 & -1 & 0 & 0 \\ -1 & -1 & 0 & 0 & -1 & 0 \\ -1 & -1 & 0 & 0 & 0 & -1 \end{smallmatrix}\right)$	$(2,4)$	5
$\mathcal{B}_6$	E_6	$I_{\mathcal{B}_6}^{(1)} = \mathbf{1}_5 \oplus H$ No such $\mathcal{B}_6$ involution!	$(6,1)$	36
		$I_{\mathcal{B}_6}^{(2)} = \mathbf{1}_3 \oplus 2H$	$(5,2)$	270
		$I_{\mathcal{B}_6}^{(3)} = \mathbf{1}_1 \oplus 3H$ No such $\mathcal{B}_6$ involution!	$(4,3)$	540
		$I_{\mathcal{B}_6}^{(4)} = I_{\mathcal{B}_5}^{(5)} \oplus \mathbf{1}_1$	$(3,4)$	45

118

Table 22 – continued from previous page

$\mathcal{B}_n$	Weyl	Action on $H_2(\mathcal{B}_n, \mathbb{Z}) = \text{span}\{l, e_1, \ldots, e_n\}$	(b_2^+, b_2^-)	$|I_{\mathcal{B}_n}^{(\cdot)}|^{\text{Weyl}}$
		$I_{\mathcal{B}_7}^{(1)} = \mathbf{1}_6 \oplus H$ $\qquad$ No such $\mathcal{B}_7$ involution!	$(7,1)$	63
		$I_{\mathcal{B}_7}^{(2)} = \mathbf{1}_4 \oplus 2H$ $\qquad$ No such $\mathcal{B}_7$ involution!	$(6,2)$	945
		$I_{\mathcal{B}_7}^{(3)} = \mathbf{1}_2 \oplus 3H$ $\qquad$ No such $\mathcal{B}_7$ involution!	$(5,3)$	3780
		$I_{\mathcal{B}_7}^{(4)} = I_{\mathcal{B}_3}^{(2)} \oplus 2H$ $\qquad$ No such $\mathcal{B}_7$ involution!	$(4,4)$	3780
		$I_{\mathcal{B}_7}^{(5)} = I_{\mathcal{B}_3}^{(3)} \oplus 2H$	$(5,3)$	315
		$I_{\mathcal{B}_7}^{(6)} = I_{\mathcal{B}_5}^{(5)} \oplus \mathbf{1}_2$	$(4,4)$	315
$\mathcal{B}_7$	E_7	$I_{\mathcal{B}_7}^{(7)} = I_{\mathcal{B}_5}^{(5)} \oplus H$	$(3,5)$	945
		$I_{\mathcal{B}_7}^{(8)} = \begin{pmatrix} 4 & 3 & 1 & 1 & 1 & 1 & 1 & 1 \\ -3 & -2 & -1 & -1 & -1 & -1 & -1 & -1 \\ -1 & -1 & -1 & 0 & 0 & 0 & 0 & 0 \\ -1 & -1 & 0 & -1 & 0 & 0 & 0 & 0 \\ -1 & -1 & 0 & 0 & -1 & 0 & 0 & 0 \\ -1 & -1 & 0 & 0 & 0 & -1 & 0 & 0 \\ -1 & -1 & 0 & 0 & 0 & 0 & -1 & 0 \\ -1 & -1 & 0 & 0 & 0 & 0 & 0 & -1 \end{pmatrix}$ No such $\mathcal{B}_7$ involution!	$(2,6)$	63
		$I_{\mathcal{B}_7}^{(9)} = \begin{pmatrix} 8 & 3 & 3 & 3 & 3 & 3 & 3 & 3 \\ -3 & -2 & -1 & -1 & -1 & -1 & -1 & -1 \\ -3 & -1 & -2 & -1 & -1 & -1 & -1 & -1 \\ -3 & -1 & -1 & -2 & -1 & -1 & -1 & -1 \\ -3 & -1 & -1 & -1 & -2 & -1 & -1 & -1 \\ -3 & -1 & -1 & -1 & -1 & -2 & -1 & -1 \\ -3 & -1 & -1 & -1 & -1 & -1 & -2 & -1 \\ -3 & -1 & -1 & -1 & -1 & -1 & -1 & -2 \end{pmatrix}$	$(1,7)$	1
		$I_{\mathcal{B}_8}^{(1)} = \mathbf{1}_7 \oplus H$ $\qquad$ No such $\mathcal{B}_8$ involution!	$(8,1)$	120
		$I_{\mathcal{B}_8}^{(2)} = \mathbf{1}_5 \oplus 2H$ $\qquad$ No such $\mathcal{B}_8$ involution!	$(7,2)$	3780
		$I_{\mathcal{B}_8}^{(3)} = \mathbf{1}_3 \oplus 3H$ $\qquad$ No such $\mathcal{B}_8$ involution!	$(6,3)$	37800
		$I_{\mathcal{B}_8}^{(4)} = \mathbf{1}_1 \oplus 4H$ $\qquad$ No such $\mathcal{B}_8$ involution!	$(5,4)$	113400
		$I_{\mathcal{B}_8}^{(5)} = I_{\mathcal{B}_5}^{(5)} \oplus \mathbf{1}_3$	$(5,4)$	3150
$\mathcal{B}_8$	E_8	$I_{\mathcal{B}_8}^{(6)} = I_{\mathcal{B}_5}^{(5)} \oplus \mathbf{1}_1 \oplus H$	$(4,5)$	37800
		$I_{\mathcal{B}_8}^{(7)} = I_{\mathcal{B}_7}^{(8)} \oplus \mathbf{1}_1$ $\qquad$ No such $\mathcal{B}_8$ involution!	$(3,6)$	3780
		$I_{\mathcal{B}_8}^{(8)} = I_{\mathcal{B}_7}^{(9)} \oplus \mathbf{1}_1$ $\qquad$ No such $\mathcal{B}_8$ involution!	$(2,7)$	120
		$I_{\mathcal{B}_8}^{(9)} = \begin{pmatrix} 17 & 6 & 6 & 6 & 6 & 6 & 6 & 6 & 6 \\ -6 & -3 & -2 & -2 & -2 & -2 & -2 & -2 & -2 \\ -6 & -2 & -3 & -2 & -2 & -2 & -2 & -2 & -2 \\ -6 & -2 & -2 & -3 & -2 & -2 & -2 & -2 & -2 \\ -6 & -2 & -2 & -2 & -3 & -2 & -2 & -2 & -2 \\ -6 & -2 & -2 & -2 & -2 & -3 & -2 & -2 & -2 \\ -6 & -2 & -2 & -2 & -2 & -2 & -3 & -2 & -2 \\ -6 & -2 & -2 & -2 & -2 & -2 & -2 & -3 & -2 \\ -6 & -2 & -2 & -2 & -2 & -2 & -2 & -2 & -3 \end{pmatrix}$	$(1,8)$	1

different matrix expressions; We pick particularly "nice" representatives by picking block-diagonal ones such that the bottom right blocks are either 2×2 permutation matrices, or identity matrices.

Note that no two (-1)-curves are homologous, that is, the homology classes of the (-1)-curves are all distinct. Hence, the homology class of a (-1)-curve can only be invariant under an involution if the (-1)-curve is geometrically invariant. Similarly, a pair of homology classes of self-intersection -1 is exchanged under an involution if and only if the actual (-1)-curves are exchanged by the involution. Hence,

- If an involution on $\mathcal{B}_n$ leaves one (-1)-class invariant, then said involution is the blow-up of an involution on $\mathcal{B}_{n-1}$ at one invariant point. In the standard basis, the group action on $H_2(\mathcal{B}_n, \mathbb{Z})$ is block diagonal, consisting of the action on $H_2(\mathcal{B}_{n-1}, \mathbb{Z})$ and one $\mathbf{1}_1$ block.

- If an involution on $\mathcal{B}_n$ exchanges two (-1)-classes that do not intersect, then said involution is the blow-up of an involution on $\mathcal{B}_{n-2}$ at a pair of points (that is, a non-fixed point and its image point). In the standard basis, the group action on $H_2(\mathcal{B}_n, \mathbb{Z})$ is block diagonal, consisting of the action on $H_2(\mathcal{B}_{n-2}, \mathbb{Z})$ and one H block.

A.8 Minimal Involutions

Analysing the list of possible actions on $H_2(S, \mathbb{Z})$ in Table 20, one easily sees that many are related by adding $\mathbf{1}_1$ or H blocks. If the action is induced from a del Pezzo surface, then these operations correspond to blowing up a fixed point and blowing up a point–image point pair, respectively. The minimal group actions, which cannot be built from simpler ones, are

- $\mathbf{1}_1$ acting on $H_2(\mathbb{P}^2, \mathbb{Z})$ Realised by $(\mathbb{P}^2, \sigma)$, eq. (231).

- $\mathbf{1}_2$ acting on $H_2(\mathbb{P}^1 \times \mathbb{P}^1, \mathbb{Z})$

    Realised by $(\mathbb{P}^1 \times \mathbb{P}^1, \sigma_1)$ and $(\mathbb{P}^1 \times \mathbb{P}^1, \sigma_2)$, eqns. (237a) and (237b).

- H acting on $H_2(\mathbb{P}^1 \times \mathbb{P}^1, \mathbb{Z})$ Realised by $(\mathbb{P}^1 \times \mathbb{P}^1, \sigma_3)$, eq. (237a).

- $I_{\mathcal{B}_5}^{(5)}$ acting on $H_2(\mathcal{B}_5, \mathbb{Z})$

- $I_{\mathcal{B}_7}^{(8)}$ acting on $H_2(\mathcal{B}_7, \mathbb{Z})$

- $I_{\mathcal{B}_7}^{(9)}$ acting on $H_2(\mathcal{B}_7, \mathbb{Z})$

- $I_{\mathcal{B}_8}^{(9)}$ acting on $H_2(\mathcal{B}_8, \mathbb{Z})$

Moreover, the first three (and only the first three) are related by adding *and subtracting* blocks of the form $\mathbf{1}_1$ and H. In terms of geometric involutions, this means that they are birational. Hence, there are five disconnected cases of involutions modulo blow-up/down. One obvious way to understand these cases is to look at the minimal involution, that is, those that cannot be further blown down. We already analysed the minimal models $(\mathbb{P}^2, \sigma)$, $(\mathbb{P}^1 \times \mathbb{P}^1, \sigma_1)$, $(\mathbb{P}^1 \times \mathbb{P}^1, \sigma_2)$, and $(\mathbb{P}^1 \times \mathbb{P}^1, \sigma_3)$, all of which are birationally equivalent[39]. The remaining four minimal involutions are classically known involutions:

$I_{\mathcal{B}_8}^{(9)}$: The Bertini involution on $\mathcal{B}_8$, which we denote by $(\mathcal{B}_8, \sigma_{\mathrm{B}})$. Its fixed point set see eq. (272), consists of a genus-4 curve and one isolated fixed point. Since $b_2^+ = 1$, all invariant homology classes must be proportional to the canonical class. The constant of proportionality determines the genus of a corresponding

---

[39]Evidently, a minimal model can be a "local minimum"

holomorphic curve via eq. (74). Using this, the homology class of the fixed point set must be

$$[\Sigma_4] = -3K = 9l - 3\sum_{i=1}^{8} e_i \ \in H_2(\mathcal{B}_8, \mathbb{Z})^{\sigma_B} = \mathbb{Z}K. \tag{265}$$

$I_{\mathcal{B}_7}^{(9)}$: The Geiser involution on $\mathcal{B}_7$, which we denote by $(\mathcal{B}_7, \sigma_G)$. The fixed point set, see eq. (272), consists of a genus-3 curve with homology class

$$[\Sigma_3] = -2K = 6l - 2\sum_{i=1}^{7} e_i \ \in H_2(\mathcal{B}_7, \mathbb{Z})^{\sigma_G} = \mathbb{Z}K. \tag{266}$$

$I_{\mathcal{B}_7}^{(8)}$: The de Jonquières involution of degree 4 on the blow-up of $\mathbb{P}^2$ at 7 points. In this case, 6 of the points necessarily lie on a conic [81], so this involution cannot be realised on a del Pezzo surface. The invariant homology classes are the rank-2 lattice generated by K and $l - e_1$. The fixed point set consists of a single genus-2 curve Σ_2. Its homology class is

$$[\Sigma_2] = -K + (l - e_1) = 4l - 2e_1 - \sum_{i=2}^{7} e_i$$
$$\in H_2(\mathcal{B}_7, \mathbb{Z})^{\sigma_{dJ}} = \mathrm{span}_{\mathbb{Z}}\{K, l - e_1\}. \tag{267}$$

$I_{\mathcal{B}_5}^{(5)}$: The de Jonquières involution of degree 3 on $\mathcal{B}_5$, which we denote by $(\mathcal{B}_5, \sigma_{dJ})$. The fixed point set, see eq. (272), consists of a single genus-1 curve (that is, an elliptic curve) Σ_1 in the class

$$[\Sigma_1] = -K = 3l - \sum_{i=1}^{5} e_i \ \in H_2(\mathcal{B}_5, \mathbb{Z})^{\sigma_{dJ}} = \mathrm{span}_{\mathbb{Z}}\{K, l - e_1\}. \tag{268}$$

Each of these involutions comes with moduli, which can be identified with the moduli of the fixed point curve Σ_g [82, 83]. For example, the moduli space of $(\mathcal{B}_5, \sigma)$ is the usual moduli space of elliptic curves[40]. Since these moduli spaces are all connected, we learn that there is (up to continuous deformation) a unique involution giving rise to the actions ($I_{\mathcal{B}_5}^{(5)}$, $I_{\mathcal{B}_7}^{(8)}$, $I_{\mathcal{B}_7}^{(9)}$, and $I_{\mathcal{B}_8}^{(9)}$, respectively) in homology.

---

[40]That is, the upper half plane modulo $PSL(2, \mathbb{Z})$.

Looking at the fixed point sets, we can understand the five different birationally connected components of involutions as follows. Note that blowing up a point on a surface always generates an exceptional divisor $\simeq \mathbb{P}^1$ and does not change the genus of other curves. Hence, all fixed points in del Pezzo involutions birationally connected to $(\mathbb{P}^2, \sigma)$ are either isolated fixed points or of genus 0. The fixed point set in the other 4 disconnected components all contain a single curve of genus 1, 2, 3, and 4, respectively. Again, since the genus of these divisors is a birational invariant, these 5 cases cannot be connected by a chain of blow-ups/downs.

A.9   Blow-ups of Minimal Models

In order to list all involutions on del Pezzo surfaces, we now just have to start with the 5 minimal involutions and perform successive blow-ups at fixed points or point–image point pairs. Recall that, by definition, the blow-up point must not lie on (-1) curves, see Footnote 17. Together with our local analysis of the fixed-point set after blow-up, Subsection A.4, we can summarise the blow-up procedure as follows:

- Blowing up an isolated fixed point is only allowed if this fixed point is not part of a (-1)-curve. After the blow-up, the isolated fixed point is replaced with the point-wise fixed exceptional divisor $e_n \simeq \mathbb{P}^1$ on $\mathcal{B}_n$. No points of e_n may be blown up any further.

- On a point-wise fixed curve C one may blow up points as long as $C^2 \geq 0$ and the point is not one of the finitely many intersection points with (-1)-curves. After the blow up to $\mathcal{B}_n$, the fixed curve C is replaced by its proper transform $\tilde{C}$ and one isolated point $\tilde{p}$. The new exceptional divisor e_n is not point-wise fixed, but intersects $\tilde{C} \cdot e_n = 1$ and contains $\tilde{p} \in e_n$. In particular, $\tilde{p}$ may not be blown up further. The homology class of the new fixed-point set is

$$[\tilde{C}] = [C - e_n] \in H_2\big(\mathcal{B}_n, \mathbb{Z}\big) \tag{269}$$

and $\tilde{C}^2 = C^2 - 1$.

- A generic point p is neither fixed nor part of the finitely many (-1)-curves. Hence, one can always find such a point p and image point q. However, since the two points are not independent, one must check that all points are still in general position, see Footnote 17. The fixed point set does not change when blowing up such a pair of points.

Clearly, the important data about the fixed points set are the curves and the isolated fixed points that can/cannot be blown up further.

The successive blow-ups of minimal involutions are then subject to the requirement that the blow-up points are in general position. This yields the following restrictions:

- Consider a generic point–image point pair on $(\mathbb{P}^2, \sigma)$,

$$p = [y : x_0 : x_1], \quad q = [-y, x_0 : x_1] \in \mathbb{P}^2. \tag{270}$$

  p, q, and the isolated fixed point $[1 : 0 : 0] \in (\mathbb{P}^2)^\sigma$ are collinear. Hence, one may either blow up this isolated fixed point or blow up a point–image point pair, but not all three.

- Amongst 4 invariant points on $(\mathbb{P}^2, \sigma)$ there are 3 collinear ones. This excludes actions containing $\mathbf{1}_5$ and higher.

- Any 3 point–image point pairs on $(\mathbb{P}^2, \sigma)$ lie on a conic. This excludes actions containing $3H$ and $4H$.

- Any 3 point–image point pairs on $(\mathbb{P}^1 \times \mathbb{P}^1, \sigma_3)$ lie on a conic. This excludes the action $I_{\mathcal{B}_3}^{(2)} \oplus 2H$.

- The de Jonquières involution of degree 4 on the blow-up of $\mathbb{P}^2$ at 7 points is excluded since there are 6 points lying on a conic.

- Recall the action of the Geiser involution on $\mathcal{B}_7 = \mathrm{Bl}_{p_1,\ldots,p_7} \mathbb{P}^2$, the image of a point $q \in \mathcal{B}_7$ is the remaining basepoint of the pencil of cubics going through the 8 points $\{p_1, \ldots, p_7, q\}$. If this remaining basepoint coincides with q, then the cubic has a node at q. Hence, blowing up a fixed point of $(\mathcal{B}_7, \sigma_{\mathrm{G}})$ is excluded as it would result in a nodal cubic going through the 8 points.

Starting from the minimal involutions, this lets us enumerate all involutions on del Pezzo surfaces. The result is presented in Table 6. These involutions are related through blowing up fixed points or point–image point pairs. This is depicted in Figure 10.

124
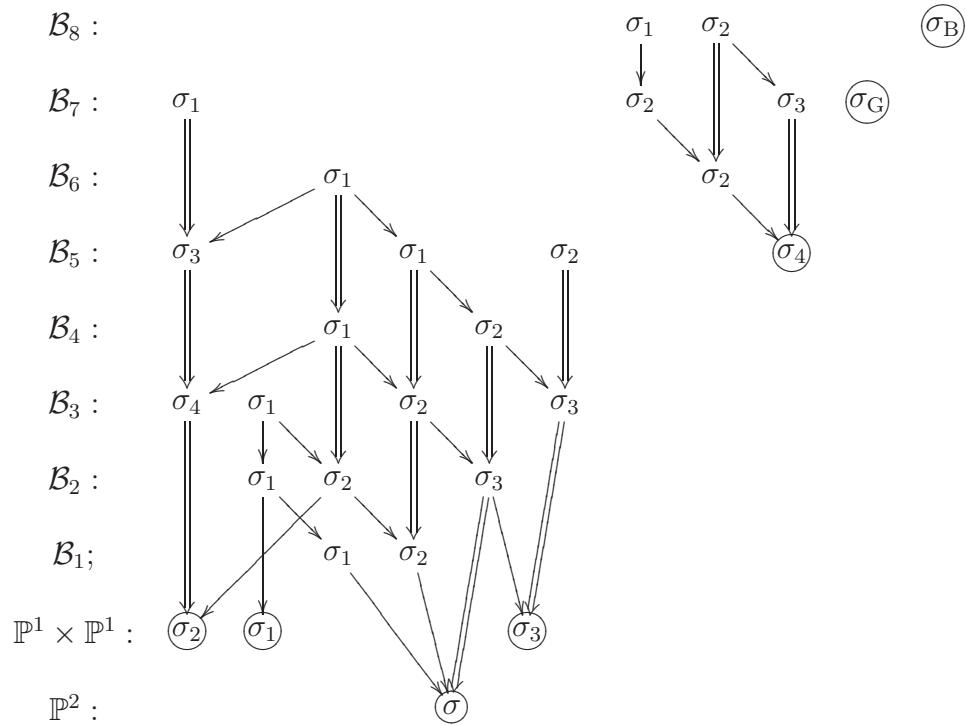
Figure 10: *Relations between the involutions on del Pezzo surfaces. The single arrows ($\rightarrow$) are the blow-downs of a fixed (-1)-curve, the double arrows ($\Rightarrow$) are the blow-downs of a (-1)-curve and its image curve. The minimal involutions are encircled.*

125

A.10 Explicit Realisations

Finally, let us list explicit examples for the involutions on del Pezzo surfaces of degree 5 and less. These can be written as hypersurfaces in weighted projective spaces. For simplicity, we pick a particular simple point in the complex moduli space in each case:

$$\mathcal{B}_6 = \left\{ x_0^3 + x_1^3 + x_2^3 + x_3^3 = 0 \right\} \quad \subset \mathbb{P}^{1,1,1,1}$$
$$\mathcal{B}_7 = \left\{ y^2 + x_0^4 + x_1^4 + x_2^4 = 0 \right\} \quad \subset \mathbb{P}^{2,1,1,1} \tag{271}$$
$$\mathcal{B}_7 = \left\{ y^2 + z^3 + x_0^6 + x_1^6 = 0 \right\} \quad \subset \mathbb{P}^{3,2,1,1}$$

The involutions listed in Table 6 then act as follows on the hypersurfaces:

$$\begin{aligned}
\sigma_1 &: \mathcal{B}_6 \to \mathcal{B}_6, & \left[x_0 : x_1 : x_2 : x_3 \right] &\mapsto \left[x_1 : x_0 : x_3 : x_2 \right], \\
\sigma_2 &: \mathcal{B}_6 \to \mathcal{B}_6, & \left[x_0 : x_1 : x_2 : x_3 \right] &\mapsto \left[x_1 : x_0 : x_2 : x_3 \right], \\
\sigma_1 &: \mathcal{B}_7 \to \mathcal{B}_7, & \left[y : x_0 : x_1 : x_2 \right] &\mapsto \left[-y : -x_0 : x_1 : x_2 \right], \\
\sigma_2 &: \mathcal{B}_7 \to \mathcal{B}_7, & \left[y : x_0 : x_1 : x_2 \right] &\mapsto \left[y : -x_0 : x_1 : x_2 \right], \\
\sigma_3 &: \mathcal{B}_7 \to \mathcal{B}_7, & \left[y : x_0 : x_1 : x_2 \right] &\mapsto \left[y : x_1 : x_0 : x_2 \right], \\
\sigma_G &: \mathcal{B}_7 \to \mathcal{B}_7, & \left[y : x_0 : x_1 : x_2 \right] &\mapsto \left[-y : x_0 : x_1 : x_2 \right], \\
\sigma_1 &: \mathcal{B}_8 \to \mathcal{B}_8, & \left[y : z : x_0 : x_1 \right] &\mapsto \left[y : z : -x_0 : x_1 \right], \\
\sigma_2 &: \mathcal{B}_8 \to \mathcal{B}_8, & \left[y : z : x_0 : x_1 \right] &\mapsto \left[y : z : x_1 : x_0 \right], \\
\sigma_B &: \mathcal{B}_8 \to \mathcal{B}_8, & \left[y : z : x_0 : x_1 \right] &\mapsto \left[-y : z : x_0 : x_1 \right].
\end{aligned} \tag{272}$$

B Cohomology of Line Bundles over del Pezzo Surfaces

On a del Pezzo surface $\mathcal{B}_n = \mathrm{Bl}_{p_1, p_2, \ldots, p_n} \left(\mathbb{P}^2 \right)$, $n \le 8$, the line bundles[41]

$$\mathrm{Pic}(\mathcal{B}_n) = H^2(\mathcal{B}_n, \mathbb{Z}) = \mathrm{span}_{\mathbb{Z}} \left\{ l, e_1, e_2, \ldots, e_n \right\} \simeq \mathbb{Z}^{n+1} \tag{273}$$

are classified by their first Chern class. We will parametrise the first Chern class of any line bundle L as

$$L = \mathcal{O}\left(al + \sum_{i \in I} b_i e_i - \sum_{j \in J} c_j e_j \right), \quad a \in \mathbb{Z}, \ b_i \in \mathbb{Z}_{\ge}, \ c_j \in \mathbb{Z}_{>}, \tag{274}$$

---

[41] We are going to label the exceptional divisors such that $e_k \subset \mathcal{B}_n$ corresponds to the blow-up point $p_k \in \mathbb{P}^2$, $k = 1, \ldots, n$.

where we split the index range $\{1, 2, \ldots, n\} = I \cup J$ into two disjoint index sets.

In order to compute the bundle cohomology groups of L, we fist recall the following two facts:

- The index of L is

$$
\begin{aligned}
\chi(L) &= \sum_{k=0}^{2} (-1)^k h^k(\mathcal{B}_n, L) = \int_{\mathcal{B}_n} \mathrm{ch}(L) \, \mathrm{Td}(T\mathcal{B}_n) = \\
&= \binom{a+2}{2} - \sum_{i \in I} \frac{b_i(b_i - 1)}{2} - \sum_{j \in J} \frac{c_j(c_j + 1)}{2}.
\end{aligned}
\tag{275}
$$

- Serre duality relates

$$
\begin{aligned}
H^k(\mathcal{B}_n, L)^\vee &= H^{2-k}(\mathcal{B}_n, L^\vee \otimes K) \\
&= H^{2-k}(\mathcal{B}_n, L^\vee \otimes \mathcal{O}(-3l + e_1 + \cdots + e_n))
\end{aligned}
\tag{276}
$$

Using Serre duality if necessary, it therefore suffices to calculate the cohomology groups of L for $a \geq -2$. In the following, we will always assume this to be the case.

First, the cohomology of $\mathcal{O}(al)$ is clearly identical to the cohomology of $\mathcal{O}_{\mathbb{P}^2}(a)$, which is

$$
H^*\Big(\mathcal{B}_n, \mathcal{O}(al)\Big) = \begin{cases} 0 & * = 2 \\ 0 & * = 1 \\ \binom{a+2}{2} & * = 0. \end{cases}
\tag{277}
$$

The $\binom{a+2}{2}$ global sections are nothing but the degree-a homogeneous polynomials in the 3 homogeneous variables. Similarly, the global sections of $\mathcal{O}(al - \sum c_i e_i)$ can be identified with the degree-a homogeneous polynomials that vanish at the blow-up point p_j to the degree c_j, $j \in J$. Note that the homogeneous polynomials are a linear space spanned by the monomials, and, therefore, counting the dimension of the space of such sections is a simple linear algebra problem. We denote the dimension of the sections vanishing at p_1, \ldots, p_n by[42]

$$
A_{\sum c_i p_i}(a) = \dim \big\{ P_a(x, y, z) \big| P_a(p_i) = 0 \text{ to order } c_i \big\}.
\tag{280}
$$

---

[42]The expected dimension is

$$
A_{\sum c_i p_i}^{\mathrm{expect}}(a) = \max \left\{ 0, \ \binom{a+2}{2} - \sum \frac{c_j(c_j + 1)}{2} \right\},
\tag{278}
$$

and this is often the actual value. However, for example, $\mathcal{O}_{\mathcal{B}_3}(3 - 3e_1 - 2e_2 - e_3)$ has $A_{3e_1 + 2e_2 + e_1}^{\mathrm{expect}}(3) = 0$ while the actual value is $A_{3e_1 + 2e_2 + e_1}(3) = 1$. Moreover, for special values of the complex structure

To obtain the higher-degree cohomology groups, consider the standard short exact sequence

$$0 \longrightarrow \mathcal{O}_{\mathcal{B}_n}\left(al - \sum c_j e_j\right) \longrightarrow \mathcal{O}_{\mathcal{B}_n}\left(al\right) \longrightarrow \oplus_{j \in J} \mathcal{O}_{c_j e_j} \longrightarrow 0. \tag{281}$$

From the corresponding long exact sequence[43],

$$0 \longrightarrow H^0\left(\mathcal{O}_{\mathcal{B}_n}\left(al - \sum c_j e_j\right)\right) \longrightarrow \binom{a+2}{2} \longrightarrow \sum \frac{c_j(c_j+1)}{2} \longrightarrow$$
$$\longrightarrow H^1\left(\mathcal{O}_{\mathcal{B}_n}\left(al - \sum c_j e_j\right)\right) \longrightarrow 0 \longrightarrow 0, \tag{282}$$

it follows that the cohomology is concentrated in degrees 0 and 1 only. Hence, using the index, one obtains that

$$H^2\left(\mathcal{B}_n, \mathcal{O}(al - \sum c_j e_j)\right) = 0. \tag{283}$$

Finally, consider the short exact sequence

$$0 \longrightarrow \mathcal{O}_{\mathcal{B}_n}\left(al - \sum c_j e_j\right) \longrightarrow L \longrightarrow \oplus_{i \in I} \mathcal{O}_{b_i e_i}(-b_i) \longrightarrow 0 . \tag{284}$$

The corresponding long exact sequence reads

$$0 \longrightarrow H^0\left(\mathcal{O}_{\mathcal{B}_n}\left(al - \sum c_i e_i\right)\right) \longrightarrow H^0(L) \longrightarrow 0$$
$$\longrightarrow H^1\left(\mathcal{O}_{\mathcal{B}_n}\left(al - \sum c_i e_i\right)\right) \longrightarrow H^1(L) \longrightarrow \sum \frac{b_i(b_i+1)}{2} \longrightarrow \tag{285}$$
$$\longrightarrow 0 \longrightarrow H^2(L) \longrightarrow 0 \longrightarrow 0.$$

---

moduli of $\mathcal{B}_n$, the dimension of the cohomology group jumps and $A_{\sum c_i p_i}(a) > A^{\text{expect}}_{\sum c_i p_i}(a)$. Note that one can always pick coordinates on $\mathbb{P}^2$ such that

$$p_1 = [1 : 0 : 0], \ p_2 = [0 : 1 : 0], \ p_3 = [0 : 0 : 1], \ p_4 = [1 : 1 : 1]. \tag{279}$$

In other words, only $\mathcal{B}_n$ with $n \geq 5$ have complex structure moduli, parametrised by the position of the points $p_5, \ldots, p_n$.

[43]By abuse of notation, we just write k instead of a k-dimensional vector space in long exact sequences.

128

One immediately notices that the cohomology of L is concentrated in degrees 0 and 1, and therefore is determined by the index and A. Therefore, the cohomology of $L = \mathcal{O}(al + \sum b_i e_i - \sum c_j e_j)$ with $a \geq -2$ is given by

$$H^*\left(\mathcal{B}_n, L\right) = \begin{cases} 0 & * = 2 \\ -\chi(L) - A_{\sum c_i p_i}(a) & * = 1 \\ A_{\sum c_i p_i}(a) & * = 0. \end{cases} \tag{286}$$

C   Cohomology of Line Bundles On Rational Elliptic Surfaces

By definition, a dP_9 surface is a rational elliptic surface, meaning that it is simultaneously a blow-up of $\mathbb{P}^2$ and elliptically fibred. Given this definition, one can show that there must be precisely 9 blow-up points[44]

$$\mathrm{dP}_9 = \mathrm{Bl}_{\{p_1,\dots,p_9\}}\left(\mathbb{P}^2\right), \tag{287}$$

that the base of the fibration must be $\mathbb{P}^1$ and can[45] be taken to be e_9), and that the fibre class is

$$f = 3l - \sum_{i=1}^{9} e_i \quad \in H_2\left(\mathrm{dP}_9, \mathbb{Z}\right). \tag{288}$$

However, the position of the 9 points are not arbitrary. In other words, not every blow-up of $\mathbb{P}^2$ at 9 points is elliptically fibred, but, rather, the blow-up points have to be in the right position. The immediate consequence for line bundles is that often the actual cohomology groups are larger than what one would obtain from the naive application of Appendix B. For example [84],

$$H^*\left(\mathrm{dP}_9, \mathcal{O}_{\mathrm{dP}_9}(f)\right) = (2, 1, 0), \tag{289}$$

while eq. (286) would have yielded[46] $(1, 0, 0)$.

---

[44]In contrast to the del Pezzo case, the blow-up points can be "infinitesimally close". This generates (-2)-curves in the blown-up surface, which are allowed on a dP_9 but not on a del Pezzo surface. In fact, the irreducible components of most Kodaira fibres (all except I_0, I_1, and III) have self-intersection -2.

[45]And we will make this choice always in the following.

[46]Of course, the index is the same since it is a topological quantity.

However, there are two special cases[47] where we can, in fact, simply apply the results of Appendix B for $\mathcal{B}_r$, $r = 0, \ldots, 8$:

- Consider the case where one of the exceptional divisors (say, e_9) does not appear in the line bundle, that is,

$$L = \mathcal{O}\Big(al + \sum_{i \in I} b_i e_i - \sum_{j \in J} c_j e_j + 0 \cdot e_9\Big), \quad a \in \mathbb{Z}, \ b_i \in \mathbb{Z}_{\geq}, \ c_j \in \mathbb{Z}_{>}, \quad (290)$$

  with $I \cup J = \{1, \ldots, 8\}$ disjoint index sets. Then, we can identify the cohomology with the analogue

$$H^*\big(\mathrm{dP}_9, L\big) = H^*\Big(\mathcal{B}_8, \mathcal{O}_{\mathcal{B}_8}\big(al + \sum_{i \in I} b_i e_i - \sum_{j \in J} c_j e_j\big)\Big) \quad (291)$$

  on $\mathcal{B}_8$, where eq. (286) holds.

- The canonical bundle is

$$K_{\mathrm{dP}_9} = \mathcal{O}_{\mathrm{dP}_9}(-f), \quad (292)$$

  and, therefore, Serre duality allows us to identify

$$H^*\big(\mathrm{dP}_9, L \otimes \mathcal{O}_{\mathrm{dP}_9}(-f)\big) = H^{2-*}\big(\mathrm{dP}_9, L^\vee\big)^\vee. \quad (293)$$

However, in general one has to use the use the program detailed in [84], and use the Leray-Serre spectral sequence for the elliptic fibration $\pi : \mathrm{dP}_9 \to \mathbb{P}^1$. This revolves around the three steps:

1. Compute the push-down $R^q \pi_* L$ for linear combinations of sections, adding and subtracting one section s at a time. This amounts to repeated applications of the short exact sequence

$$0 \longrightarrow \mathcal{O}_{\mathrm{dP}_9}(D - s) \longrightarrow \mathcal{O}_{\mathrm{dP}_9}(D) \longrightarrow \mathcal{O}_s(D \cdot s) \longrightarrow 0 \quad (294)$$

   and the corresponding long exact sequence

$$0 \longrightarrow \pi_*\big(\mathcal{O}_{\mathrm{dP}_9}(D - s)\big) \longrightarrow \pi_*\big(\mathcal{O}_{\mathrm{dP}_9}(D)\big) \longrightarrow \mathcal{O}_{\mathbb{P}^1}(D \cdot s) \longrightarrow$$
$$\longrightarrow R^1 \pi_*\big(\mathcal{O}_{\mathrm{dP}_9}(D - s)\big) \longrightarrow R^1 \pi_*\big(\mathcal{O}_{\mathrm{dP}_9}(D)\big) \longrightarrow 0, \quad (295)$$

   for push-downs.

---

[47]Here, and in the following, we will assume that we are on a sufficiently generic dP$_9$ surface where all blow-up points $p_1, \ldots, p_9$ can be chosen to be distinct.

2. Use the *projection formula*

$$R^q \pi_* \left(L \otimes \mathcal{O}_{\mathrm{dP}_9}(nf) \right) = R^q \pi_* \left(L \right) \otimes \mathcal{O}_{\mathbb{P}^1}(n) \qquad (296)$$

to shift fibre classes to the base $\mathbb{P}^1$.

3. Compute the cohomology groups of $R^q \pi_*(L)$ (on $\mathbb{P}^1$) and use the Leray-Serre spectral sequence to conclude

$$H^* \left(\mathrm{dP}_9, L \right) = \begin{cases} H^1 \left(\mathbb{P}^1, R^1 \pi_*(L) \right) & * = 2, \\ H^1 \left(\mathbb{P}^1, \pi_*(L) \right) \oplus H^0 \left(\mathbb{P}^1, R^1 \pi_*(L) \right) & * = 1, \\ H^0 \left(\mathbb{P}^1, \pi_*(L) \right) & * = 0. \end{cases} \qquad (297)$$

As an example, let us consider $L = \mathcal{L}^{-2} \otimes \mathcal{L}_Y^{-1} = \mathcal{O}_{\mathrm{dP}_9}(2e_9 + e_1 - e_2 - 2f)$ in Table 8. Adding and subtracting sections yields (vanishing $R^1 \pi_*$s are skipped)

$$\begin{aligned} \pi_* \left(\mathcal{O}_{\mathrm{dP}_9} \right) &= \mathcal{O}_{\mathbb{P}^1}, \quad R^1 \pi_* \left(\mathcal{O}_{\mathrm{dP}_9} \right) = \mathcal{O}_{\mathbb{P}^1}(-1), \\ \pi_* \left(\mathcal{O}_{\mathrm{dP}_9}(e_9) \right) &= \mathcal{O}_{\mathbb{P}^1}, \\ \pi_* \left(\mathcal{O}_{\mathrm{dP}_9}(2e_9) \right) &= \mathcal{O}_{\mathbb{P}^1} \oplus \mathcal{O}_{\mathbb{P}^1}(-2), \\ \pi_* \left(\mathcal{O}_{\mathrm{dP}_9}(2e_9 + e_1) \right) &= \mathcal{O}_{\mathbb{P}^1} \oplus \mathcal{O}_{\mathbb{P}^1}(-2) \oplus \mathcal{O}_{\mathbb{P}^1}(-1), \\ \pi_* \left(\mathcal{O}_{\mathrm{dP}_9}(2e_9 + e_1 - e_2) \right) &= \mathcal{O}_{\mathbb{P}^1}(-2) \oplus \mathcal{O}_{\mathbb{P}^1}(-1). \end{aligned} \qquad (298)$$

Hence, using eq. (296),

$$\begin{aligned} \pi_* \left(L \right) &= \mathcal{O}_{\mathbb{P}^1}(-4) \oplus \mathcal{O}_{\mathbb{P}^1}(-3) \\ R^1 \pi_* \left(L \right) &= 0. \end{aligned} \qquad (299)$$

Finally, the Leray-Serre spectral sequence yields

$$H^* \left(\mathrm{dP}_9, L \right) = (0, 5, 0). \qquad (300)$$

Bibliography

[1] R. Blumenhagen, M. Cvetič, P. Langacker, and G. Shiu, "Toward realistic intersecting D-brane models," *Ann. Rev. Nucl. Part. Sci.* **55** (2005) 71–139, hep-th/0502005.

[2] M. R. Douglas and S. Kachru, "Flux compactification," *Rev. Mod. Phys.* **79** (2007) 733–796, `hep-th/0610102`.

[3] R. Blumenhagen, B. Kors, D. Lüst, and S. Stieberger, "Four-dimensional String Compactifications with D-Branes, Orientifolds and Fluxes," *Phys. Rept.* **445** (2007) 1–193, `hep-th/0610327`.

[4] F. Denef, M. R. Douglas, and S. Kachru, "Physics of string flux compactifications," *Ann. Rev. Nucl. Part. Sci.* **57** (2007) 119–144, `hep-th/0701050`.

[5] H. P. Nilles, S. Ramos-Sanchez, M. Ratz, and P. K. S. Vaudrevange, "From strings to the MSSM," `0806.3905`.

[6] S. Kachru, R. Kallosh, A. Linde, and S. P. Trivedi, "De Sitter vacua in string theory," *Phys. Rev.* **D68** (2003) 046005, `hep-th/0301240`.

[7] V. Balasubramanian, P. Berglund, J. P. Conlon, and F. Quevedo, "Systematics of moduli stabilisation in Calabi-Yau flux compactifications," *JHEP* **03** (2005) 007, `hep-th/0502058`.

[8] J. P. Conlon, F. Quevedo, and K. Suruliz, "Large-volume flux compactifications: Moduli spectrum and D3/D7 soft supersymmetry breaking," *JHEP* **08** (2005) 007, `hep-th/0505076`.

[9] L. Aparicio, D. G. Cerdeno, and L. E. Ibanez, "Modulus-dominated SUSY-breaking soft terms in F-theory and their test at LHC," *JHEP* **07** (2008) 099, `0805.2943`.

[10] R. Blumenhagen, S. Moster, and E. Plauschinn, "String GUT Scenarios with Stabilised Moduli," `0806.2667`.

[11] R. Blumenhagen, B. Körs, D. Lüst, and T. Ott, "The standard model from stable intersecting brane world orbifolds," *Nucl. Phys.* **B616** (2001) 3–33, `hep-th/0107138`.

[12] C. Vafa, "Evidence for F-Theory," *Nucl. Phys.* **B469** (1996) 403–418, `hep-th/9602022`.

[13] R. Donagi and M. Wijnholt, "Model Building with F-Theory," `0802.2969`.

[14] C. Beasley, J. J. Heckman, and C. Vafa, "GUTs and Exceptional Branes in F-theory - I," 0802.3391.

[15] H. Hayashi, R. Tatar, Y. Toda, T. Watari, and M. Yamazaki, "New Aspects of Heterotic–F Theory Duality," 0805.1057.

[16] C. Beasley, J. J. Heckman, and C. Vafa, "GUTs and Exceptional Branes in F-theory - II: Experimental Predictions," 0806.0102.

[17] R. Donagi and M. Wijnholt, "Breaking GUT Groups in F-Theory," 0808.2223.

[18] A. Font and L. E. Ibanez, "Yukawa Structure from U(1) Fluxes in F-theory Grand Unification," 0811.2157.

[19] J. J. Heckman and C. Vafa, "Flavor Hierarchy From F-theory," 0811.2417.

[20] D. Lüst, P. Mayr, S. Reffert, and S. Stieberger, "F-theory flux, destabilization of orientifolds and soft terms on D7-branes," *Nucl. Phys.* **B732** (2006) 243–290, hep-th/0501139.

[21] P. Aluffi and M. Esole, "Chern class identities from tadpole matching in type IIB and F-theory," 0710.2544.

[22] A. P. Braun, A. Hebecker, and H. Triendl, "D7-Brane Motion from M-Theory Cycles and Obstructions in the Weak Coupling Limit," *Nucl. Phys.* **B800** (2008) 298–329, 0801.2163.

[23] A. Collinucci, F. Denef, and M. Esole, "D-brane Deconstructions in IIB Orientifolds," 0805.1573.

[24] A. P. Braun, A. Hebecker, C. Ludeling, and R. Valandro, "Fixing D7 Brane Positions by F-Theory Fluxes," 0811.2416.

[25] R. Blumenhagen, M. Cvetič, and T. Weigand, "Spacetime instanton corrections in 4D string vacua - the seesaw mechanism for D-brane models," *Nucl. Phys.* **B771** (2007) 113–142, hep-th/0609191.

[26] L. E. Ibanez and A. M. Uranga, "Neutrino Majorana masses from string theory instanton effects," *JHEP* **03** (2007) 052, hep-th/0609213.

[27] B. Florea, S. Kachru, J. McGreevy, and N. Saulina, "Stringy instantons and quiver gauge theories," *JHEP* **05** (2007) 024, `hep-th/0610003`.

[28] R. Blumenhagen, M. Cvetič, D. Lüst, R. Richter, and T. Weigand, "Non-perturbative Yukawa Couplings from String Instantons," *Phys. Rev. Lett.* **100** (2008) 061602, `0707.1871`.

[29] H. Verlinde and M. Wijnholt, "Building the standard model on a D3-brane," *JHEP* **01** (2007) 106, `hep-th/0508089`.

[30] M. Buican, D. Malyshev, D. R. Morrison, H. Verlinde, and M. Wijnholt, "D-branes at singularities, compactification, and hypercharge," *JHEP* **01** (2007) 107, `hep-th/0610007`.

[31] E. Witten, "New Issues in Manifolds of SU(3) Holonomy," *Nucl. Phys.* **B268** (1986) 79.

[32] R. Blumenhagen, G. Honecker, and T. Weigand, "Loop-corrected compactifications of the heterotic string with line bundles," *JHEP* **06** (2005) 020, `hep-th/0504232`.

[33] R. Tatar and T. Watari, "Proton decay, Yukawa couplings and underlying gauge symmetry in string theory," *Nucl. Phys.* **B747** (2006) 212–265, `hep-th/0602238`.

[34] R. Blumenhagen, S. Moster, and T. Weigand, "Heterotic GUT and standard model vacua from simply connected Calabi-Yau manifolds," *Nucl. Phys.* **B751** (2006) 186–221, `hep-th/0603015`.

[35] R. Blumenhagen, S. Moster, R. Reinbacher, and T. Weigand, "Massless spectra of three generation U(N) heterotic string vacua," *JHEP* **05** (2007) 041, `hep-th/0612039`.

[36] R. Tatar and T. Watari, "GUT Relations from String Theory Compactifications," `0806.0634`.

[37] J. J. Heckman, J. Marsano, N. Saulina, S. Schafer-Nameki, and C. Vafa, "Instantons and SUSY breaking in F-theory," `0808.1286`.

[38] J. Marsano, N. Saulina, and S. Schafer-Nameki, "An Instanton Toolbox for F-Theory Model Building," `0808.2450`.

[39] J. Marsano, N. Saulina, and S. Schafer-Nameki, "Gauge Mediation in F-Theory GUT Models," `0808.1571`.

[40] E. Witten, "PiTP Lecture: String Compactifications I," `http://video.ias.edu/PiTP-2008-Witten1`.

[41] T. W. Grimm and A. Klemm, "U(1) Mediation of Flux Supersymmetry Breaking," *JHEP* **10** (2008) 077, `0805.3361`.

[42] D. S. Freed and E. Witten, "Anomalies in string theory with D-branes," `hep-th/9907189`.

[43] I. Antoniadis, E. Kiritsis, and T. N. Tomaras, "A D-brane alternative to unification," *Phys. Lett.* **B486** (2000) 186–193, `hep-ph/0004214`.

[44] J. R. Ellis, P. Kanti, and D. V. Nanopoulos, "Intersecting branes flip SU(5)," *Nucl. Phys.* **B647** (2002) 235–251, `hep-th/0206087`.

[45] M. Cvetič, I. Papadimitriou, and G. Shiu, "Supersymmetric three family SU(5) grand unified models from type IIA orientifolds with intersecting D6-branes," *Nucl. Phys.* **B659** (2003) 193–223, `hep-th/0212177`.

[46] F. Gmeiner and M. Stein, "Statistics of SU(5) D-brane models on a type II orientifold," *Phys. Rev.* **D73** (2006) 126008, `hep-th/0603019`.

[47] M. Cvetič and P. Langacker, "New grand unified models with intersecting D6-branes, neutrino masses, and flipped SU(5)," *Nucl. Phys.* **B776** (2007) 118–137, `hep-th/0607238`.

[48] I. Antoniadis, A. Kumar, and B. Panda, "Supersymmetric SU(5) GUT with Stabilized Moduli," *Nucl. Phys.* **B795** (2008) 69–104, `0709.2799`.

[49] T. W. Grimm and J. Louis, "The effective action of N = 1 Calabi-Yau orientifolds," *Nucl. Phys.* **B699** (2004) 387–426, `hep-th/0403067`.

[50] T. W. Grimm, "The effective action of type II Calabi-Yau orientifolds," *Fortsch. Phys.* **53** (2005) 1179–1271, `hep-th/0507153`.

[51] M. Marino, R. Minasian, G. W. Moore, and A. Strominger, "Nonlinear instantons from supersymmetric p-branes," *JHEP* **01** (2000) 005, `hep-th/9911206`.

[52] R. Blumenhagen, G. Honecker, and T. Weigand, "Supersymmetric (non-)abelian bundles in the type I and SO(32) heterotic string," *JHEP* **08** (2005) 009, `hep-th/0507041`.

[53] R. Blumenhagen, G. Honecker, and T. Weigand, "Non-abelian brane worlds: The open string story," `hep-th/0510050`.

[54] E. Plauschinn, "The generalized Green-Schwarz mechanism for Type IIB orientifolds with D3- and D7-branes," `0811.2804`.

[55] H. Jockers and J. Louis, "The effective action of D7-branes in N = 1 Calabi-Yau orientifolds," *Nucl. Phys.* **B705** (2005) 167–211, `hep-th/0409098`.

[56] H. Jockers and J. Louis, "D-terms and F-terms from D7-brane fluxes," *Nucl. Phys.* **B718** (2005) 203–246, `hep-th/0502059`.

[57] E. Witten, "Toroidal compactification without vector structure," *JHEP* **02** (1998) 006, `hep-th/9712028`.

[58] C. Bachas, M. Bianchi, R. Blumenhagen, D. Lüst, and T. Weigand, "Comments on Orientifolds without Vector Structure," *JHEP* **08** (2008) 016, `0805.3696`.

[59] A. M. Uranga, "D-brane probes, RR tadpole cancellation and K-theory charge," *Nucl. Phys.* **B598** (2001) 225–246, `hep-th/0011048`.

[60] R. Blumenhagen, S. Moster, and E. Plauschinn, "Moduli Stabilisation versus Chirality for MSSM like Type IIB Orientifolds," *JHEP* **01** (2008) 058, `0711.3389`.

[61] S. H. Katz and E. Sharpe, "D-branes, open string vertex operators, and Ext groups," *Adv. Theor. Math. Phys.* **6** (2003) 979–1030, `hep-th/0208104`.

[62] T. W. Grimm and J. Louis, "The effective action of type IIA Calabi-Yau orientifolds," *Nucl. Phys.* **B718** (2005) 153–202, `hep-th/0412277`.

[63] M. Cvetič, R. Richter, and T. Weigand, "Computation of D-brane instanton induced superpotential couplings - Majorana masses from string theory," *Phys. Rev.* **D76** (2007) 086002, `hep-th/0703028`.

[64] L. E. Ibanez, A. N. Schellekens, and A. M. Uranga, "Instanton Induced Neutrino Majorana Masses in CFT Orientifolds with MSSM-like spectra," *JHEP* **06** (2007) 011, `0704.1079`.

[65] M. Cicoli, J. P. Conlon, and F. Quevedo, "General Analysis of LARGE Volume Scenarios with String Loop Moduli Stabilisation," `0805.1029`.

[66] M. Demazure, *Séminaire sur les singularités des surface*, ch. Surfaces de Del Pezzo, II, III, IV et V. Springer-Verlag, 1980.

[67] K. Kodaira, "On compact analytic surfaces II," *Annals of Math.* **77** (1963) 563–626.

[68] K. Kodaira, "On compact analytic surfaces III," *Annals of Math.* **78** (1963) 1–40.

[69] A. Klemm, B. Lian, S. S. Roan, and S.-T. Yau, "Calabi-Yau fourfolds for M- and F-theory compactifications," *Nucl. Phys.* **B518** (1998) 515–574, `hep-th/9701023`.

[70] D. R. Morrison and C. Vafa, "Compactifications of F-Theory on Calabi–Yau Threefolds – II," *Nucl. Phys.* **B476** (1996) 437–469, `hep-th/9603161`.

[71] J. Louis, J. Sonnenschein, S. Theisen, and S. Yankielowicz, "Non-perturbative properties of heterotic string vacua compactified on K3 x T**2," *Nucl. Phys.* **B480** (1996) 185–212, `hep-th/9606049`.

[72] W. Barth, C. Peters, and A. Van den Ven, "Compact Complex Surfaces," *Springer-Verlag, Berlin* (1984).

[73] D.-E. Diaconescu, R. Donagi, and B. Florea, "Metastable quivers in string compactifications," *Nucl. Phys.* **B774** (2007) 102–126, `hep-th/0701104`.

[74] M. R. Douglas and G. W. Moore, "D-branes, Quivers, and ALE Instantons," `hep-th/9603167`.

[75] G. Aldazabal, L. E. Ibanez, F. Quevedo, and A. M. Uranga, "D-branes at singularities: A bottom-up approach to the string embedding of the standard model," *JHEP* **08** (2000) 002, `hep-th/0005067`.

[76] J. P. Conlon, A. Maharana, and F. Quevedo, "Towards Realistic String Vacua," `0810.5660`.

[77] R. Blumenhagen, M. Cvetič, R. Richter, and T. Weigand, "Lifting D-Instanton Zero Modes by Recombination and Background Fluxes," *JHEP* **10** (2007) 098, `0708.0403`.

[78] J. P. Conlon, S. S. Abdussalam, F. Quevedo, and K. Suruliz, "Soft SUSY breaking terms for chiral matter in IIB string compactifications," *JHEP* **01** (2007) 032, `hep-th/0610129`.

[79] I. Garcia-Etxebarria and A. M. Uranga, "From F/M-theory to K-theory and back," *JHEP* **02** (2006) 008, `hep-th/0510073`.

[80] Y. I. Manin, "Rational surfaces over perfect fields. II," *Mat. Sb. (N.S.)* **72** (1967) 161–192.

[81] I. V. Dolgachev and V. A. Iskovskikh, "Finite subgroups of the plane Cremona group," `math/0610595`.

[82] L. Bayle and A. Beauville, "Birational involutions of P^2," `math/9907028`.

[83] T. de Fernex, "On planar Cremona maps of prime order," *NAGOYA MATH.J.* **174** (2004) 1, `math/0302175`.

[84] V. Braun, Y.-H. He, B. A. Ovrut, and T. Pantev, "Vector bundle extensions, sheaf cohomology, and the heterotic standard model," *Adv. Theor. Math. Phys.* **10** (2006) 4, `hep-th/0505041`.